Asymmetric Catalysis Mediated by Synthetic Peptides

Elizabeth A. Colby Davie,*,‡,§ Steven M. Mennen,‡ Yingju Xu,‡ and Scott J. Miller*,†,‡

Department of Chemistry, Yale University, P.O. Box 208107, New Haven, Connecticut 06520-8107, Department of Chemistry, Boston College, Chestnut Hill, Massachusetts 02467, and Assumption College, 500 Salisbury Street, Worcester, Massachusetts 01609

Contents

* To whom correspondence should be addressed. E-mail: scott.miller@yale.edu.
† Yale University.
‡ Boston College.
§ Assumption College.

1. Introduction

Exquisitely selective reactions are ubiquitous in the natural world. In such processes, enzymes exhibit extraordinary degrees of stereoselectivity and can also display remarkable substrate specificity, allowing for very high levels of chemo- and regioselectivity. The intricate macromolecular structure of enzymes plays a significant role in selective substrate binding by creating clefts or pockets in which compounds may only fit in a certain orientation. Topological shape alone is not responsible for enzymatic activity, however. Specific amino acid residues are arrayed in space so that certain functional groups are in close proximity to act in concert and achieve catalysis. Primary structural features are often equally vital to the mode of catalysis through interactions such as hydrogen bonding, proton transfer, or nucleophilic assistance at the binding site, among others. Considering the finite number of coded amino acids that compose enzymes, the diversity of reactivity and selectivity found is astounding.

Enzymes have fascinated chemists on many levels for decades. Synthetic chemists have attempted to harness the power of nature's catalysts in the laboratory in several ways. The building blocks of enzymes, single amino acids, have provided the foundations of several beautiful methods for asymmetric synthesis, as both auxiliary scaffolds and catalysts. In contrast, the secondary and tertiary structures of large proteins have been ingeniously mimicked through advances in de novo protein design.

Toward the middle of the catalyst size continuum, peptides composed of 2−50 amino acids have gained momentum as effective catalysts for a number of enantioselective methods. Peptide catalysts possessing only a few amino acid residues

Elizabeth A. Colby Davie was born in St. Paul, MN, in 1977. She attended Macalester College, receiving her B.A. in chemistry in 2000. She then conducted graduate research in the laboratory of Professor Timothy F. Jamison at the Massachusetts Institute of Technology, earning her Ph.D. in 2005. She joined the group of Professor Scott J. Miller at Boston College in 2005 as a National Institute of Health Postdoctoral Research Fellow. Currently, she is an assistant professor of chemistry at Assumption College.
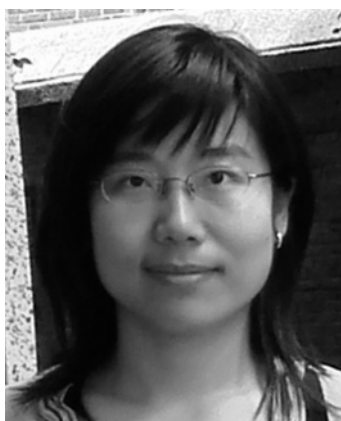
Yingju Xu received her Bachelor's and Master's degrees in organic chemistry from Nanjing University, China, in 2002. She then began her graduate research under the direction of Professor Scott J. Miller at Boston College. She received her Ph.D. in 2007 and is currently a process chemist at Merck in Rahway, New Jersey.

Steven M. Mennen was born and raised in Appleton, Wisconsin, in 1980. He received his B.S. in chemistry from the University of Wisconsin—Stevens Point in 2002 and completed his doctoral dissertation in 2007 with Professor Scott J. Miller at Boston College. Dr. Mennen is currently an NIH Posdoctoral Fellow with Professor Larry E. Overman at the University of California—Irvine.

Scott J. Miller was born December 11, 1966, in Buffalo, NY. He received his B.A. (1989), M.A. (1989), and Ph.D. (1994) from Harvard University, where he worked in the laboratories of Professor David Evans as a National Science Foundation Predoctoral Fellow. Subsequently, he traveled to the California Institute of Technology where he was a National Science Foundation Postdoctoral Fellow in the laboratories of Professor Robert Grubbs. In 1996, he joined the faculty at Boston College, and in 2006 he moved to Yale University. Professor Miller's research program focuses on problems in asymmetric catalysis. His group employs strategies that include catalyst design, the development of combinatorial techniques for catalyst screening, and the application of these approaches to the preparation of biologically active agents.

may adopt a secondary structure suitable for the transfer of chirality. Additionally, the modular nature of peptides allows for fine-tuning of reactivity and selectivity by replacing single amino acid residues. Together, these factors produce an attractive catalyst platform for asymmetric synthesis, which has been realized for decades. As early as the 1970s, Inoue demonstrated that poly(amino acids) are effective catalysts for the conjugate addition of thiols to enones. A few years later, Juliá and Colonna reported the use of such polymers in the enantioselective epoxidation of chalcones and related enones. Poly(amino acids) have also been employed by Nonaka as chiral coatings for electrodes, allowing both reductive and oxidative electrochemical processes. Polymers are far from the only effective peptide catalysts for asymmetric synthesis; smaller peptide catalysts have also played a prominent role in enantioselective catalysis. Inoue developed diketopiperazine catalysts for cyanohydrin synthesis in the 1970s and 1980s. In 1996, Lipton showed that these diketopiperazine catalysts are effective for the enantioselective Strecker reaction. More recent work by several groups in the arena of group transfer reactions, enantioselective aldol reactions, formal acyl anion chemistry, enantioselective protonation of enolates, Michael additions, and the Morita—Baylis—Hillman reaction have firmly established small peptides as versatile, enantioselective catalysts. It is this burgeoning subfield of peptide chemistry that will be covered in this review.

2. Metal-Free Asymmetric Carbon—Carbon Bond-Forming Reactions Catalyzed by Synthetic Peptides

2.1. Addition of Hydrogen Cyanide to Carbonyl Electrophiles

One of the original studies of peptides as potential catalysts for asymmetric induction involved the addition of hydrogen cyanide to aldehydes. Over a century ago, Strecker showed that what appears to be a straighforward reaction would
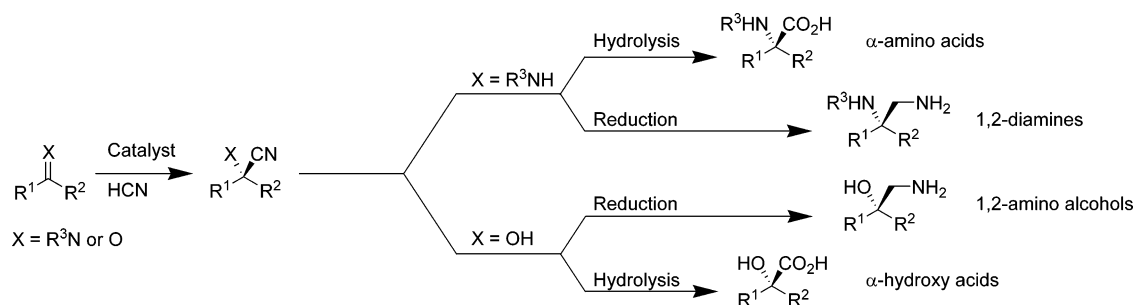
Figure 1. Addition of hydrogen cyanide to carbonyls.

proceed in basic media.[1] The direct product of this class of reactions is either a cyanohydrin or an α-aminonitrile, which upon hydrolysis or reduction provides direct access to α-amino acids, 1,2-diamines, 1,2-amino alcohols, or α-hydroxy acids (Figure 1).[2]

2.1.1. Hydrocyanation of Aldehydes

In 1979, Oku and Inoue published a pioneering study of cyclic dipeptides (2,5-dioxopiperazines or diketopiperazines) as catalysts for the asymmetric addition of hydrogen cyanide to benzaldehyde.[3] At this time, the enzyme oxynitrilase[4] and several alkaloids[5] were known to mediate the synthesis of cyanohydrins from aldehydes and hydrogen cyanide, but peptide-based catalysis had not yet been documented for carbon−carbon bond-forming reactions.

Examination of the diastereomers of several dipeptides revealed which structural features most efficiently transferred chirality from the catalyst to the product (Table 1). Linear dipeptides allowed for rapid reaction rates (entries 2 and 3) but did not catalyze an enantioselective reaction. Cyclic dipeptides allowed for a reaction with modest enantioselectivity, wherein absolute stereoconfiguration is believed to predominantly originate from the absolute configuration of the histidine residue based on the small difference between diastereomeric peptides (entries 4 and 5). From these results, Oku and Inoue concluded that the conformationally rigid skeleton of the diketopiperazine is favorable for an asymmetric synthesis of cyanohydrins. At the time of these published results, Oku and Inoue's application of dipeptides to the synthesis of cyanohydrins allowed for levels of selectivity comparable to the highest known with a nonenzymatic catalyst.

Further investigation into this reaction allowed for significant improvements that made this method very attractive for the synthesis of enantiomerically enriched cyanohydrins.

Table 1. Asymmetric Addition of Hydrogen Cyanide to Benzaldehyde Catalyzed by Dipeptides
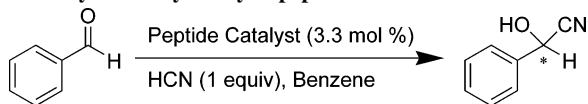
Entry	Catalyst	Time (h)	Conv. (%)	ee (%)	Absol. Config
1	cyclo-(His)$_2$	23	50	2.5	R
2	Cbz-Ala-His-OMe	3	80	0.1	S
3	Cbz-D-Ala-His-OMe	3	70	0.1	R
4	cyclo-(Ala-His)	47	50	9.9	R
5	cyclo-(D-Ala-His)	47	90	7.5	R
6	H-His-OH	7 days	60	5.1	S

Cbz, carbobenzoxy

Table 2. Asymmetric Addition of HCN to Benzaldehyde Catalyzed by cyclo-Phe-His
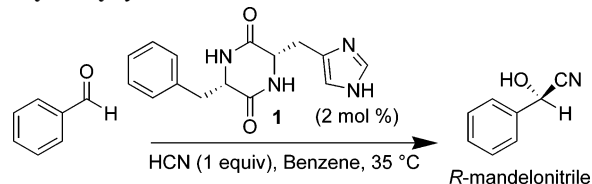
Entry	Time (h)	Conv. (%)	ee (%)
1	0.5	40	90
2	1	80	76
3	4	80	69
4	16	90	21
5	72	90	12

Monitoring the enantiomeric excess as a function of time allowed for an important developmental observation. In only 30 min, R-mandelonitrile could be obtained in an enantiomeric excess of 90% using diketopiperazine **1**, but it rapidly racemized over prolonged reaction times (Table 2).[6]

Two possible racemization mechanisms were proposed (Figure 2): base deprotonation of R-mandelonitrile, followed by the nonspecific protonation of the resulting anion (path A), or elimination of hydrogen cyanide to generate benzaldehyde, followed by nonspecific addition of hydrogen cyanide to benzaldehyde (path B).[7] Comparison of the relative rates for the cyanohydrin formation of benzaldehyde and butyraldehyde (Scheme 1) indicates that cyanohydrin **R-2b** forms significantly faster than **R-2a** ($k_{1a} \ll k_{1b}$). However, since the racemization of **R-2a** is faster than the racemization of **R-2b** ($k_{2a} \gg k_{2b}$), Inoue and co-workers conclude that anion stabilization from the aromatic ring indicates path A as the most reasonable mechanism of racemization.

Time, temperature, solvent, and mode of catalyst crystallization all play a significant role in an enantioselective reaction. Shorter reaction times allow for higher enantiose-

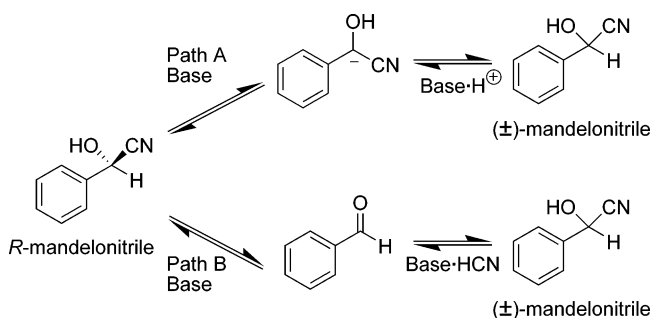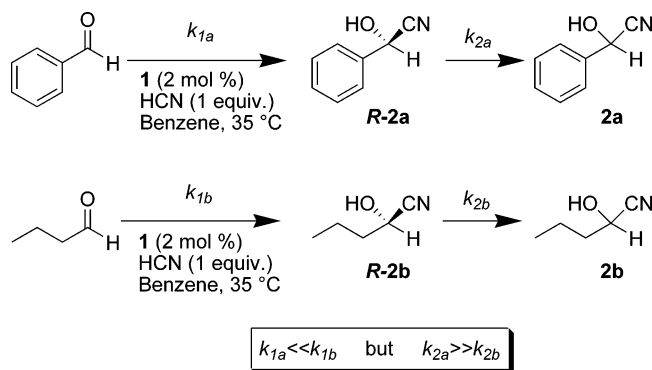**Figure 2.** Plausible mechanisms for the racemization of R-mandelonitrile.

Scheme 1. Rate Comparison for the Racemization of Cyanohydrins

$$k_{1a} \ll k_{1b} \quad \text{but} \quad k_{2a} \gg k_{2b}$$

Table 3. Asymmetric Addition of Hydrogen Cyanide to Aldehydes Catalyzed by *cyclo*-Phe-His and D-Oxynitrilase

Entry	Aldehyde	Time (min.)	Conv. (%)	ee (%) by 1	ee (%) by D-oxynitrilase
1	benzaldehyde	30	40	90	100
2	benzaldehyde	240	80	69	100
3	benzaldehyde (*p*-Me)	30	80	33	28
4	benzaldehyde (*m*-Me)	30	83	82	60
5	benzaldehyde (*o*-Me)	30	67	70	not reported
6	benzaldehyde (*m*-MeO)	30	71	54	51
7	benzaldehyde (*m*-PhO)	30	70	61	not reported
8	butyraldehyde	35	100	28	20
9	pentanal	40	100	43	31
10	*iso*-butyraldehyde	35	100	35	25
11	cyclohexane carboxaldehyde	15	100	25	not reported

lectivity at the expense of yield. In the case of butyraldehyde, lowering the temperature from 35 to −6 °C (toluene as solvent) increased the enantioselectivity from 19% ee to 40% ee.[8] Short reaction times demonstrated that *cyclo*-Phe-His (**1**) catalyzed the asymmetric addition of hydrogen cyanide to aldehydes with enantiomeric excesses comparable to those obtained from the enzyme D-oxynitrilase (Table 3).[8,9]

Nonpolar and aprotic solvents were important for achieving an efficient asymmetric reaction. Solvents with moderate polarity such as tetrahydrofuran, diethyl ether, and ethyl acetate afforded moderate reductions in both conversion and enantioselectivity, whereas use of the polar and protic solvent methanol led to eroded enantioselectivity. Conducting the reaction in toluene at −20 °C with 2 equiv of hydrogen cyanide allowed for improvement in the selectivity and substrate scope, as shown in Table 4.[10]

The purification method of *cyclo*-Phe-His (**1**) was found to be critical for maintaining an enantioselective reaction.[10] When catalyst **1** was purified using nonaqueous solvents, high catalytic activities and asymmetric induction were observed. On the contrary, when **1** was purified with solvents containing water, low enantioselectivities and catalytic activities were observed. This dichotomy was empirically supported by X-ray diffraction[10] and scanning electron microscope[11] studies of solid **1**. When **1** was crystallized and dried under different conditions, significant variances in the physical state were observed.

Table 4. Asymmetric Addition of Hydrogen Cyanide to Aldehydes Catalyzed by *cyclo*-Phe-His

Entry	Aldehyde	Time (h)	Conv. (%)	ee (%)
1	benzaldehyde	8	97	97
2	benzaldehyde (*p*-MeO)	10	57	78
3	benzaldehyde (*m*-MeO)	8	83	97
4	benzaldehyde (*o*-MeO)	10	45	84
5	benzaldehyde (*m*-PhO)	8	97	92
6	benzaldehyde (*m*-Me)	10	78	96
7	benzaldehyde (*p*-NO2)	2.5	99	53
8	benzaldehyde (*m*-NO2)	8	100	4
9	benzaldehyde (*p*-CN)	8	100	32
10	2-napthaldehyde	1.5	61	91
11	6-methoxy-2-napthaldehyde	6	88	73
12	furfural	8	60	42
13	nicotin-3-napthaldehyde	0.5	73	54
14	cyclohexanecarboxaldehyde	2.5	96	58
15	*iso*-butyraldehyde	5	79	71
16	*iso*-valeraldehyde	5	44	18
17	hexanal	8	90	56
18	pivaldehyde	5	60	58

Table 5. Influence of Thixotropy in Asymmetric Addition of Hydrogen Cyanide to *m*-Phenoxybenzaldehyde Catalyzed by *ent*-1

Entry	Rate of Stirring (rpm)	Yield (%)	ee (%)
1	150	97	74
2	200	97	86
3	250	97	92
4	300	97	92

Danda documented further nuances in the asymmetric addition of hydrogen cyanide to *m*-phenoxybenzaldehyde.[12] The reaction maintained a clear gel state when dipeptide catalyst ***ent*-1** was rapidly crystallized prior to use. The amorphous solid provided both high enantioselectivities and catalytic activities. When ***ent*-1** was prepared as a crystalline solid or needles, the state of the reaction was observed as a slightly opaque gel or a suspension. Under these conditions, the enantioselectivity and catalytic activities were significantly diminished. Monitoring the physical properties of the gelled reaction mixture showed that the viscosity decreased as a function of increased stirring rate, a property known as thixotropy. The influence of thixotropy on the enantioselectivity was demonstrated by showing that faster rates of stirring translated into increased enantioselectivities (Table 5).

On the basis of the effect of solvent and the knowledge that the acyclic systems were inferior for the addition of hydrogen cyanide to aldehydes, a hydrogen bond in the
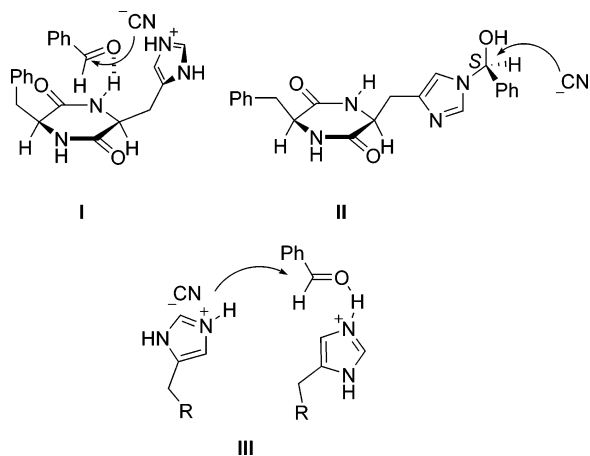
Figure 3. Proposed transition-state diagrams for the *cyclo*-Phe-His-catalyzed hydrocyanation of aldehydes.

Figure 4. Cyclic dipeptide catalysts for the asymmetric Strecker reaction.

transition state was hypothesized. Inoue and co-workers proposed transition state **I** (Figure 3), wherein cyanide adds preferentially to the *re* face of benzaldehyde.[10]

Danda[12] inaugurated mechanistic interest when he observed that the reaction exhibited asymmetric autocatalysis. When catalyst **1** (2% ee) was allowed to react under Inoue's optimized conditions, optically enriched cyanohydrin could be obtained in 82% ee if the reaction was doped with only 9 mol % of ring-substituted *R*-mandelonitrile at 92% ee. This suggested that *R*-mandelonitrile could either break down an aggregate of catalyst molecules or that *R*-mandelonitrile may be involved in the active catalyst.

In a related study by North and co-workers, hemiaminal intermediate **II** (Figure 3) was proposed.[13] Computational studies indicated that the *S* configuration at the aminal center was 5 kJ/mol more stable than the *R* configuration (Figure 3, **II**). S$_N$2 addition of cyanide to intermediate **II** yields *R*-mandelonitrile. Kim and Jackson found that immobilization of the *cyclo*-Tyr-His analogue of *cyclo*-Phe-His (**1**) on polystyrene or polysiloxane polymer provided a 10% enantiomeric excess. In contrast, *cyclo*-(MeO)Tyr-His allowed for 70% enantiomeric excess under the conditions investigated.[14] The studies using immobilized catalyst suggested that a second-order reaction may be responsible for the high enantiomeric excess. A detailed kinetic analysis by Shvo et al. provided the necessary evidence to conclude that the reaction was indeed second order in *cyclo*-Phe-His (**1**) (Figure 3, **III**).[11] Further studies into elucidating the details of the mechanism have been attempted using solution[15] and solid-state[16] NMR studies as well as computational studies.[15a,16] A significant obstacle remaining is the experimental complication related to the heterogeneous nature of the reaction, which makes the interpretation and comparison of experimental data difficult.

2.1.2. Cyclic Dipeptide-Catalyzed Asymmetric Strecker Reaction

The Strecker reaction has long been regarded as a means for the de novo synthesis of nonproteinogenic α-amino acids (See Figure 1).[1] Several methods for the synthesis of optically enriched α-aminonitriles, the precursors to α-amino acids in the Strecker synthesis, have been documented. These chemical technologies typically apply chiral auxiliaries[17] or asymmetric catalysts[18] as the source of chirality. The following discussion will be limited to metal-free peptidebased catalysts, keeping within the scope of this review. At the
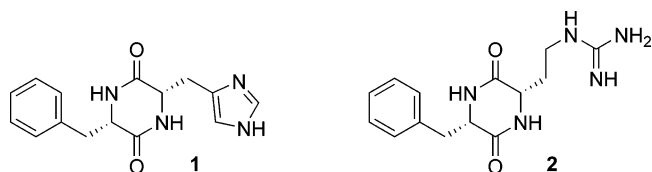
same time, a number of metal-free peptide-like catalysts have been found to be excellent catalysts for these processes.[19]

In 1996, Lipton and co-workers documented a study into the development of an asymmetric Strecker reaction using cyclic dipeptides as the source of chirality.[20] Given the mechanistic similarities to the addition of hydrogen cyanide to aldehydes (see section 2.1.1), Lipton took into consideration the design elements described by Inoue and co-workers. *cyclo*-Phe-His (**1**) failed to catalyze the Strecker reaction of benzaldehyde aldimine; presumably, the basicity of the histidine side chain was insufficient to accelerate proton transfer. Exchanging the imidazole side chain of **1** for the more basic guanidine catalyst **2** provided a competent catalyst for the Strecker reaction (Figure 4).

The asymmetric addition of hydrogen cyanide to benzaldehyde in the presence of ammonia provided the desired 2-aminophenylacetonitrile, which proved to be configurationally unstable, ultimately leading to the application of *N*-substituted imines as carbonyl surrogates. Preformed *N*-benzylhydrylimines could be converted to the corresponding α-aminonitriles using **2** as a catalyst in varying enantioselectivities (Table 6). Aromatic aldehydes generally provided high enantiomeric excesses, except in the cases of highly electron-deficient derivatives, which afford nearly racemic products. The question of whether racemization was occurring by an enolization mechanism, in analogy to that observed in the addition of hydrogen cyanide to benzaldehyde (see Figure 2), was investigated through an attempt to observe deuterium exchange. A lack of ^{1}H$-^2$H exchange suggested enolization is not operative in this case. However, the possibility of racemization through rapid and reversible addition of hydrogen cyanide could not be discounted.

Table 6. Conversion of *N*-Benzhydrylimines to α-Aminonitriles
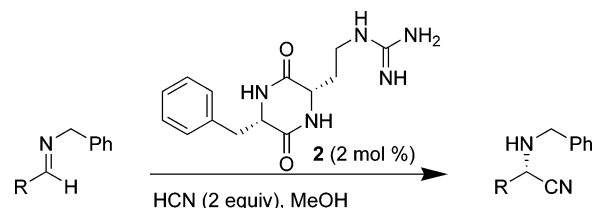
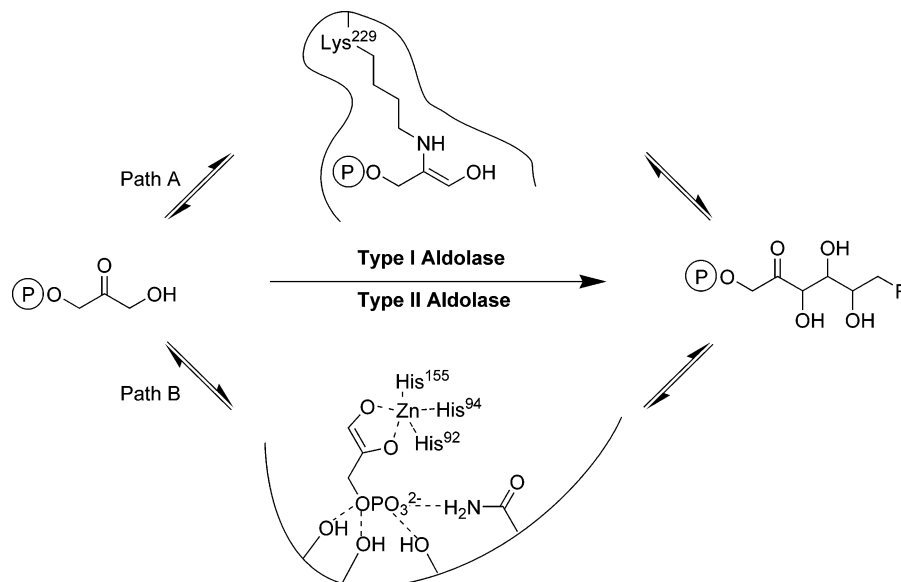| Entry	R=	Temp (°C)	Yield (%)	ee (%)
1	Ph	-25	97	>99
2	4-ClPh	-25	97	83
3	4-ClPh	-75	94	>99
4	4-OMePh	-25	96	64
5	4-OMePh	-75	90	96
6	3-ClPh	-75	80	>99
7	3-OMePh	-75	82	80
8	3-NO$_2$Ph	-75	71	<10
9	3-pyridyl	-75	86	<10
10	2-furyl	-75	94	32
11	*i*-Pr	-75	81	<10
12	*t*-Bu	-75	80	17

Figure 5. Mechanisms of Type I and Type II aldolases.

The arrow-pushing mechanisms for the *cyclo*-Phe-His (**1**) catalyzed asymmetric addition of hydrogen cyanide to aldehydes and the *cyclo*-Phe-(*S*)-α-amino-γ-guanidinobutyryl (**2**) catalyzed Strecker reaction appear to be similar. However, **1** and **2** mediate the formation of enantiomeric products, even though **1** and **2** are composed entirely of *S* amino acids. Inoue and Danda have clearly demonstrated that several factors (crystallization method, solvent viscosity, and asymmetric autocatalysis) can have a dramatic effect on the experimental results. The asymmetric Strecker reaction catalyzed by **2** operates as a homogeneous solution, which is in contrast to the amorphous gel required for the successful asymmetric addition of hydrogen cyanide to aldehydes. Recently, a subsequent investigation into the asymmetric Strecker reaction catalyzed by **2** has documented difficulties in the preparation of **2** in a form capable of yielding satisfactory levels of catalysis and enantioselectivity, even though the correct structure of **2** was unambiguously determined by single-crystal X-ray diffraction analysis of the hydronitrate salt.[21] Further investigation into factors such as the method of crystallization, which proved critical for the *cyclo*-Phe-His (**1**) catalyzed asymmetric addition of hydrogen cyanide to aldehydes, may prove valuable in expanding our understanding of this technology and guide further applications.

2.2. Aldol Reaction

The aldol reaction combines an enolate (or an enolate equivalent) and either an aldehyde or a ketone to yield a β-hydroxycarbonyl compound. This powerful methodology has been applied to countless accounts of natural-product synthesis and has been a popular area for the development of metal-catalyzed chemical technologies. Nature has provided outstanding examples of the versatility of this reaction with Type I and Type II aldolases (Figure 5).[22] The Type I aldolase is an enzyme with a functional primary amine component in the hydrophobic active site (path A), while the Type II employs a coordinated zinc(II) ion (path B). The Type I aldolase, which proceeds through an enamine, has inspired synthetic chemists to delve into the possibility of miniaturizing these enzymes to short peptides. Several approaches have served as platforms for future investigations. Both the development and implementation of a high-

throughput method to identify catalysts, as well as the construction of rationally designed catalysts possessing a terminal amine, have led to the documentation of effective catalysts.

2.2.1. Aldol Reaction Catalyzed by N-Terminal Prolyl Peptides

The proteinogenic amino acid proline has received an enormous amount of attention in the literature because of the reactive enamine associated with the secondary amine.[23] Not surprisingly, proline has been installed as a reactive residue in peptide-catalyzed reactions. The amidation of the carboxyl group of proline has been shown to be incompatible with catalysis of the asymmetric aldol reaction, and this may have slowed the initial investigations of peptide chemists.[24]

One of the first examples of a peptide-catalyzed aldol reaction was documented by Reymond and co-workers in 2003.[25] In this initial communication, Reymond and co-workers examined several different classes of peptides as potential catalysts (Figure 6). Classes IA and IB both involve primary amines, with Class IA containing a quaternary ammonium salt to lower the pK_a of the amine to p$K_a = 7$, as seen in Type I aldolases. Both Classes IIA and IIB contain

Class I-A
-primary amine
-quaternary amonium salt

Class I-B
-primary amine

Class II-A
-secondary amine
-free carboxyl

Class II-B
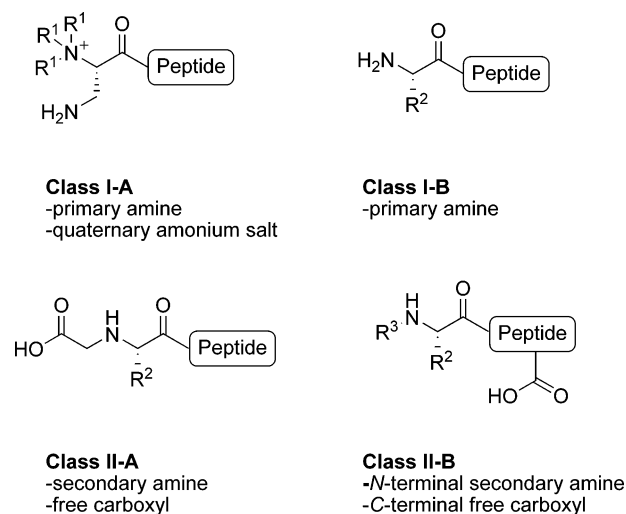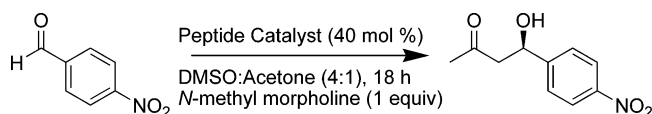-*N*-terminal secondary amine
-*C*-terminal free carboxyl

Figure 6. Design of potential peptide catalysts.

Table 7. Direct Asymmetric Aldol Reaction between Acetone and *p*-Nitrobenzaldehyde Catalyzed by Simple Peptides and Derivatives


Entry	Class	Peptide	Conv. (%)	ee (%)
1	I-A	5 Peptides, R^1 = Me	<5	-
2	I-B	3 Peptides, R^2 = Ser, Phe or Leu	<5	-
3	II-A	2 Peptides, R^2 = Pro, or C_6H_{11}	<5	-
4	II-B	H-Pro-Leu-NH$_2$	<5	-
5	II-B	H-Pro-Leu-OH	<5	-
6	II-B	H-Pro-Asp-NH$_2$	39	<5
7	II-B	H-Pro-Gly-OH	99	46
8	II-B	H-Pro-Glu-Leu-Phe-OH	96	66
9	II-B	H-Pro-Aib-Glu-Phe-OH	94	37
10	II-B	H-Pro-Asp-Leu-Phe-OH	95	50
11	II-B	H-Pro-Aib-Asp-Phe-OH	97	12

Aib, α-aminoisobutyric acid

Table 8. Peptide-Catalyzed Aldol Reactions
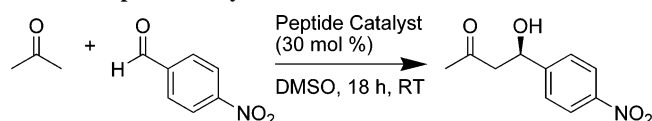
Entry	Peptide	Yield (%)	ee (%)
1	H-Pro-OH	68	76
2	H-Pro-Ala-OH	90	70
3	H-Pro-Trp-OH	77	65
4	H-Pro-Asp-OH	75	74
5	H-Pro-Glu-OH	72	68
6	H-Pro-Val-OH	89	70
7	H-Pro-Arg-OH	91	31
8	H-Pro-Ser-OH	87	77
9	H-Pro-Lys-OH·HCl	62	66
10	H-Pro-Gly-Gly-OH	68	53
11	H-Pro-His-Ala-OH	85	56

secondary amines but differ in the location within the peptide sequence. In a Class IIA peptide, the secondary amine is located within the peptide chain, and the Class IIB peptides display *N*-terminal prolines as the secondary amine component. Reymond and co-workers's Class II peptides also incorporate free carboxyl groups based on the observed necessity for the carboxyl in proline-catalyzed aldol reactions.[24] After comparing Classes IA, IB, IIA, and IIB peptides for the aldol reaction of acetone and *p*-nitrobenzaldehyde (Table 7), it was observed that Class IA (entry 1), Class IB (entry 2), and Class IIA (entry 3) all demonstrated low reactivity. *N*-Terminal prolyl peptides (Class IIB) emerged as the superior class of catalysts for the conditions investigated. High conversions to the desired aldol adduct and asymmetric induction up to 66% enantiomeric excess (entries 6−11) were observed.

In a publication appearing soon after Reymond's initial work, Martin and List showed that *N*-terminal prolyl peptides could be competent aldol-promoting catalysts.[26] In a study of di- and tripeptide-catalyzed aldol reactions of acetone with *p*-nitrobenzaldehyde, Martin and List illustrated that dipeptides (Table 8, entries 2−9) and tripeptides (entries 10 and 11) could perform equally well if not better than proline (entry 1).

**Table 9. Direct Aldol Reactions of Acetone with Aldehydes by Peptide Catalyst 3 or 4**
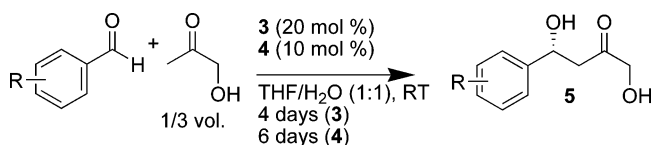
Entry	Aldehyde	Catalyst	Yield (%)	ee (%)
1	4-NO$_2$	3	82	82
2		4	76	87
3	4-CN	3	88	84
4		4	70	84
5	4-CF$_3$	3	82	86
6		4	66	88
7	3-NO$_2$	3	82	85
8		4	80	89
9	3,5-Br$_2$	3	68	91
10		4	59	92[a]
11	2-Cl	3	78	85
12		4	56	86
13	2-NO$_2$	3	83	91
14		4	71	93
15	2,6-Cl$_2$	3	84	96
16		4	73	96

[a] THF/H$_2$O (2:1).
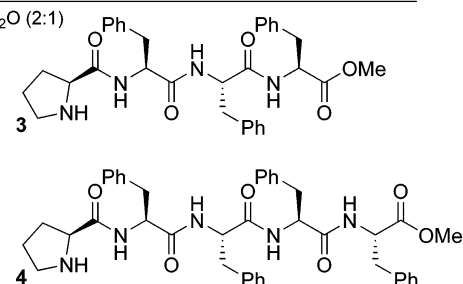
The *N*-terminal prolyl peptide-catalyzed aldol reaction has been studied in the context of simultaneously controlling regioisomeric/enantiomeric excesses. Gong and co-workers investigated a series of *N*-terminal prolyl peptides as catalysts for the reaction of electron-deficient aromatic aldehydes with hydroxyacetone.[27] Tetra- and pentapeptides **3** and **4** showed great promise in controlling the formation of regioisomer **5** as the major isolated product (Table 9). It is noteworthy that the major product in the analogous reaction catalyzed by L-proline[28] or aldolase[22] is the alternative regioisomer (not pictured). With a mixture of tetrahydrofuran and water as the best solvent system, up to 96% enantiomeric excess could be obtained with a simple peptide containing only L-proline and L-phenylalanine.

The possibility that micelles might accelerate the peptide-catalyzed aldol reaction was the focus of Li and co-workers.[29,30] H-Pro-Phe-OH catalyzed the aldol reaction of aromatic (Table 10, entries 1−7) and aliphatic aldehydes (entries 8 and 9) with almost equal efficiencies and asymmetric inductions. Replacing acetone with cyclohexanone (entry 10) allowed for complete conversion to the *anti*-isomer as the only observable isomer with >99% enantiomeric excess. H-Pro-Phe-OH could also be easily precipitated with aqueous ammonium chloride after the reaction was complete and reused for three additional rounds with no apparent change in reactivity or selectivity.

Peptides that contain several hydrophobic residues can be operationally troublesome in aqueous solvent mixtures

Table 10. Substrate Screen for the Aldol Reaction between Acetone and Aldehydes Catalyzed by H-Pro-Phe-OH
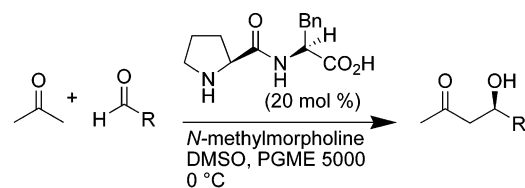
Entry	R	Time (h)	Yield (%)	ee (%)
1	4-Nitrophenyl	24	96	73
2	Phenyl	36	62	64
3	3-Nitrophenyl	24	84	67
4	2-Nitro-3,4-methyl-enedioxyphenyl	28	80	83
5	2-Chlorophenyl	30	81	55
6	3,4-Dichlorophenyl	32	72	61
7	2-Methoxyphenyl	36	70	53
8	i-Propyl	48	92	77
9	Cyclohexanyl	48	80	79
10[a]	2-Nitrophenyl	24	90	>99

[a] Cyclohexanone instead of acetone, nearly 100% *anti* conformation.

Table 11. Aldol Reactions between Acetone and Aldehydes with a Solid-Supported Catalyst
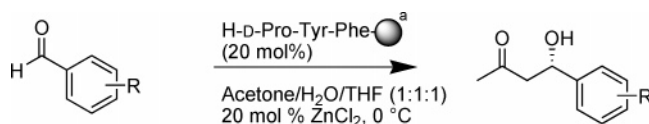
Entry	Aldehyde (R =)	Time (h)	Yield (%)	ee (%)
1	2-NO$_2$	18	89	84
2	3-NO$_2$	24	83	76
3	4-Cl	30	50	72
4	2-Cl	30	93	74
5	4-OMe	N.R.	N.R.	N.R.
6	4-NO$_2$ (1st use of cat.)	20	100	71
7	(1st reuse of cat.)	20	99	73
8	(2nd reuse of cat.)	20	92	75
9	(3rd reuse of cat.)	20	96	74
10	(4th reuse of cat.)	20	96	71

[a] The symbol ⬤ denotes amino group terminated PEG-PS resin.

because of their tendencies toward aggregation or sedimentation. One possible solution is to run the reaction at high dilution to solubilize the peptide. However, dilution does have the inherent problem of slowing reaction rates for bimolecular reactions. Immobilizing peptides on an amphiphilic resin such as poly(ethylene glycol) grafted on cross-linked polystyrene (PEG-PS) allows reactions to be run at higher concentration and prevents aggregation or sedimentation. Kudo and co-workers have studied *N*-terminal prolyl peptides immobilized on PEG-PS as catalysts for the aldol reaction.[31] The peptide catalyst H-D-Pro-Tyr-Phe-(PEG-PS) in the presence of ZnCl$_2$ as an additive could effect the aldol reaction of acetone with several electron-deficient aromatic aldehydes (Table 11, entries 1−4). Aromatic aldehydes containing an electron donating group were unreactive (entry 5). Additionally, H-D-Pro-Tyr-Phe-(PEG-PS) could be easily recovered by simple filtration and reused with minimal loss in reactivity. The use of additional ZnCl$_2$ improved catalyst recycling.

The apparent requirement of an acidic proton in the *N*-terminal prolyl peptide-catalyzed aldol reaction adds an
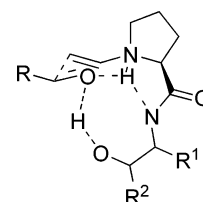
Figure 7. Zimmerman−Traxler-like transition state in the hydroxyproline amide-catalyzed aldol reaction.

Table 12. Catalysis of *p*-Nitrobenzaldehyde and Acetone by H-Pro-Ser-NH-TG
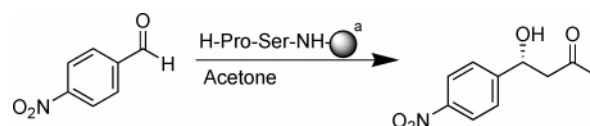
Entry	Solvent	Temp (°C)	Time (h)	Conv. (%)	ee (%)
1	Acetone:H$_2$O (1:1)	20	16	Quant.	22
2	DMSO:Acetone (4:1)	20	16	70	59
3	DMF:Acetone (4:1)	20	16	<10[a]	39
4	CH$_2$Cl$_2$:Acetone (4:1)	20	16	<4	N.D.
5	Acetone	-15	72	>98	71
6	Acetone	-25	41	>98	82
7	Acetone	-45	48	35	68

[a] The symbol ⬤ denotes Novasyn TG resin.

additional challenge to developing catalysts immobilized on solid phase. However, Gong, Wu, and co-workers have demonstrated that, in specific cases, catalysis can be accomplished in the absence of a carboxyl group. With an appropriately placed alcohol, modified single amino acids were shown to effect an enantioselective aldol reaction.[32] Presumably, a hydrogen bond with the alcohol and the amide N−H reinforces the Zimmerman−Traxler-like transition state and restores the catalytic activity (Figure 7). Andreae and Davis showed that this hypothesis holds true for *N*-terminal prolyl peptides.[33] Specifically, the *N*-terminal proline could be attached to either a serine or threonine residue to reinstate the catalytic activity of the proline amide peptide. Examining H-Pro-Ser-TG immobilized on Novasyn TentaGel resin for the aldol reaction of *p*-nitrobenzaldehyde in various solvents, they showed that, in neat acetone at −25 °C, H-Pro-Ser-TG affords >98% conversion to the desired aldol product in 82% enantiomeric excess (Table 12, entry 6).

Polymer-supported catalysts not only have a straightforward operational advantage of solubility and ease of reuse but also have the ability to be easily amended to on-bead high-throughput screening technologies. Wennemers and co-workers have developed a strategy for the rapid identification of bimolecular reactions.[34] This chemical technology employs a peptide catalyst immobilized on resin that is linked via a spacer to one reactant. The other reactant for the bimolecular reaction would incorporate a colored or fluorescent tag to allow for easy identification of a "hit" catalyst (Figure 8).

Wennemers and co-workers applied their "catalyst−substrate coimmobilization strategy" to the development of an *N*-terminal prolyl peptide-catalyzed aldol reaction of acetone and aldehydes.[35] By preparing a split-and-mix library of tripeptides at one end of a bifunctional lysine linker and a ketone at the other end, the library could be immobilized on TentaGel resin (Figure 9). With only 15 different D- and L-amino acids in each of the three positions, a library consisting of a maximum of 15^3 = 3375 tripeptides was
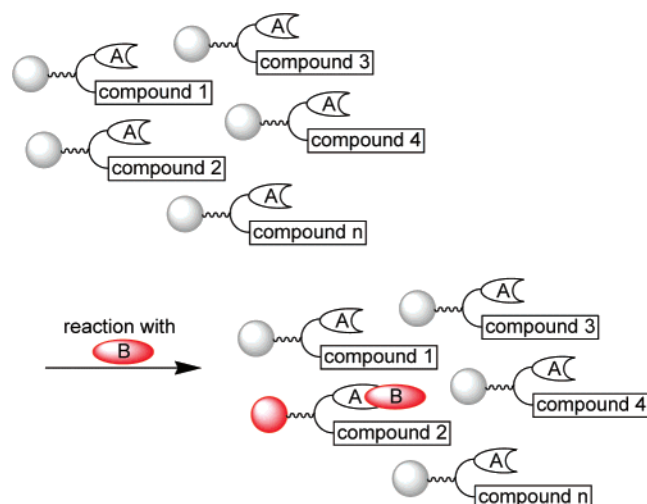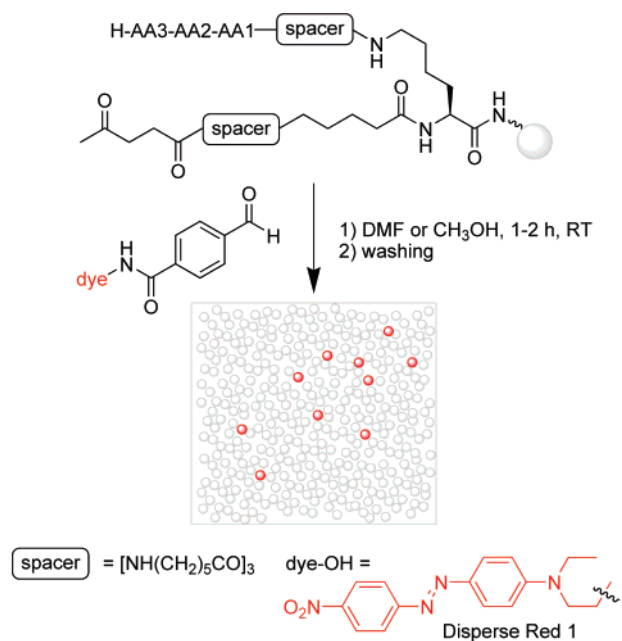
Figure 8. Catalyst−substrate co-immobilization strategy.

AA1 and AA3 = Gly, D-Val, Ala, Leu, D-Pro, Pro, D-Phe, Tyr, D-His, His, D-Arg, D-Asp, Glu, D-Asn, Gln; AA2 = Gly, Val, D-Ala, D-Leu, D-Pro, Pro, Phe, D-Tyr, D-His, His, Arg, Asp, D-Glu, Asn, D-Gln

Figure 9. Substrate−catalyst co-immobilization for the discovery of peptides as aldol catalysts.

synthesized. The library was reacted with dye-marked benzaldehyde at ambient temperature for only 1−2 h, followed by extensive washing to remove all noncovalently bonded dyed compounds. Analysis by ocular inspection indicated ∼1 out of 100 beads with a distinct red color, which revealed two main sequences [H-Pro-D-Ala-D-Asp-NH-TG (**6**) and H-Pro−Pro-Asp-NH-TG (**7**)]. It is noteworthy that switching to the alternate strategy of immobilizing the aldehyde and reacting with a dye-marked ketone was also effective in identifying similar catalysts.[36]

Using solid-phase peptide synthesis, peptide catalysts **6** and **7** were resynthesized and examined in solution. Peptide catalysts **6** and **7**, for the aldol reaction of acetone and *p*-nitrobenzaldehyde, demonstrate two important highlights. Each catalyzed the formation of enantiomeric aldol products even though both *N*-terminal proline residues were of the same absolute configuration. Additionally, peptide **7** catalyzes the formation of the aldol product in 99% yield and

Table 13. Aldol Reactions Catalyzed by Peptides 6 and 7

Entry	R	10 mol % **6**		1 mol % **7**		30 mol % H-Pro-OH	
		Yield (%)	ee (%)	Yield (%)	ee (%)	Yield (%)	ee (%)
1	4-NO$_2$Ph	73	70 (*R*)	99	80 (*S*)	68	76 (*R*)
2	Ph	58	66 (*R*)	69	78 (*S*)	62	60 (*R*)
3	*c*-Hex	56	83 *(R)*	66	82 (*S*)	63	84 *(R)*
4	*i*-Pr	75	91 (*R*)	79	79 (*S*)	97	96 (*R*)
5	*neo*-Pent	24	70 (*S*)	28	73 (*R*)	22	36 (*S*)

80% ee, employing only 1 mol % catalyst at room temperature in only 4 h! Comparing catalysts **6** and **7** against the single amino acid proline (Table 13) demonstrates that both peptides provide similar results to proline (entries 3 and 4) or better results (entries 1, 2, and 5) with at least one of the two peptides.

The *N*-terminal prolyl peptide H-Pro-Pro-Asp-NH-TG (**7-TG**), discovered by Wennemers and co-workers, is the most reactive and provides enantioselectivities comparable to the highest reported for a peptide-catalyzed aldol reaction to date. Further studies were performed to increase the operational convenience by studying the effects of several different polymer supported versions of H-Pro-Pro-Asp-NH-TG (**7-TG**), as well as the effect of loading of catalyst **7-TG**.[37] Comparison of several resins (polystyrene, SPAR, TentaGel, and PEGA) revealed TentaGel and PEGA as the optimal solid supports for maintaining the reactivity and selectivity. Furthermore, lowering the catalyst loading on solid support (TentaGel and PEGA) increased the rate of the reaction. At catalyst loadings ranging between 0.1 and 0.2 mmol g^{-1}, an ideal compromise is reached between catalysis and diffusion of starting materials and products into and out of the resin. It was then shown that catalyst **7-TG** could be reused three times without any significant loss in catalytic activity or selectivity.

A further extension was then shown when catalyst **7** was pegylated to provide solubility in a broad range of common solvents such as CH$_2$Cl$_2$, CHCl$_3$, tetrahydrofuran (THF), dioxane, acetone, DMSO, and H$_2$O.[37] The pegylated catalyst H-Pro-Pro-Asp-Ahx-NH(CH$_2$CH$_2$O)$_3$-CH$_3$ (**7-Peg**) provides enhanced solubility and reactivity. Using only 0.5 mol % of pegylated peptide **7-Peg** at −20 °C catalyzes the aldol reaction in 95% yield and 91% enantiomeric excess in only 8 h (entry 4, Table 14).

In a study directed at the discovery of peptide dendrimers as aldolase mimics, Reymond and co-workers employed on-

Table 14. Comparison of the Catalytic Activity of the Pegylated Catalyst 7-Peg with That of 7

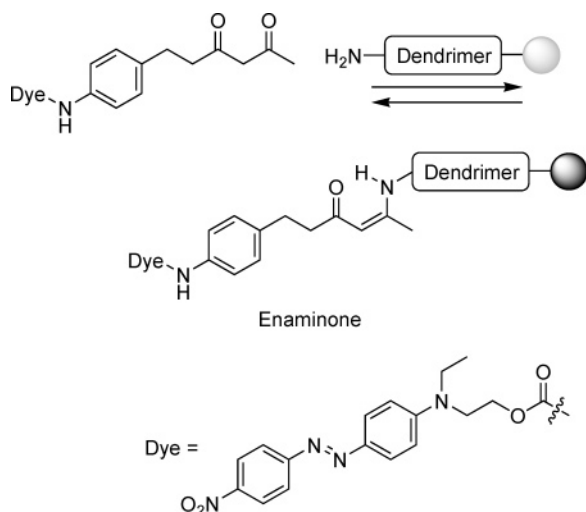| Entry	Catalyst	mol % Peptide Catalyst	Temp (°C)	Time (h)	Yield (%)	ee (%)
1	**7-Peg**	1	RT	1	94	80
2	**7-Peg**	0.5	RT	4	93	80
3	**7-Peg**	1	-20	4	96	91
4	**7-Peg**	0.5	-20	8	95	91
5	**7**	1	RT	4	99	80
6	**7**	5	-20	24	98	91

Figure 10. Enaminone aldolase probe.

bead probes specific for aldolase active residues.[38] Two different categories of probes were successfully applied to the identification of active peptide dendrimers for the asymmetric aldol reaction. The first probe was a dye-labeled 1,3-diketone, which, upon condensation with an amine, forms an enaminone, which is easily identified by color (Figure 10). Mixing the beads of the library of dendrimers with a solution of the diketone probe for a 30 min incubation time produced ~0.1% staining per batch. Sequencing revealed that the stained beads contained dendrimers with 1−3 lysine residues, consistent with enaminone formation.

The second successful strategy applied toward the identification of a proficient peptide dendrimer catalyst was a fluorogenic enolization probe. As depicted in Figure 11, condensation of an amine, followed by enolization, will allow for β-elimination of the fluorescent product umbelliferone.

Suspending the beads with a freshly prepared solution of enolization probe for 40 min followed by plating onto a silica gel plate allowed each bead to be well-separated from the others as a free-standing reactor. Segregation of the beads on the silica gel plate ensured that umbelliferone could not diffuse away. Fluorescence analysis, as well as subsequent sequencing of the active beads, revealed that the majority of the active beads contained N-terminal proline residues. From this series of compounds, dendrimer **8** was identified as a catalyst for the aldol reaction of acetone and p-nitrobenzaldehyde, providing 69% conversion and 61% enantiomeric excess in 36 h (Table 15, entry 1). In an aqueous environment, dendrimer **8** displays a dramatic rate increase for the aldol reaction, consistent with aldolase behavior, affording >99% conversion in only 3 h (entry 2).
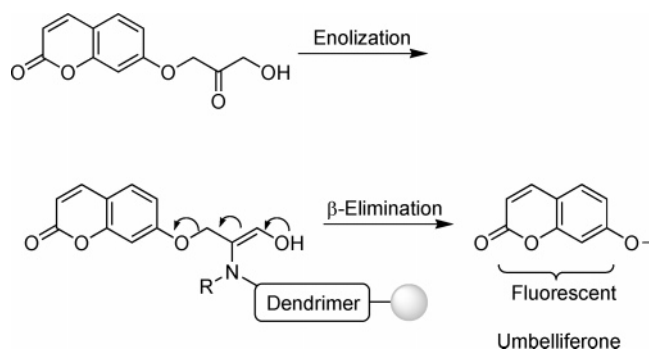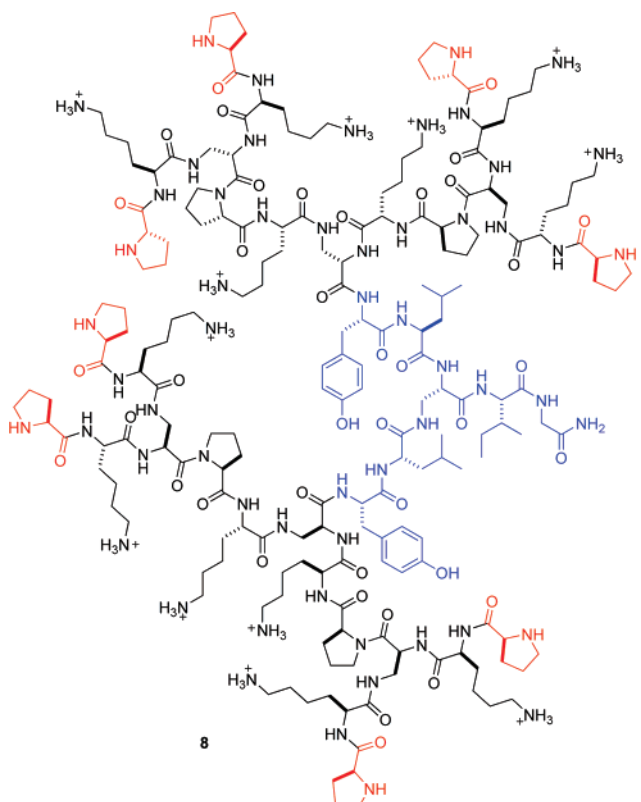

Figure 11. Enolization aldolase probe.

Table 15. Dendrimer-Catalyzed Aldol Reaction

Entry	Solvent	Time (h)	Conv. (%)	ee (%)
1	DMSO-acetone (4:1)	36	69	61
2	aq. buffer-acetone (1:1)	3	>99	<5

The majority of N-terminal prolyl peptide-catalyzed asymmetric aldol reactions employ an aldehyde as the electrophilic partner. Tomasini and co-workers have shown that ketones are also viable electrophiles for the peptide-catalyzed aldol reaction.[39] After examining several dipeptides, H-D-Pro-β^3-hPhg-OBn was shown to catalyze the asymmetric aldol reaction of acetone and isatin in quantitative yield and 73% enantiomeric excess (Table 16, entry 1). The asymmetric aldol reaction was tolerant to various N-substitutions (entries 2−4), as well as an electron-withdrawing group on the aryl ring (entry 5).

2.2.2. Aldol Reaction Catalyzed by N-Terminal Primary Amino Peptides

The application of N-terminal prolyl peptides has indeed proven to be a fertile ground for the development of peptide-catalyzed asymmetric aldol reactions. The ability to apply primary amino acid derivatives to peptide-catalyzed aldol reactions would provide a further level of diversity and modularity to catalyst development. Although some may consider proline to be *special*, it is not uniquely equipped to perform reactions that proceed via an enamine intermediate.

The initial interest of Tsogoeva and Wei in the aldol reaction began with peptides containing histidine as a potential catalyst. Early investigations into the aldol reaction began with an examination of the acetone/p-nitrobenzalde-hyde aldol reaction mediated by a dipeptide.[40] The peptide

**Table 16. Aldol Reaction of Isatin Derivatives with Acetone-Catalyzed by H-D-Pro-β^3-hPhg-OBn**
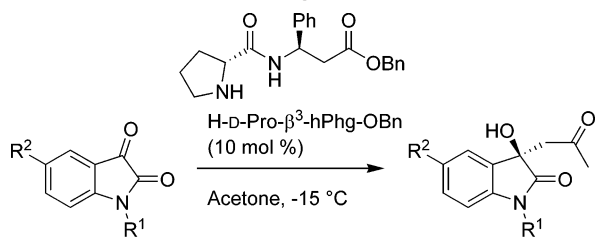
Entry	R^1	R^2	Time (h)	Yield (%)	ee (%)	Abs. Config.
1	H	H	16	quantative	73	R
2	Me	H	17	quantative	77	R
3	Et	H	16	92	74	R
4	Bn	H	17	90	74	R
5	H	Br	17	quantative	73	R

Table 17. Aldol Reactions of Acetone with Several Aromatic Aldehydes Catalyzed by H-Leu-His-OH
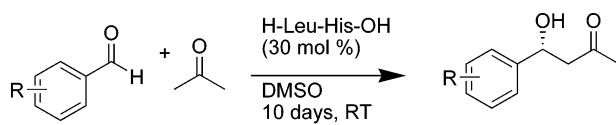
Entry	Aldehyde	Conv. (%)	Yield (%)	ee (%)
1	4-NO$_2$	96	87	71
2	2-NO$_2$	82	62	72
3	2-Cl	100	96	76
4	4-Br	89	65	68
5	4-Cl	94	67	60
6	2-Naphthaldehyde	65	53	50

design contained two amino acid residues (His, Phe, Leu, or Lys), with both free *C*- and *N*-termini providing superior results to methyl ester, Cbz-protected *N*-terminus, and *cyclo*-dipeptides. Of the peptides investigated, H-Leu-His-OH was determined to be optimal and was demonstrated to afford comparable levels of selectivity for several electron-poor aromatic aldehydes (Table 17). Additionally, an examination of a series of cocatalysts revealed that *trans*-2,5-dimethylpiperazine (10 mol %) could decrease the reaction time from 10 days to 22 h with only a moderate sacrifice in asymmetric induction.[40]

Córdova and co-workers have documented studies concerning the aldol reaction of primarily cyclic ketones and aldehydes.[41] Peptides based on the simple amino acids alanine and valine were investigated for their ability to catalyze the reaction of cyclohexanone and *p*-nitrobenzaldehyde. It was found that the use of water as an additive (5−20 equiv) was necessary to obtain the highest levels of enantioselectivity. H-Ala-Ala-OH and H-Ala-Phe-OH were found to be competent catalysts for mediating the aldol reaction of cyclic ketones with high chemo-, diastereo-, and enantioselectivity (Table 18). When using hydroxyacetone as the aldol donor, the *vic*-diol was obtained as the exclusive regioisomer. The exclusivity of hydroxyacetone is complementary to the results observed by Gong and co-workers when studying *N*-terminal prolyl peptides as catalysts (c.f., Table 9).[27] On the basis of the relative and absolute stereochemistry of the aldol products observed, Córdova and

Table 18. Peptide- and Peptide Analogue-Catalyzed Direct Asymmetric Aldol Reactions
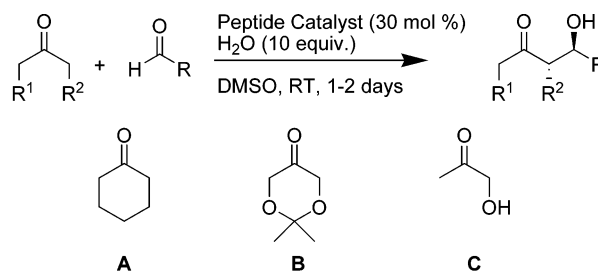
Entry	Catalyst	Ketone	R	Yield (%)	D.R.[b]	ee (%)
1	H-Ala-Ala-OH	A	4-NO$_2$C$_6$H$_4$	73	8 : 1	91
2	H-Ala-Ala-OH	B	4-NO$_2$C$_6$H$_4$	70	3 : 1	99
3	H-Ala-Phe-OH	B	4-NO$_2$C$_6$H$_4$	88	5 : 1	99
4	H-Val-D-phenylalaninol	B	4-NO$_2$C$_6$H$_4$	80	4 : 1	99
5[a]	H-Ala-Ala-OH	B	4-CNC$_6$H$_4$	65	13 : 1	99
6[a]	H-Ala-Ala-OH	B	4-BrC$_6$H$_4$	55	2 : 1	92
7[a]	H-Ala-Phe-OH	A	4-BrC$_6$H$_4$	88	2 : 1	99
8[a]	H-Ala-Ala-OH	A	4-BrC$_6$H$_4$	86	2 : 1	96
9[a]	H-Ala-Ala-OH	A	4-ClC$_6$H$_4$	67	2 : 1	98
10[a]	H-Ala-Ala-OH	B	*i*-Pr	50	2 : 1	97
11	H-Ala-Ala-OH	C	4-NO$_2$C$_6$H$_4$	93	1 : 1	75

[a] 5 equiv H$_2$O. [b] *anti : syn*

co-workers proposed the possibility of chairlike transition states **IV** and **V** for both the peptide-catalyzed and the amino acid amide-catalyzed aldol reactions, respectively (Figure 12).

Using water as the main constituent of the reaction mixture for the dipeptide-catalyzed aldol reaction was the focus of a subsequent study by Córdova and co-workers.[42] As with their previous study, peptides were shown to outperform the single amino acid for the aldol reaction of cyclic ketones with aromatic aldehydes. Using density functional theory (DFT) calculations to decipher the mechanistic subtleties suggested that a dipeptide transition state **VI** (Figure 13) more efficiently shielded water from breaking down the six-membered transition state. The analogous single amino acid transition state (**VII**) could not efficiently stabilize the resulting alkoxide, making the single amino acid less enantioselective.
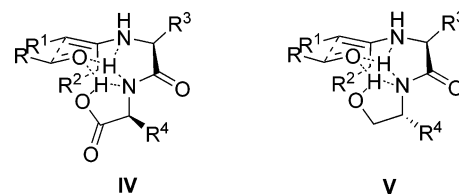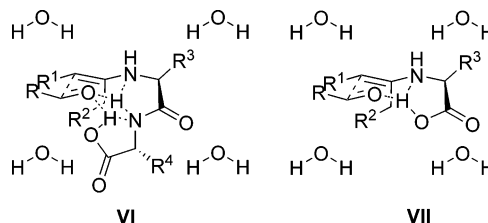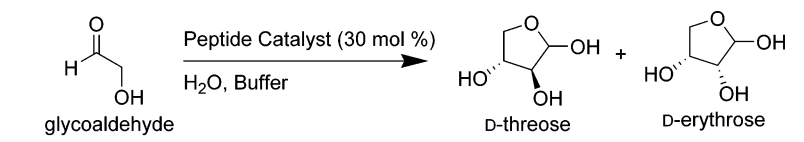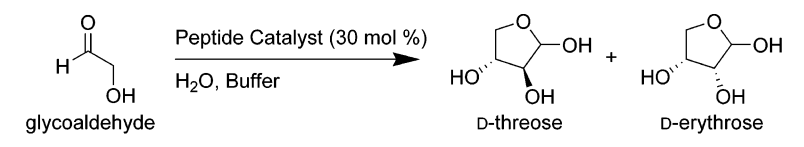
Figure 12. Plausible transition states IV and V for the dipeptide- and amino acid amide-catalyzed direct asymmetric aldol reaction.

Figure 13. Plausible transition states VI and VII for the dipeptide and primary amino acid-catalyzed asymmetric aldol reactions in water.

Table 19. Stereospecific Synthesis of Tetroses by the Condensation of Glycoaldehyde Using Dipeptide Catalysts Containing a β-Branched Amino Acid

| Entry	Peptide Catalyst	Temp, °C (time, h)	Buffer	pH	D-thr ee (%)	D-ery ee (%)	Yield (%) thr + ery	ery/thr
1	H-Val-Gly-OH	50 (3)	0.25 M TEAA	5.4	2	-11	50	1
2	H-Gly-Val-OH	50 (3)	0.25 M TEAA	5.4	2	53	20	1.2
3	H-Gly-Ile-OH	50 (3)	0.25 M TEAA	5.4	3	53	15	1.5
4	H-Ala-Val-OH	50 (3)	0.25 M TEAA	5.4	0	40	17	1.2
5	H-Ala-Ile-OH	50 (3)	0.25 M TEAA	5.4	2	38	5	1
6	H-Val-Val-OH	50 (3)	0.25 M TEAA	5.4	-1	59	25	1
7	H-Ile-Val-OH	50 (3)	0.25 M TEAA	5.4	-1	61	25	1
8	H-Val-Val-OH	50 (3)	0.05 M TEAA	5.4	-2	75	22	1
9	H-Val-Val-OH	25 (18)	0.25 M TEAA	5.4	-1	72	5	1.5
10	H-Val-Val-OH	25 (18)	0.05 M NaAc	5.4	-7	80	23	1.5
11	H-Val-Val-OH	25 (18)	0.05 M CaAc	5.4	-10	78.5	20	1.5
12	H-Val-Val-OH	25 (18)	0.05 M NaAc	4.9	-1	82	12	1.5
13	H-Val-Val-OH	0 (32)	0.05 M NaAc	5.4	1.5	13	29	1.7

Table 20. Stereospecific Synthesis of Tetroses by the Condensation of Glycoaldehyde Using Dipeptide Catalysts without a β-Branched Amino Acid

Entry	Peptide Catalyst	Temp, °C (time, h)	Buffer	pH	D-thr ee (%)	D-ery ee (%)	Yield (%) thr + ery	ery/thr
1	H-Ala-Gly-OH	50 (3)	0.25 M TEAA	5.4	-16	2	50	1
2	H-Ala-Gly-Gly-OH	50 (3)	0.25 M TEAA	5.4	-16	-3	15	1
3	H-Phe-Gly-OH	50 (3)	0.25 M TEAA	5.4	-5	7	63	1
4	H-Gly-Pro-OH	50 (3)	0.25 M TEAA	5.4	0	0	17	0.8
5	H-Gly-Ala-OH	50 (3)	0.25 M TEAA	5.4	0	43	10	1.8
6	H-Ala-Ala-OH	50 (3)	0.25 M TEAA	5.4	-7	33	45	1.5
7	H-Ala-Ala-OH	50 (1.5)	0.25 M TEAA	5.4	-9	33	10	2
8	H-Ala-Ala-OH	0 (96)	0.25 M TEAA	5.4	0	0	50	0.8
9	H-Tri-Ala-OH	50 (3)	0.25 M TEAA	5.4	-13	22	17	0.8
10	H-Tetra-Ala-OH	50 (3)	0.25 M TEAA	5.4	-12	17	5	1.2
11	H-Leu-Ala-OH	50 (3)	0.25 M TEAA	5.4	-4	35	38	1
12	H-Ala-Phe-OH	50 (3)	0.25 M TEAA	5.4	1	31	5	1
13	H-Ala-Glu-OH	50 (3)	0.25 M TEAA	5.4	32	32	11	1
14	H-Ala-Leu-Ala-OH	50 (3)	0.25 M TEAA	5.4	-13	33	13	1
15	H-Ala-His-OH	50 (3)	0.25 M TEAA	5.4	ND	ND	Trace	ND
16	H-D-Ala-Ala-Ala-OH	50 (3)	0.25 M TEAA	5.4	9	7	15	1.2
17	H-Ala-Ala-OH	50 (3)	0.05 M NaAc	5.4	-4	17	34	1
18	H-D-Ala-D-Ala-OH	50 (3)	0.05 M NaAc	5.4	2	-13	60	0.8
19	H-D-Ala-D-Ala-OH	25 (18)	0.05 M NaAc	5.4	0.5	-11	34	1.2
20	H-Glu-Glu-OH	50 (3)	0.25 M TEAA	5.4	-1.5	34	34	1.2
21	H-Leu-Leu-OH	50 (3)	0.25 M TEAA	5.4	0	0	<5	1
22	H–β-Ala-Ala-OH	50 (3)	0.25 M TEAA	5.4	0	10	25	1
23	Ac-(Ala)₃-OH	50 (3)	0.25 M TEAA	5.4	ND	ND	None	ND

The asymmetric induction by simple ancient building blocks is of intense interest in trying to understand a prebiotic scenario on Earth. Pizzarello and Weber have been studying how simple ancient amino acids[43] and peptides[44] can catalyze the dimerization of glycoaldehyde to D-erythrose and D-threose. The peptidic investigation was carried out exclusively in aqueous buffers with simple dipeptides as catalysts. Peptides with β-branched (Table 19) and non-β-branched

(Table 20) amino acid residues were both investigated. The most efficient peptide catalysts for asymmetric induction were the β-branched ones (Table 19). The peptide catalyst H-Val-Val-OH (entries 6, 8−13) was employed for the dimerization of glycoaldehyde, producing D-erythrose with >80% enantiomeric excess (entries 10 and 12).

Córdova et al. further showed how the simple ancient dipeptides H-Ala-Ala-OH, and H-Val-Val-OH could catalyze

Scheme 2. Ancient Peptide-Catalyzed Sugar Synthesis from Glycoaldehyde

H-Ala-Ala-OH	48% ee
H-Val-Val-OH	82% ee
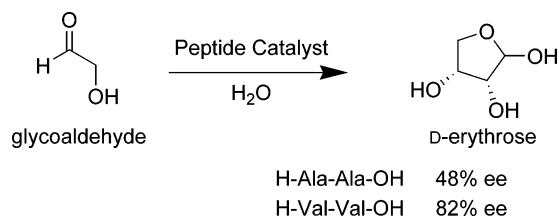
Scheme 3. Peptide-Catalyzed Aldol Reaction between Cyclohexanone and Phenylglyoxylate

60% Yield
2:1 *anti:syn*
68% ee
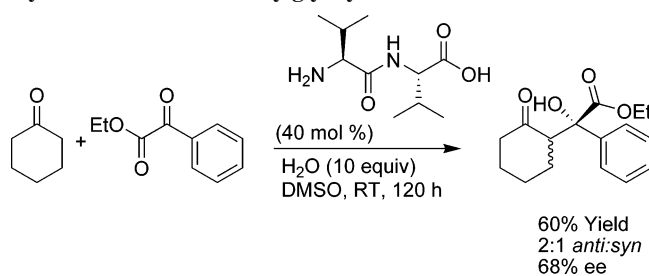
the aldol dimerization of glycoaldehyde to D-erythrose in 48% and 82% enantiomeric excess, respectively (Scheme 2).[45] The asymmetric induction of H-Ala-Ala-OH is significantly higher than the ancient amino acid alanine.[46]

As with the *N*-terminal prolyl peptide-catalyzed asymmetric aldol reaction, the use of ketones as electrophiles has received less attention for the *N*-terminal primary amino peptide-catalyzed asymmetric aldol reaction. Córdova and co-workers demonstrated that the dipeptide H-Val-Val-OH could catalyze the aldol reaction of cyclohexanone and phenylglyoxylate in 60% yield and 68% enantiomeric excess (Scheme 3).[45] The single amino acids valine and tetrazole valine were able to catalyze the same reaction in 96% and 98% enantiomeric excess, respectively.

2.3. Michael Reaction

N-Terminal prolyl peptides and *N*-terminal primary amino peptides have proven to be fruitful categories for peptide catalysis, especially with regards to their ability to catalyze the aldol reaction. A mechanistic similarity between the prolyl peptide-catalyzed Michael reaction and the peptide-catalyzed aldol reaction is the initial formation of an enamine, which subsequently reacts with its electrophilic partner (Figure 14). The conjugate addition of an enolate (or equivalent) provides direct access to a 1,5-dicarbonyl compound, a synthon which has proven to be tremendously valuable in organic synthesis.[47]

2.3.1. Addition of Ketones to Nitroolefins

In a maiden publication by Martin and List regarding their study of *N*-terminal prolyl peptides, they documented a series of dipeptides that could catalyze the Michael addition of acetone to *trans-β*-nitrostyrene (Table 21).[26] Dipeptide H-Pro-Val-OH (entry 6) afforded the Michael product in modest enantiomeric excess and yield. Additionally, the single amino acid proline provided significantly higher reactivity, albeit with a reduced level of asymmetric induction.

Córdova and co-workers were interested in the asymmetric addition of cyclic ketones to *trans-β*-nitrostyrene catalyzed
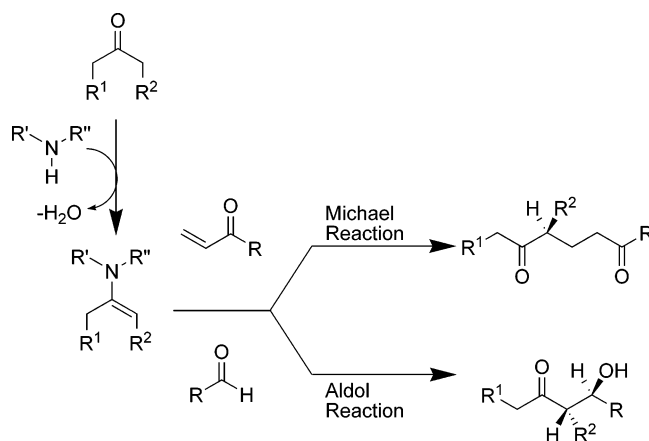
Figure 14. Michael reaction vs. aldol reaction.

Table 21. Peptide-Catalyzed Michael Reactions
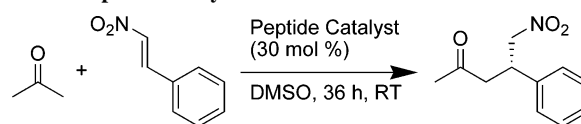
Entry	Peptide	Yield (%)	ee (%)
1	H-Pro-OH	97	7
2	H-Pro-Ala-OH	71	5
3	H-Pro-Trp-OH	68	0
4	H-Pro-Asp-OH	75	3
5	H-Pro-Glu-OH	91	8
6	H-Pro-Val-OH	65	31
7	H-Pro-Arg-OH	65	19
8	H-Pro-Ser-OH	81	8
9	H-Pro-Lys-OH·HCl	66	8
10	H-Pro-Gly-Gly-OH	79	10
11	H-Pro-His-Ala-OH	70	7

by *N*-terminal primary amino peptides.[48] A series of single amino acids and di- and tripeptides was investigated for the conjugate addition of cyclohexanone to *trans-β*-nitrostyrene. The optimal catalysts of those investigated were determined to be H-Ala-Ala-OH and H-Ala-D-Ala-OH. Examination of the substrate scope demonstrated that at least one of the two peptides was able to catalyze the Michael addition of cyclohexanone to electron-rich (entry 4) and electron-poor (entry 5) *trans-β*-nitrostyrene derivatives with high diastereo- and enantiocontrol (Table 22). Several substituted cyclohexanone derivatives (entries 6 and 7) and heterocyclic variants (entries 8, 10, and 11) were produced with comparable chemical and optical efficiencies.

2.3.2. Addition of Nitroalkanes to α,β-Unsaturated Carbonyl Compounds

The addition of nitroalkanes to α,β-unsaturated carbonyl compounds has become an area of intense interest for investigations involving asymmetric catalysis. Tsogoeva and Jagtap became interested in the possibility of *N*-terminal primary amino peptides as potential catalysts for the addition of 2-nitropropane to cyclohexenone.[49] After examination of peptides **9** and **10** along with chiral amine additives (**11**– **15**), H-Leu-His-OH (**9**) in the presence of (1*R*,2*R*)-1,2-diphenylethylenediamine (**15**) was selected for further examination (Table 23, entry 18). Catalyst loading with respect

Table 22. H-Ala-Ala-OH and H-Ala-D-Ala-OH Catalyzed Direct Enantioselective Michael Addition of Ketones to Nitroolefins

Condition A: H-Ala-Ala-OH (30 mol %), 3 days, 4 °C
-OR-
Condition B: H-Ala-D-Ala-OH (45 mol %), 3 days, -20 °C

DMSO:NMP (1:1) (10 equiv H_2O)

Entry	Ketone	R	Product	Condition	Yield (%)	D.R.[a]	ee (%)
1	cyclohexanone	Ph	Ph, NO$_2$	A	67	22 : 1	91
2	cyclohexanone	Ph	Ph, NO$_2$	B	62	17 : 1	97
3	cyclohexanone	Napthyl	2-Naphthyl, NO$_2$	B	79	22 : 1	98
4	cyclohexanone	4-MeOC$_6$H$_4$	Ph(4-OMe), NO$_2$	B	76	20 : 1	92
5[b]	cyclohexanone	4-NO$_2$C$_6$H$_4$	Ph(4-NO$_2$), NO$_2$	B	68	25 : 1	94
6	1,4-dioxaspiro ketone	Ph	Ph, NO$_2$	A	58	36 : 1	94
7[c]	4-methylcyclohexanone	Ph	Ph, NO$_2$ (2 : 1)	A	69	19 : 1	92
8	dioxanone	Ph	Ph, NO$_2$	B	30	12 : 1	92
9	hydroxyacetaldehyde	Ph	Ph, NO$_2$, OH	A	60 (23)[d]	1 : 2 (1 : 2)[d]	29 (40)[d]
10[e]	thiopyranone	Ph	Ph, NO$_2$	B	66	25 : 1	98
11	tetrahydropyranone	Ph	Ph, NO$_2$	B	95	15 : 1	90
12[f]	isobutyraldehyde	Ph	Ph, NO$_2$	B	57	-	58
13[g]	cyclopentanone	Ph	Ph, NO$_2$	A	35	1 : 1	64 (79)[h]

[a] D.R. *(syn:anti)*. [b] 2 days. [c] Combined yield of both isomers, D.R. of both isomers, %ee of second isomer. [d] -20 °C for 2 days. [e] 4 °C for 2 days. [f] 15 mol % peptide catalyst. [g] R.T. [h] %ee for the *anti*-diastereomer.

to additive loading had a significant effect on the chemical efficiency. With 30 mol % of H-Leu-His-OH (**9**) and 30 mol % (1*R*,2*R*)-1,2-diphenylethylenediamine (**15**), the Michael addition of 2-nitropropane to cyclohexenone could be achieved in up to 86% yield and 75% enantiomeric excess.

Tsogoeva and co-workers turned their attention to *N*-terminal prolyl peptides as catalysts for the conjugate addition of nitroalkanes to cyclic α,β-unsaturated ketones. 4-*trans*-Aminoproline-based di-,[50] tri-,[51] and tetrapeptides[50] were the focus of a series of investigations into the Michael reaction. The initial study illustrated that arginine-containing peptides **16** and **17** and tri-*trans*-aminoprolyl peptide **18** could catalyze

the asymmetric addition of 2-nitropropane to cyclohexenone in the presence of *trans*-2,5-dimethylpiperazine[52] in 80% yield and 77% enantiomeric excess (Table 24).[51] Less polar solvents (CHCl$_3$ and acetone) were shown to increase the optical induction, while more polar solvents (DMF, DMSO, and [bmim]PF$_6$) allowed for higher yields, albeit with eroded selectivity. A comparison of a 4-*trans*-aminoproline based di- (**19**),[50] tri- (**18**),[51] and tetrapeptide (**20**)[50] for the conjugate addition of nitroalkanes to cyclic α,β-unsaturated ketones is summarized in Table 25.

The β-turn structural motif has received attention by Miller in his studies of group transfer reactions.[53] Only recently

Table 23. Michael Addition Catalyzed by Dipeptides in the Presence of Additives
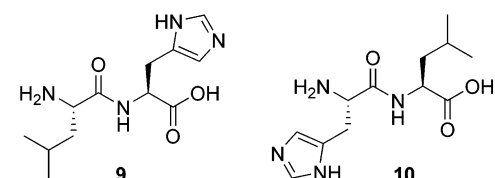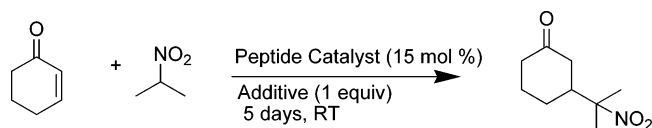
Entry	Catalyst	Additive	Solvent	Yield (%)	ee (%)
1	9	11	DMSO	53	29 (R)
2	9	11	DMF	24	31 (R)
3	10	11	DMSO	95	26 (R)
4	10	11	DMF	29	41 (R)
5	9	-	DMSO	13	42 (R)
6	9	-	DMF	6	21 (R)
7	-	11	DMSO	39.5	-
8	-	11	DMF	5	-
9	9	12	DMSO	>99	3 (S)
10	9	12	DMF	77	31 (S)
11	10	12	DMSO	93	7 (S)
12	10	12	DMF	70	28 (S)
13	-	12	DMSO	60	2 (S)
14	-	12	DMF	14	28 (S)
15	9	13	DMF	79	32 (R)
16	-	13	DMF	21	32 (R)
17	9	14	DMF	74	45 (S)
18	9	15	DMF	**62**	**61 (R)**
19	10	15	DMF	34	49 (R)
20	-	15	DMF	12	45 (R)
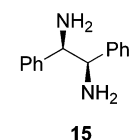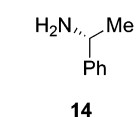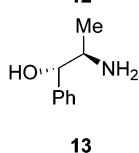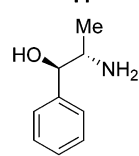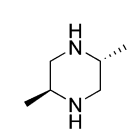
has this structural element proven to be within the prowess of carbon−carbon bond-forming reactions. Specifically, Linton, Miller, and co-workers have recently demonstrated that bifunctional β-turn peptides containing a modified arginine and a τ-benzyl histidine could catalyze an asymmetric Michael addition of α-nitroketones.[54] The development of a selective peptide catalyst began with the examination of several residues and their diastereomers. Further screening of arginine-protecting groups, including ureas and thioureas, led to the peptide catalyst 1-Oct-Arg(Pfb)-D-Pro-Aib-His(τ-Bn)-Phe-OMe, which could catalyze the Michael addition of α-nitrocarbonyls with only 2 mol % catalyst in up to 74% enantiomeric excess (Table 26, entry 2).

2.4. Morita–Baylis–Hillman Reaction

The Morita−Baylis−Hillman reaction was first documented by Morita and co-workers[55] in 1968 and further patented by Baylis and Hillman[56] in 1972. This reaction is believed to proceed by the conjugate addition of a nucleophile to an α,β-unsaturated carbonyl compound (**22**), which generates a latent enolate (Figure 15, **23**). This latent enolate reacts with an electrophile such as an aldehyde (**21**) to produce intermediate **24**. Upon proton transfer and elimination of the catalyst, the reaction affords the Morita−Baylis−Hillman product (**25**). Although the mechanism in Figure 15 is generally accepted,[57] recent reports have found that, in specific cases ($R^2 = OR$), the reaction is second order in aldehyde and that proton transfer is the rate-determining step. This suggests that intermediate **26** is responsible for proton transfer.[58]

2.4.1. Amino Acid Peptide-Catalyzed Morita–Baylis–Hillman Reaction

Miller and co-workers have documented some progress in peptide catalysis by employing π-methyl histidine (Pmh) as the catalytic moiety for numerous group transfer reactions.

Table 24. Conjugate Additions of 2-Nitropropane to Cyclohexenone Catalyzed by Peptides in the Presence of *trans*-2,5-Dimethylpiperazine
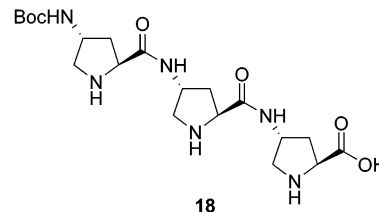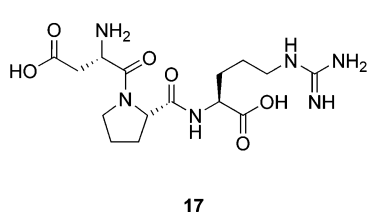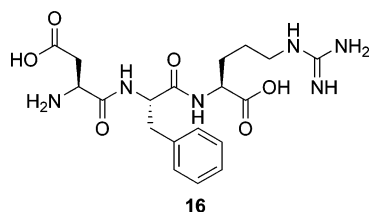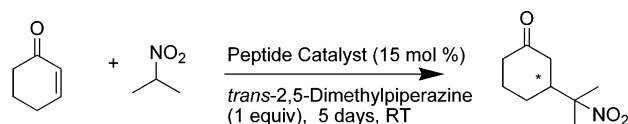
| Solvent	Peptide **16**			Peptide **17**			Peptide **18**			No Peptide	
	Entry	Yield (%)	ee (%)	Entry	Yield (%)	ee (%)	Entry	Yield (%)	ee (%)	Entry	Yield (%)
CHCl₃	1	<10	18	6	<10	71	11	80	77	16	-
Acetone	2	N.R.	-	7	N.R.	-	12	43	80	17	-
DMF	3	16	28	8	<10	17	13	>99	63	18	5
DMSO	4	53	29	9	73	23	14	85	7	19	39.5
[bmim]PF₆	5	44	5	10	35	<5	15	>95	51	20	25

bmim, 1-*n*-butyl-3-methylimidazolium

Table 25. Michael Addition of Nitroalkanes to Cyclic α,β-Unsaturated Ketones Catalyzed by 4-*trans*-Aminoproline-Based Di-, Tri-, and Tetrapeptides
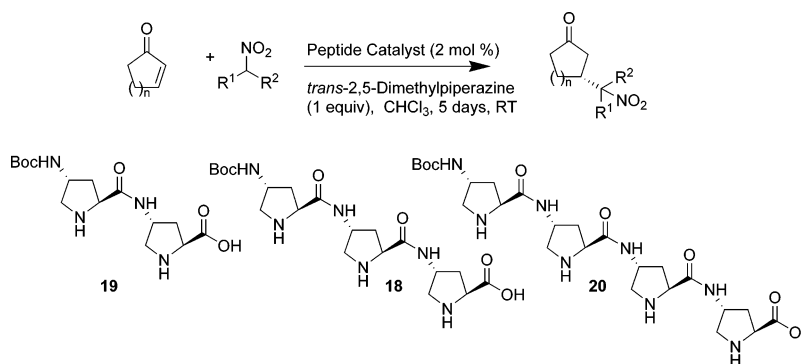
Entry	Nitroalkane	Product	Dipeptide **19**		Tripeptide **18**		Tetrapeptide **20**	
			Yield (%)	ee (%)	Yield (%)	ee (%)	Yield (%)	ee (%)
1	CH₃NO₂		75	57	95	58	75	55
2	CH₃CH₂NO₂		100	LP: 66[a] MP: 67[b]	83	LP: 56[a] MP: 65[b]	100	LP: 58[a] MP: 59[b]
3			46	77	-	-	80	81
4			100	88	71	84	57	82
5			-	-	24	78	-	-
6	CH₃CH₂NO₂		65	LP: 61[a] MP: 54[b]	-	-	71	LP: 47[a] MP: 48[b]
7			40	76	-	-	50	64
8			64	77	-	-	41	60

[a] ee of less polar isomer (LP). [b] ee of more polar isomer (MP).
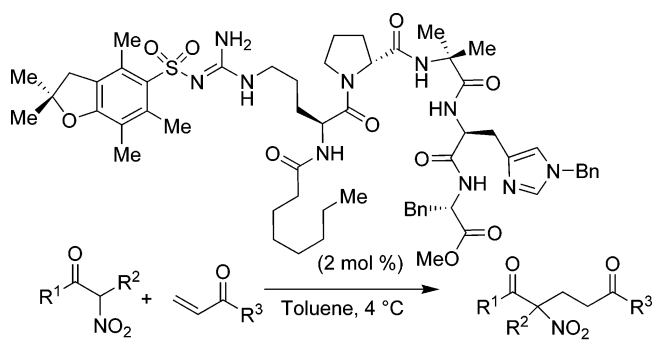
These enantioselective processes include, but are not limited to, acylation,[59] phosphorylation,[60] and sulfinylation.[61] Additionally, the modified histidine residue τ-benzyl histidine has been shown to be an effective catalyst for the conjugate
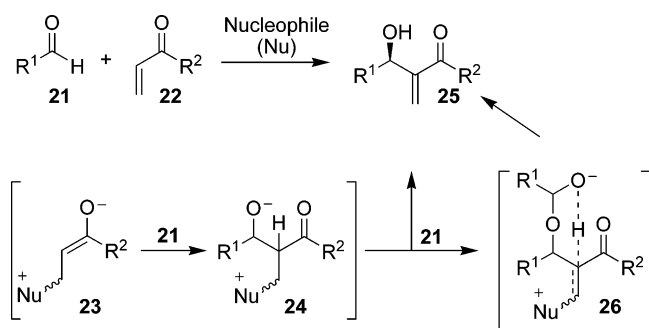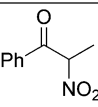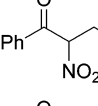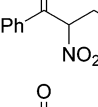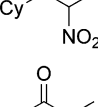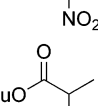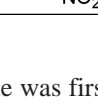

Figure 15. Proposed mechanism of the Morita−Baylis−Hillman reaction.

addition of azide ion.[62] The prospect of expanding the diversity of accessible structures within the outreaches of Pmh peptide catalysis to carbon−carbon bond-forming reactions was a hypothesis in the contexts of the Morita−Baylis−Hillman reaction.

In the initial stages of reaction development, Miller and co-workers began their investigation into the methyl vinyl ketone (MVK) Morita−Baylis−Hillman reaction with *o*-nitrobenzaldehyde. Using only *N*-methylimidazole (NMI) as a simple model catalyst, sluggish reaction rates were observed (40% conversion in 24 h). In analogy to observations by Shi and Jiang,[63] in their studies with the Hatakeyama[64] cinchona alkaloid catalyst, the cocatalyst proline almost doubled the observed reaction rates when combined in equal quantities with NMI (75% conversion in 24 h).[65]

A peptide library consisting of 105 randomly generated peptide sequences containing an *N*-terminal π-methyl his-
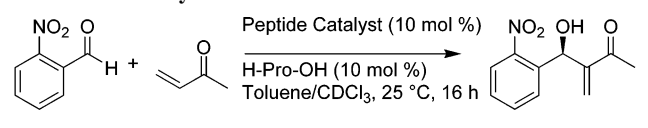
Table 26. Selectivity and Yields Observed with Various Nitrocarbonyls Using 1-Oct-Arg(Pfb)-D-Pro-Aib-His(τ-Bn)-Phe-OMe as Catalyst
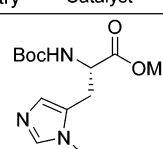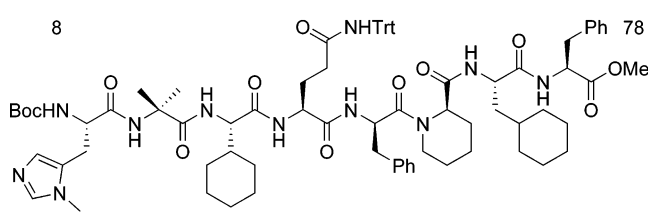

Entry	Substrate	Electrophile	Yield (%)	ee (%)
1			82	52
2			64	74
3			29	60
4			99	0
5			96	0
6			85	50

Table 27. Catalyst Screen for the MVK–MBH Reaction with o-Nitrobenzaldehyde

Entry	Catalyst	ee (%)
1	(Boc-Pmh-OMe)	19
2	Boc-Pmh-Aib-OMe	33
3	Boc-Pmh-Aib-Phe-OMe	33
4	Boc-Pmh-Aib-Phe-D-Phe-OMe	40
5	Boc-Pmh-Aib-Cha-hPhe-D-Phe-OMe	47
6	Boc-Pmh-Aib-Chg-Gln(Trt)-D-Phe-Phe-OMe	61
7	Boc-Pmh-Aib-Chg-Gln(Trt)-D-Phe-(Boc)Trp-Phe-OMe	73
8		78
9	Boc-Pmh-Aib-Chg-Gln(Trt)-D-Phe-D-Pip-Cha-Phe-Phe-OMe	75
10	Boc-Pmh-Aib-Chg-Gln(Trt)-D-Phe-D-Pip-Cha-Val-(Boc)Trp-Phe-OMe	74

hPhe, homophenylalanine
Cha, cyclohexylalanine

tidine residue was first synthesized and analyzed for stereo-selectivity in the Morita–Baylis–Hillman (MBH) reaction. By comparing the most reactive and selective catalysts in the initial screen, the sequence Boc-Pmh-Aib-Peptide was identified as a promising lead for the N-terminus of the peptide catalyst. Exploration of the structure–activity relationship (SAR) of each position of the peptide by single substitution led to a peptide that could catalyze the Morita–Baylis–Hillman reaction in 61% enantiomeric excess (Table 27, entry 6). At this point, a direct relationship was observed between peptide length and selectivity (Table 27). The correlated increase in selectivity that was observed with increasing main chain length leveled off at the stage of an octamer peptide, which catalyzed the Morita–Baylis–Hillman reaction in 78% enantiomeric excess (entry 8).

The use of a cocatalyst allows for a unique opportunity to investigate noncovalent interactions. In an attempt to further optimize the reaction, numerous single amino acids, N-methyl amino acids, and proline derivatives were surveyed for their ability to act as adept cocatalysts.[66] After a thorough investigation, the amino acid proline unequivocally outperformed any of the other cocatalysts investigated.

Examination of the scope of the peptide–amino-acid cocatalyzed Morita–Baylis–Hillman reaction demonstrates

that a variety of electron-withdrawing groups could be tolerated (Table 28). Optimal asymmetric induction was obtained when these electron-withdrawing groups were ortho or para on the benzaldehyde derivative. Meta electron-donating substituents allowed for the highest selectivity observed when an ortho electron-withdrawing substituent was also present (entry 6).

2.5. Acyl Anion Equivalents

The use of enamines and their counterparts has received considerable attention in the peptide-catalysis literature. This may stem from the straightforward modus operandi in terms of bond polarization of enamine chemistry. Acyl anions and their in situ generated equivalents have received significantly less attention in the literature. Classical solutions to the generation of an acyl anion include the deprotonation of a dithiane or cyanohydrin.[67] These synthetic sequences involve multiple operations to generate their respective precursors and terminate with deprotection sequences that are not necessarily straightforward. Additionally, the necessity of a strong base for deprotonation would likely degrade the peptide itself. The use of a thiamine pyrophosphate mimic could indeed be a new bond disconnection for peptide-catalyzed asymmetric catalysis.

Pioneering studies by Breslow on the mechanism of thiamine pyrophosphate catalysis and the analogous benzoin reaction have proven to be seminal contributions to organic chemistry.[68] This multistep, complex reaction coordinate still stands as the leading depiction of the plausible mechanism. As depicted in Figure 16, a thiazolium ylide (**28**), or

Table 28. Substrate Scope for the Peptide-Catalyzed MVK−MBH with H-Pro-OH Cocatalyst

Entry	Aldehyde	Product	Yield (%)	ee (%)	Entry	Aldehyde	Product	Yield (%)	ee (%)
1			81	78	6			88	81
2			92	73	7			52	71
3			81	69	8			74	45
4			>95	63	9			55	65
5			89	63	10			55	41

isoelectronic *N*-heteterocyclic carbene (**29**) generated from salt **27** and a base, adds to an aldehyde (**30**). This is followed by a proton tautomerization of **31** to generate the acyl-anion equivalent (**32**)/enamine (**33**) resonance structure, commonly referred to as the "Breslow intermediate". Nucleophilic addition to an electrophile (**34**, aldehyde = benzoin reaction, α,β-unsaturated carbonyl = Stetter reaction) with production of **35**, followed by proton transfer and catalyst elimination completes the catalytic cycle and produces **36**.

2.5.1. Peptide-Catalyzed Asymmetric Intramolecular Stetter Cyclization

The use of proteinogenic amino acids has generated a vast number of carbon−carbon bond-forming reactions. In particular, reaction developments that proceed via enamine/enolate chemistry have been a flourishing area of peptide research. In an attempt to move beyond the use of proteinogenic amino acids, Miller and co-workers have embarked on a journey into chemical reactions that proceed via in situ formed acyl-anion equivalents, which is commonly referred to as *umpolung*.[69] The incorporation of the appropriately functionalized nonproteinogenic amino acid thiazolylalanine (Taz) into short peptides has proven to be a novel mimic of the enzymatic cofactor thiamine pyrophosphate.[70]

Miller and co-workers began their study with an investigation into the intramolecular Stetter cyclization. Preliminary studies with quaternized single amino acid derivatives of Taz demonstrated the proof-of-principle experiments to support the hypothesis that peptide-containing *N*-heterocyclic carbene could catalyze the desired cyclization. A series of peptides

was investigated for their ability to catalyze an enantioselective variant of the intramolecular Stetter cyclization. *C*- and *N*- terminal Taz quaternized peptides were capable of catalyzing the cyclization with low selectivity. On the other hand, a peptide containing a Taz residue flanked by the bulky chiral (*S*)-(−)-1-(1-napthyl)ethylamine and Boc-Thr(Bn)- could catalyze the enantioselective Stetter cyclization in up to 73% ee and 67% yield (Table 29, entry 1). Substrates containing electron-donating groups could be cyclized with comparable levels of asymmetric induction (entries 2−5). However, substrates bearing strongly electron-withdrawing groups were shown to rapidly racemize under the reaction conditions (entry 6).

2.5.2. Aldehyde N-Acylimine Cross-Coupling Reaction

After demonstrating peptides were competent *N*-heterocyclic carbene organocatalysts in the intramolecular Stetter reaction, Miller and co-workers focused their efforts toward an arena in which asymmetric catalysis had no available precedent, specifically, a peptide-catalyzed intermolecular aldehyde *N*-acylimine cross-coupling reaction.[71,72] Early investigations were complicated by racemization as a deleterious side reaction. On the basis of empirical evidence collected during initial optimization, it was hypothesized that base-induced enolization was the racemization pathway. Using the extremely hindered tertiary amine base 1,2,2,6,6-pentamethylpiperidine (PEMP) minimized the degree of racemization observed throughout the course of the reaction. Racemization rate comparison of isotopically labeled
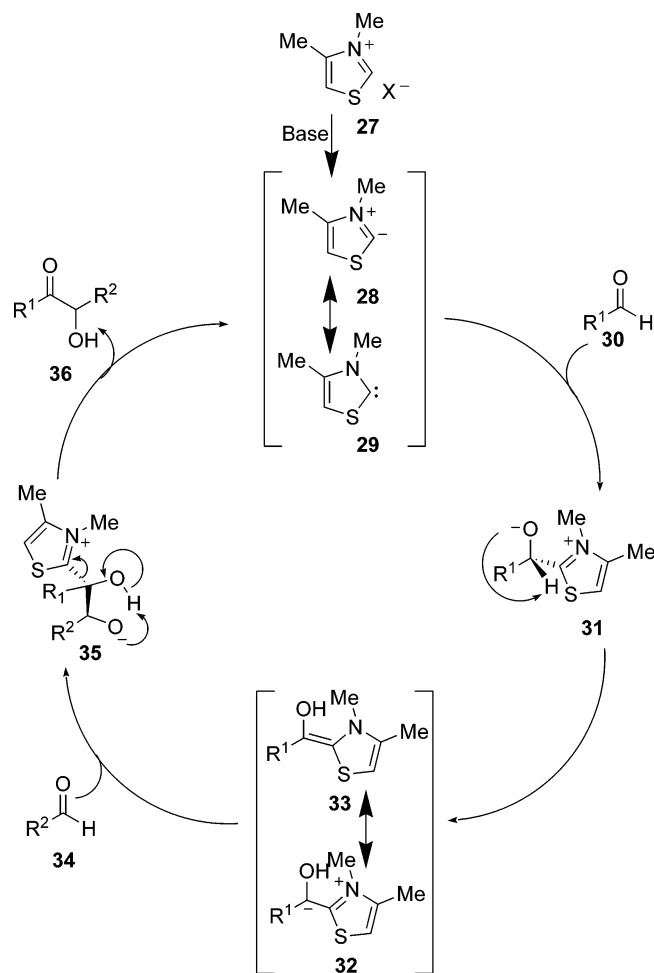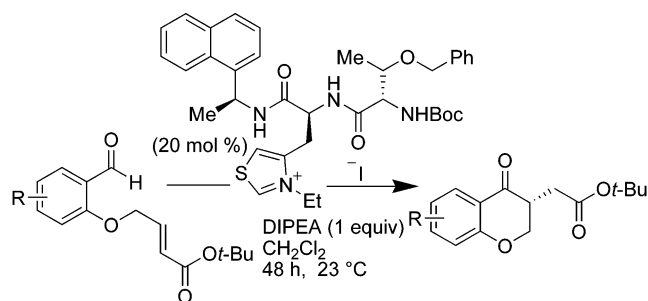
Figure 16. Mechanism of the benzoin reaction.

Table 29. Substrate Scope for the Peptide-Catalyzed Intramolecular Stetter Cyclization

Entry	Product	Yield (%) (0.25 M)	ee (%)	Yield (%) (0.40 M)	ee (%)
1		67	73	-	-
2		32	72	45	75
3		45	73	43	69
4		13	69	47	64
5		17	73	39	76
6		78	0	88	0

materials provided strong evidence to support the hypothesis of base-induced enolization (Figure 17).

Throughout the course of this study, electronic perturbations revealed meta and para electron-withdrawing substituents on the aromatic aldehyde accelerated the reaction rates, while meta and para electron-donating substituents on the *N*-acylimine suppressed the racemization (Table 30). Asymmetric inductions of up to 87% enantiomeric excess (entry

3) with 90% isolated yield could be obtained in only 2 h at ambient temperature. Furthermore, a single recrystallization could be used for a straightforward upgrade to >98% enantiomeric excess.
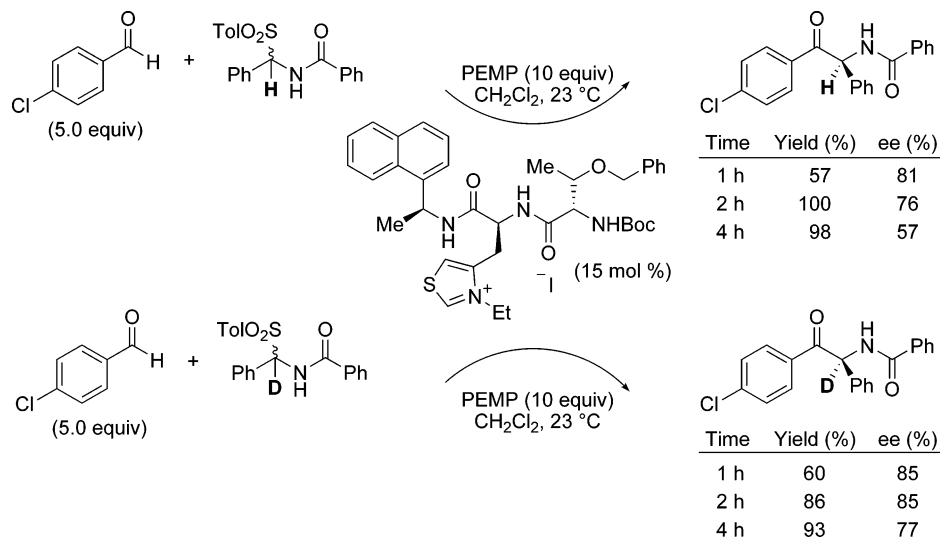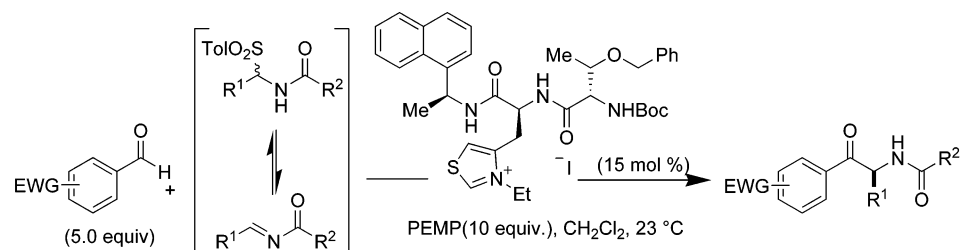

Time	Yield (%)	ee (%)
1 h	57	81
2 h	100	76
4 h	98	57

Time	Yield (%)	ee (%)
1 h	60	85
2 h	86	85
4 h	93	77

Figure 17. Effects of isotopic labeling for the peptide-catalyzed aldehyde *N*-acylimine cross-coupling reaction.

Table 30. Substrate Scope for Aldehyde Acylimine Cross-Couping Reaction

Entry	Aldehyde	Tosyl Amide	Product	Time	Yield (%)	ee (%)
1				1 h	57	81
2				2 h	100 (60)[a]	76 (>98)[b]
3				2 h	90	87
4[c]				2 h	91 (71)[a]	85 (>98)[b]
5				15 min	77	82
6				15 min	63 (23)[a]	79 (>98)[b]
7				2 h	97 (48)[a]	75 (>98)[b]
8				1 h	80	81
9				2 h	15	83 (S)

[a] mass isolated after one recrystalization. [b] %ee after one recrystalization. [c] 13 x Scale.

3. Enantioselective Oxidative Methods

3.1. Juliá–Colonna Epoxidation

One of the most well-known enantioselective, peptide-catalyzed oxidation reactions is the asymmetric Weitz–Scheffer epoxidation of chalcones, originally developed by Juliá and Colonna in the early 1980s.[73–76] Because of the high enantioselectivity, easily accessible catalysts, and somewhat unusual reaction conditions, this method has drawn considerable attention. Many efforts have focused on streamlining the process as well as delineating the mode of asymmetric induction.[77]

3.1.1. Initial System

In 1980, Juliá and co-workers first reported the discovery of a poly(amino acid)-catalyzed epoxidation of chalcone **37a** under triphasic conditions.[73] As shown in Scheme 4, it was found that (E)-chalcone, when treated with aqueous sodium hydroxide and hydrogen peroxide in the presence of solid poly-L-alanine (**39**), undergoes epoxidation with a very high degree of enantioselectivity, furnishing product **38a** with up to 96% ee in 24–48 h.

Several important observations were made, including the following: (1) poly-L-alanine is far superior to poly(γ-benzyl-L-glutamate) and poly(γ-butyl-L-glutamate) in terms of both chemical yield and enantioselectivity; (2) a catalyst

Scheme 4.
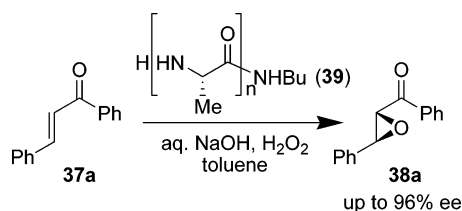
Scheme 5.
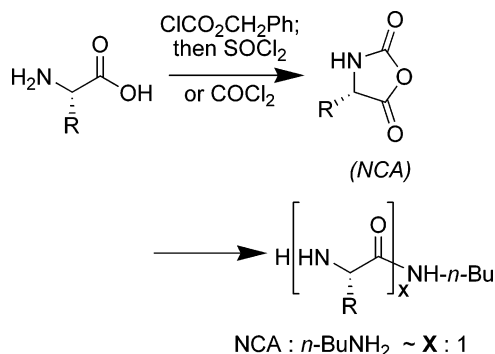
is required for both reactivity and selectivity; (3) recovered catalyst may be used in subsequent reactions, but yield and enantioselectivity suffer; and (4) while the catalyst loading does not have a large effect on enantioselectivity, the relative phase distribution (by weight) is important for optimal yield and enantioselectivity.

Polypeptide catalysts may be prepared in a straightforward manner using the N-carboxyanhydride (NCA) of the appropriate amino acid (Scheme 5). The polymeric catalyst is a mixture of peptides of varying lengths, but the average length is approximately controlled by the ratio of NCA to initiator (n-butylamine for catalyst **39**).

In a series of subsequent publications by Juliá and Colonna and their co-workers, the scope of the enantioselective epoxidation, reaction condition effects,[74] and catalyst structure effects[74−76] was communicated. It was found that several aromatic enones undergo poly-L-alanine-catalyzed epoxidation with good levels of enantioselectivity and moderate-to-excellent chemical yields (Table 31,[74] entries 1−6). Cyclic enones (**41** and **42**) and nitroalkenes (**40**), however, are not enantioselectively epoxidized under the same conditions (entries 7−9).

A number of reaction parameters were explored in the epoxidation of **37a** using catalyst **39** including organic solvent, temperature, and oxidizing agent.[74] Toluene and tetrachloromethane were found to be the most competent organic solvents in terms of rate and enantioselectivity. The use of chlorobenzene or dichloromethane reduces the reaction rate but maintains good enantioselectivity. Less polar solvents such as cyclohexane and hexane furnish products in excellent yield but significantly reduced enantiomeric excess. Modest temperature effects were documented: when the reaction is run above ambient temperature, the enantioselectivity decreases, and there is essentially no difference in product enantiomeric excess when the reaction is run at 0 or 25 °C. Several oxidant systems were examined including m-chloroperbenzoic acid (m-CBPA)−NaHCO₃−H₂O, t-BuO₂H−NaOH−H₂O, t-BuO₂H, t-BuO₂H−K₂CO₃, and the original H₂O₂−H₂O system. Of these, only the use of H₂O₂−H₂O provides products in high enantiomeric excess. Notably, when t-BuO₂H alone is used (producing biphasic reaction conditions), the epoxidation does not proceed at all.

Table 31. Epoxidation Substrate Scope

Entry	Alkene	R¹	R²	Yield (%)	ee (%)
1	**37a**	Ph	Ph	78-85	78-86
2	**37b**	Ph	p-NO$_2$C$_6$H$_4$	83	82
3	**37c**	2-thiophenyl	Ph	96	80
4	**37d**	3-thiophenyl	Ph	30	70
5	**37e**	o-OMe-C$_6$H$_4$	Ph	54	50
6	**37f**	Ph	p-Cl-C$_6$H$_4$	47	66
7	**40**			50	7
8	**41**			100	0
9	**42**			19	<5%

Table 32. Catalyst Effects

Entry	R¹	R²	R³	X[a]	Yield (%)	ee (%)	Ref.
1	H	Me	NHBu	5	9	11	73
2	H	Me	NHBu	7	18	28	73
3	H	Me	NHBu	10	78	84	73
4	H	Me	NHBu	30	96	96	73
5	H	CH₂CH(CH₃)₂	NHBu	10	60	84	74
6	H	CH₂CH(CH₃)₂	NHBu	30	44	88	74
7	H	CH(CH₃)CH₂CH₃	NHBu	10	75	93	74
8	H	CH₃, CH₂CH(CH₃)₂	NHBu	10	67	95	74
9	H	CH(CH₃)₂	NHBu	10	5.5	10	74
10	H	CH₂Ph	NHBu	10	32	1	74
11	H	CH₂CO₂CH₂Ph	NHBu	10	7.5	3	74
12	H	(CH₂)₂CO₂CH₂Ph	NHBu	10	12	11.6	74
13	H	Me	NH(CH₂)₂NEt₂	10	52	15	73
14	H	Me	NH(CH₂)₂NEt₂Bu⊕ Br⊖	10	62	20	73
15	H	Me	OH	19	80	80	75
16	H	Me	OH	> 50	96	96	75
17	H	Me	OMe	> 50	26	78	75
18	H	Me	OCH₂polystyrene		82	84	75
19	Me	CH₂CH(CH₃)₂	NHBu	30	73	92	75

[a]Approximate degree of polymerization based on NCA method of preparation. NCA:initiator = X

Several catalyst structure effects on the enantioselective epoxidation of chalcone **37a** were investigated. First, the length of polypeptide catalyst was examined. A set of four poly-L-alanine catalysts were synthesized and compared (approximately 5, 7, 10, and 30 alanine residues). It was found that polymers of increasing length are more effective enantioselective catalysts (Table 32, entries 1−4), with a 30 mer catalyst providing product **38a** in 96% ee (entry 4). Next, other poly-L-peptides were evaluated for efficacy in the

Scheme 6.
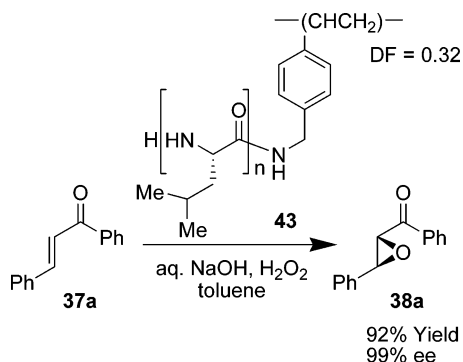
asymmetric epoxidation reaction.[75] Poly-L-leucine (entries 5 and 6) and poly-L-isoleucine (entry 7) were found to be excellent catalysts with comparable efficacy to poly-L-alanine (entries 3 and 4), as were random copolymers of leucine and alanine (entry 8). Poly-L-valine, on the other hand, was found to be a far inferior catalyst (entry 9). Random copolymers of valine and alanine show decreasing efficacy as the percentage of valine increases. Poly-L-phenylalanine, poly-β-benzyl-L-aspartate, and poly-γ-benzyl-L-glutamate are also poor catalysts for the process, reducing both the yield and the enantioselectivity of the reaction (entries 10−12). Finally, modification of the *C*- and *N*-terminal groups of the catalyst was studied.[76] When the catalyst is capped by a diamine at the *N*-terminus, the enantioselectivity is significantly reduced (entries 13 and 14). It was found that, in addition to the previously reported *C*-terminal amide catalysts, *C*-terminal carboxylic acids are excellent catalysts and furnish similar high levels of enantioselectivity (entries 15 and 16). Esters are also well-tolerated at the *C*-terminus (entries 17 and 18). Notably, this allows for attachment of the catalyst to a polystyrene solid support. Finally, dimethylation of the *N*-terminus does not significantly reduce product enantiomeric excess (entry 19 compared to entry 4).

3.1.2. Triphasic Reaction Development and Broadening of Scope

The remarkable enantioselectivity of the Juliá−Colonna epoxidation prompted a number of researchers to conduct further investigations. Many studies addressed some of the main drawbacks to the original procedure such as the issues of inconsistent catalyst preparation, catalyst degradation and recovery, and limited substrate scope. In several instances, poly(amino acid)-catalyzed epoxidation was employed for the preparation of key synthetic intermediates.

In 1990, Itsuno and co-workers[78] reported the use of polymer-supported poly(amino acids) for the asymmetric epoxidation of enones. Several polymeric amino acid catalysts were prepared, supported by a cross-linked aminomethylated polystyrene (CLAMPS) resin. The catalysts were evaluated for efficacy in the enantioselective epoxidation of **37a**, and it was found that immobilized CLAMPS−poly-L-leucine (**43**) is an excellent promoter of the reaction, providing product **38a** in 92% yield and 99% ee (Scheme 6). The optimal degree of functionality (DF) of the aromatic polymer backbone is 0.32. Notably, the catalyst can be recovered and may be recycled numerous times (after 12 cycles, product **38a** may still be obtained in 95% yield and 94% ee). Whereas the original poly(amino acid) catalysts are difficult to recycle as they take on a gel-like consistency,

the Itsuno CLAMPS catalysts have a large enough particle size to filter and represent an improvement in catalyst recovery.

An early study by Lantos, Novack, and co-workers provided more insight on reliable catalyst preparation and reuse.[79] In the process of preparing epoxide **44** en route to leukotriene antagonist SK&F 104353, it was shown that synthesis of poly-L-leucine using a modified NCA method (performed using freshly prepared L-leucine NCA in a humidity chamber) generated a reproducibly active and robust catalyst. Additionally, it was observed that activation of the polymer catalyst by stirring with hexane or CH_2Cl_2, substrate, and aqueous base for 24 h prior to addition of H_2O_2 and EDTA significantly reduces reaction times. Furthermore, recovered catalyst from these modified conditions can be used in six consecutive reactions without reduction in yield or enantioselectivity.
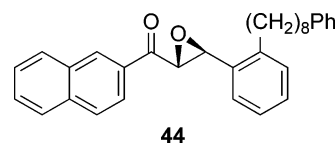
The role of oxidizing agent has been revisited since Juliá and Colonna's original investigations. The mild system of sodium perborate−NaOH was found to be suitable in place of H_2O_2−NaOH,[80,81] providing optimal results for certain sensitive dienone substrates.[80] Additionally, the use of sodium percarbonate−H_2O_2 systems has produced excellent results using lower catalyst loadings.[80,82]

Several studies have focused on broadening the substrate scope of the Juliá−Colonna epoxidation. Contributions by the research groups of Bezuidenhoudt and Ferreira,[83,84] Roberts,[80,85−87] and Falck[88] have shed considerable light on the process, which displays a much wider scope than originally reported. For instance, it has been shown that the process is not limited to simple chalcone-like substrates. Highly substituted aryl enones also undergo stereoselective epoxidation, as do di- and trienones, stannyl enones, and alkyl-substituted enones.

Further broadening of the scope was accomplished by the employment of phase-transfer catalysts (PTCs). Militzer and co-workers found that the addition of tetrabutylammonium bromide (TBAB) provides a significant rate acceleration relative to the original triphasic conditions.[89] Under the triphasic PTC conditions, catalyst loading may be drastically reduced from 200 wt % to <1 wt %, resulting in nearly biphasic conditions as the amount of solid catalyst is much less than the volume of the organic and aqueous phases. In the same report, a reliable procedure for preparing poly-L-leucine catalysts is noted. High-purity leucine−NCA may be formed via phosgenation of leucine. Polymerization using 1,3-diaminopropane as intiator is best performed in refluxing toluene. Precipitation or centrifugation followed by drying furnishes highly active catalysts. Additionally, some previously unsuccessful substrates are epoxidized efficiently using the PTC conditions (such as alkenyl sulfones).[90]

Roberts and co-workers have also investigated PTCs for the Juliá−Colonna epoxidation of alkenyl sulfones.[91] They reported modified conditions in which poly-L-leucine catalyst is incubated with toluene, PTC, NaOH, and H_2O_2. Removal of the aqueous layer, re-exposure of the organic and solid

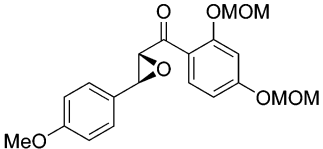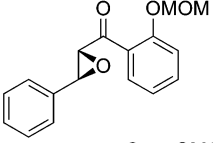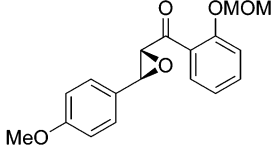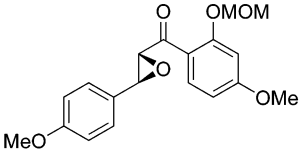**Table 33. Poly(amino acid)-Catalyzed Epoxidation under Triphasic Conditions[92]**
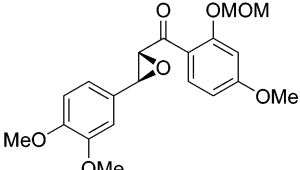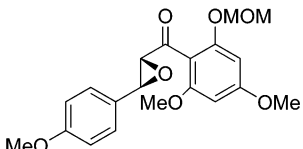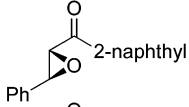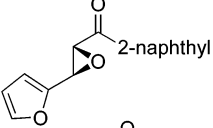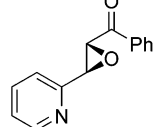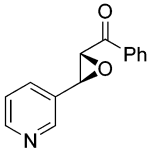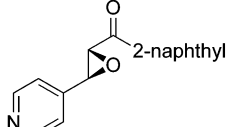
Entry	Product	Method	Yield (%)	ee (%)	Ref.
1		A		70	83a
2		A	65	38	83b
3		A	64 99	66 84	83b 84
4		A	74 98	84 86	83b 84
5		A	46	62	83b
6		A		32	83b
7		B	90	93	80
8		B	75	>96	80
9		B H	84 >99	72 84	80 90
10		C	70	94	80
11		B	67	>96	80

Table 33. (Continued)
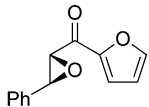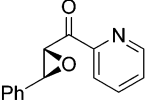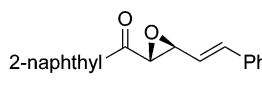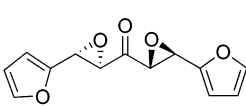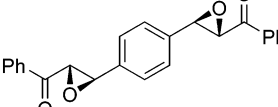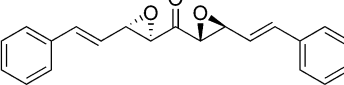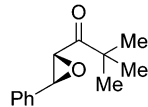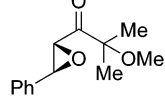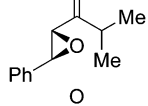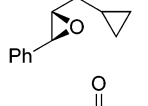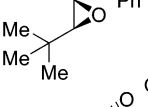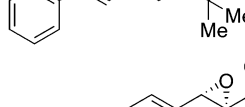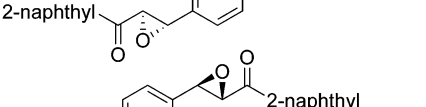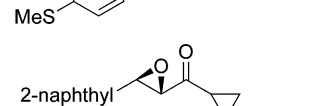
Entry	Product	Method	Yield (%)	ee (%)	Ref.
12		C	98	93	80
13		B	74	79	80
14		D	78	>96	80
15		B	60	90 >88 de	80
16		C	91	>99 >88 de	80
17		B	50	80	80
18		B	92	>98	80
19		B	70	63	86
20		B	60	62	86
21		B G	85 40	77 90	86 90
22		B	85	90	80
23		B	90	>97	80
24		E	82	>98 >99 de	80
25		C	82	>96	85
26		C	61	90	86

Table 33. (Continued)

Entry	Product	Method	Yield (%)	ee (%)	Ref.
27		B	73	74	86
		E	52	98	86
28		F	57	90	86
29		F	100	>95	86
30		B	51	>94	86
31		F	66	>95	86
32		F	78	59	87
33		B	76	76	87
		G	>99	92	90
34		D	90	>99	88
35		G	82	68	90
		I	66	91	91
36		I	49	94	91
37		I	61	95	91
38		I	76	70	91

A = poly-L-alanine (100 weight %), H_2O_2-NaOH, CCl_4
B = poly-L-leucine (11 mol %), H_2O_2-NaOH, CH_2Cl_2
C = poly-D-leucine (11 mol %), H_2O_2-NaOH, CH_2Cl_2
D = poly-L-leucine (11 mol %), H_2O_2-NaOH, hexane
E = poly-L-leucine (11 mol %), $NaBO_3$-$4H_2O$, NaOH CH_2Cl_2
F = CLAMPS-poly-L-leucine (11 mol %), H_2O_2-NaOH, toluene (Itsuno catalyst)
G = poly-L-leucine (11 mol %), H_2O_2-NaOH, TBAB, toluene
H = poly-L-leucine (0.5 mol %), H_2O_2-NaOH, TBAB, toluene
I = poly-L-leucine (0.1 mol %), H_2O_2-NaOH, Bu_4NHSO_4, toluene (then aq. layer removed)

phases to fresh NaOH and H_2O_2, repeated removal of the aqueous phase, and addition of substrate provides the best results.

Table 33 shows the range of substrates that undergo enantioselective epoxidation under triphasic Juliá−Colonna conditions.[92]

Scheme 7.

A: 18 h, 87% yield, 88% ee
B: 0.5 h, 85% yield, >95% ee

A: 72 h, 78% yield, >95% ee
B: 3 h, 85% conversion, >95% ee

A: 168 h, no conversion
B: 4 h, 70% yield, 83% ee

Method A: poly-L-leucine
CH$_2$Cl$_2$, H$_2$O$_2$-NaOH
(triphasic conditions)

Method B: poly-L-leucine
THF, DBU, UHP
(biphasic conditions)
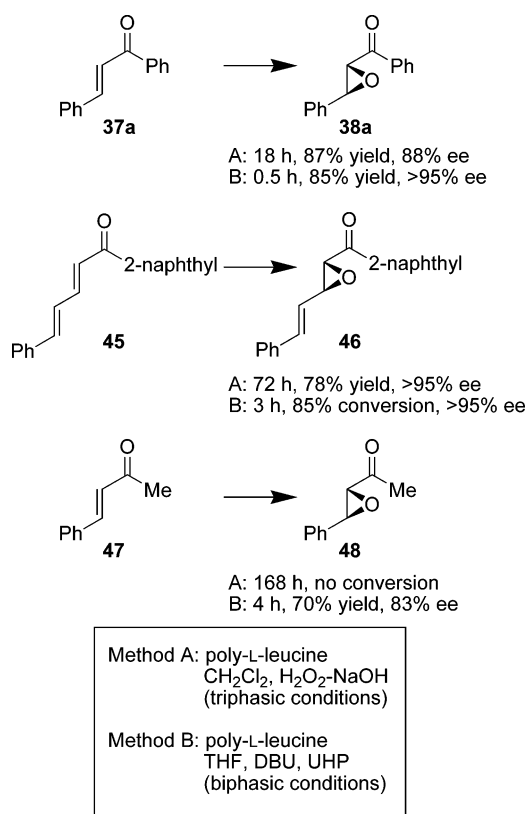
Scheme 8.

3.1.3. Biphasic Systems

In 1997, Roberts and co-workers reported a significant advance in the poly(amino acid)-catalyzed epoxidation of enones with elimination of the aqueous phase that was originally required.[93] These cond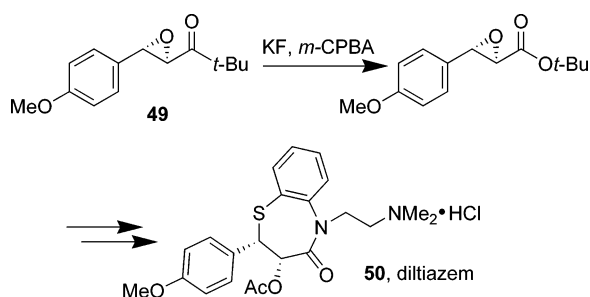itions replace aqueous H$_2$O$_2$−NaOH with an organic base 1,8-diazabicyclo[5.4.0]-undec-7-ene (DBU) and an organic-soluble peroxide source, urea−hydrogen peroxide[94] (UHP). Using UHP, DBU, and poly-L-leucine in THF, the resulting biphasic system provides a marked rate increase, allowing isolation of epoxide **38a** after only 30 min compared to 18 h under the original triphasic conditions (Scheme 7). Similar effects are noted for a range of substrates, including dienone **45** and methyl ketone **47**, which produced epoxides **46** and **47**, respectively.

It was found that 1,5-diazabicyclo[4.3.0]non-5-ene (DBN) is just as effective as DBU. Diisopropylethylamine (Hünig's base) may be used but causes a reduction in yield and enantioselectivity; triethylamine is completely ineffective. The oxidant may be changed to 1,4-diazabicyclo[2.2.2]-octane−peroxide complex (DABCO−1.5 H$_2$O$_2$) with comparable results to UHP, but 90% H$_2$O$_2$ is much less effective.

These biphasic conditions led to several studies by Roberts and co-workers,[95−100] resulting in an impressive expansion of substrate scope for the asymmetric expoxidation of enones. Several substrates that were unreactive or slow to react under triphasic conditions are efficiently epoxidized with high enantioselectivity using the biphasic conditions. Additionally, PTC conditions may be applied using the biphasic protocol.[90]

Table 34 has been compiled to display the range of epoxides that may be generated by employing the new conditions.[92] Notably, several simple enones (not chalcone-like) are good substrates for the epoxidation (entries 9−11 and 20−22). Additionally, it was found that poly-L-leucine catalysts are competent catalysts for substrates possessing stereogenic centers. In some cases, the catalyst is powerful enough to overwhelm the inherent substrate-controlled diastereoselectivity (entry 23).

The biphasic conditions for asymmetric epoxidation have been employed in the efficient preparation of a number of key intermediates in the total syntheses of several target compounds. Diltiazem (**50**), a blood-pressure-lowering agent, can be produced in four steps from epoxide **49** (Scheme 8).[96] Key to the process is oxidizing an epoxy ketone to an epoxy ester, which is further elaborated to **50**. The Juliá−Colonna epoxidation biphasic conditions have also been employed to synthesize a key side chain of Taxol (**51**, Scheme 9)[96] and clausenamide (**52**, Scheme 10).[101]

Roberts and co-workers have also examined other solid-supported poly(amino acid) catalysts under biphasic epoxidation conditions. It was noted that poly(ethylene glycol) polystyrene amines can support active catalysts.[101] These catalysts may be prepared using either the NCA method described above or a peptide synthesizer (producing catalysts of specific lengths). Additionally, the use of CLAMPS−poly-L-leucine in a miniature continuous-flow system was reported.[101] In this system, a small Pasteur pipet is slurry-packed with CLAMPS−poly-L-leucine and oxidant. Substrate dissolved in solvent containing DBU (0.5%) is passed through this fixed bed of catalyst (15−20 min residence time), allowing direct product isolation with excellent conversion and enantioselectivity. Finally, Roberts and co-workers discovered that poly(amino acids) may be immobilized on silica,[102a,b] resulting in granular catalysts that are particularly easy to handle and, importantly, to recover and recycle. Epoxidation occurs under biphasic conditions, generating epoxides in high yield and enantioselectivity, with short reaction times. Recycled catalysts do not lose catalytic activity, and a high level of enantioselectivity is maintained in subsequent runs. Improvement to catalyst preparation and activity was observed when polymerization with leucine NCA was performed in DME at 90 °C followed by adsorption onto silica.[102c]

Tang and co-workers have reported the use of silica-grafted poly-L-leucine catalysts (covalently bound to silica) for asymmetric epoxidation under triphasic and biphasic conditions.[103] The catalysts can be recovered by filtration and are reusable in subsequent runs with modest decreases in enantioselectivity.
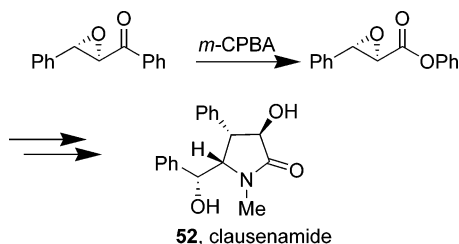
3.1.4. Homogeneous Systems

Roberts and co-workers have played an important and continuing role in the evolution of poly(amino acid) catalysts. In addition to their work on solid-supported catalysts, they have found that catalysts may be supported by organic soluble polymers (poly(ethylene glycol)-based), allowing the

Scheme 9.

51, side-chain of Taxol™

Scheme 10.

52, clausenamide
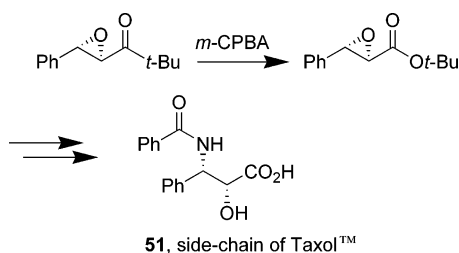
Juliá−Colonna epoxidation to be conducted under homogeneous conditions.[104,105] The soluble catalyst may be combined with UHP and DBU in organic solvent, producing a homogeneous system that has comparable efficiency to the biphasic system described above.

Tsogoeva and a group from Degussa further developed organic-soluble catalysts for use in a continuously operated reactor.[106] They found that a membrane reactor is suitable for conducting the reaction and provides a method for nanofiltration. The reactor allows substrate and oxidant to be incubated with catalyst for the designated reaction time. Filtration through a membrane allows unreacted substrate and product to pass through for isolation but sequesters the polymeric catalyst. In this way, the reaction chamber maintains the original catalyst and is primed for further operations. High enantioselectivities can be achieved for up to 50 residence times.

3.1.5. Mechanistic Investigations

The initial reports of Juliá and Colonna included the hypothesis that the most effective enantioselective poly-(amino acid) catalysts are those that adopt α-helical structures.[75] Several investigations have been carried out in an attempt to further delineate the mechanism of asymmetric induction in the Juliá−Colonna epoxidation. A number of approaches have been taken, including the synthesis of catalysts of varying length, structure, and solubility as well as the use of spectroscopic and computational methods.

Early mechanistic studies by Roberts and co-workers involved the synthesis of polyleucine catalysts containing varying amounts of D-leucine.[107] These initial experiments led to the observation that the residues at the *N*-terminus have the greatest effect on enantioselectivity, whereas residues toward the middle and *C*-terminus have little effect. Next, PEG-supported polyleucine catalysts of discrete lengths were designed to systematically investigate this effect. Specifically, D-leucine was integrated into catalysts possessing 10 and 20 total leucine residues, with variation in location and total D-leucine content.[104] Again, it was found that stereochemistry near the *N*-terminus dictates the overall sense of asymmetric induction in the epoxidation of **37a**. At least five *C*-terminal residues were found to be necessary to confer asymmetric induction, with longer-chain catalysts displaying

higher reactivity and selectivity. Examination of the *N*-terminal residue of unsupported poly(amino acid) catalysts revealed that a free amino group is optimal, but methyl, dimethyl, or acetyl substitution at the *N*-terminus results in catalysts that are still active but cause a slight-to-moderate decrease in enantioselectivity.[108] Additionally, soluble PEG-bound poly-L-leucine catalysts of varying lengths were studied by Fourier transform infrared (FTIR).[105] Less-effective catalysts were found to have a disordered structure, while catalysts that conferred high enantioselectivity were found to display a helical structure. Further analysis of PEG-supported catalysts using circular dichroism (CD) analysis as well as computational (AGADIR) methods supported findings of the correlation between catalyst activity and helicity.[109]

Ohkata and co-workers also documented the importance of peptide catalyst helicity for enantioselectivity in the Juliá−Colonna epoxidation.[110] A set of leucine oligomers possessing the helix-inducing residue Aib was prepared. Notably, these catalysts are soluble in a variety of organic solvents, allowing IR absorption spectra to be taken in solution. From IR measurements, a correlation between catalyst activity and degree of helicity was established.

In 2001, Berkessel and co-workers made further contributions to deciphering the mechanism with a combination of synthetic and computational methods.[111] A series of discrete-length leucine oligomers bound to NH$_2$-TentaGel-S were prepared. Under triphasic conditions, the epoxidation of **37a** was found to be highly enantioselective (>96% ee) using catalysts containing five or more leucine residues. The yield of the reaction improves with increasing main-chain length up to 14 then reaches a plateau. From these experiments, it was concluded that a minimum of one helical turn (i.e., four or more leucine residues) is necessary, with additional residues providing a more highly ordered helix and, thus, a more selective catalyst. The role of the *N*-terminus was also studied. Inverse peptides, or those bound to the solid support at the *N*-terminus in contrast to those bound to the *C*-terminus, with free carboxylic acid termini were found to be completely inactive. Likewise, oligomers of β-amino acids that induce helicity with the opposite orientation of hydrogen bonds were also found to be inactive. These observations suggest that the *N*-terminus is the region of the catalyst responsible for reactivity and selectivity (in corroboration with early mechanistic studies).

Beyond these experimental studies, Berkessel and co-workers also carried out significant computational modeling of peptide−substrate interactions using a Monte Carlo search. These computations suggest that hydrogen bonding between the chalcone carbonyl oxygen atom and the NH of the *N*-terminal (*n*) residue and *n*-2 residue is favored, but there does not appear to be a facial bias. Figure 18a shows one possible orientation of bound **37a**. The resulting peptide−chalcone adduct may bind peroxide through hydrogen bonding with the NH at the *n*-1 position. After this binding, it appears that transfer of peroxide to chalcone can only occur with one orientation of chalcone (thus providing enantioselectivity, Figure 18b). Additionally, binding of (*Z*)-chalcone to the peptide blocks binding of peroxide, explaining the poor reactivity of such substrates (Figure 18c). This three-point binding mode implies that the chirality of the helix determines the stereochemical outcome of the epoxidation, not the chirality of the α-carbon atoms in the backbone of the peptide catalyst. Finally, it was found that the side chains of

Table 34. Poly(amino acid)-Catalyzed Epoxidation under Biphasic Conditions[92]
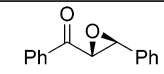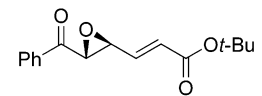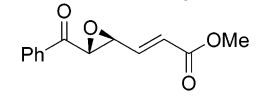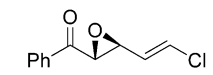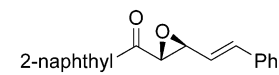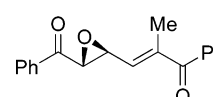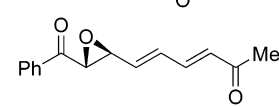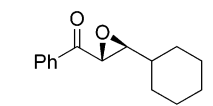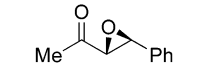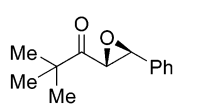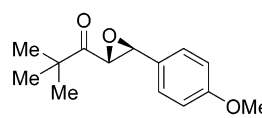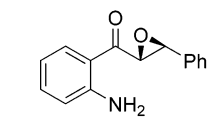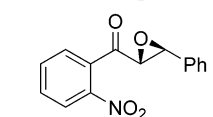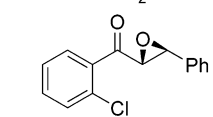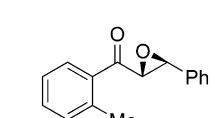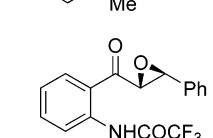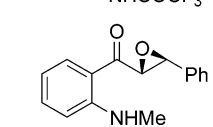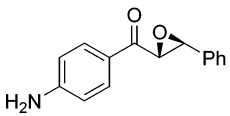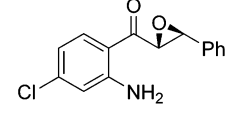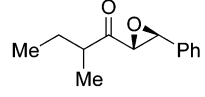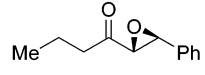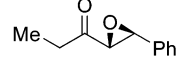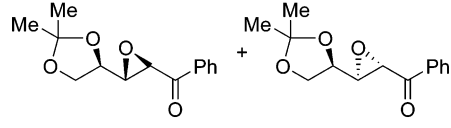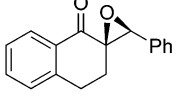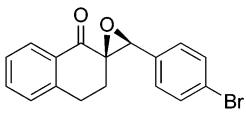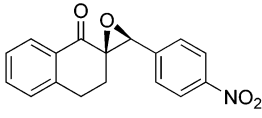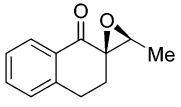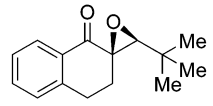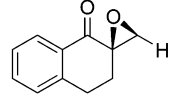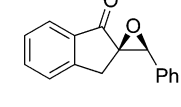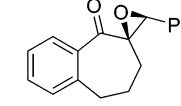
Entry	Product	Method	Yield (%)	ee (%)	Ref.
1		A	85	>95	93
		B	85	>95	96
2		A	95	90	95
3		A	90	90	95
4		A	57	86	95
5		A	85	96	95
		B	85	>98	96
6		A	70	92	95
7		A	43	90	95
8		B	91	89	96
9		B	70	80	96
10		B	76	94	96
11		B	>90	>96	96
12		B	81	>98	97
13		B	91	91	97
14		B	90	89	97
15		B	94	81	97
16		B	59	91	97
17		B	62	96	97

Table 34 (Continued)

Entry	Product	Method	Yield (%)	ee (%)	Ref.
18		B	n.r.	-	97
19		B	91	>98	97
20		A	87	96	98
21		A	85	94	98
22		A	80	82	98
23		B C D E	92 95 96 97	1 : 1 1 : 30 2.4 : 1 1 : 20	99 99 99 99
24		F	76	84	100
25		F	81	82	100
26		F	85	96	100
27		F	66	92	100
28		F	63	83	100
29		F	64	94	100
30		F	72	88	100
31		F	74	59	100

A: UHP, DBU, poly-L-leucine, THF
B: UHP, DBU, CLAMPS-poly-L-leucine, THF
C: UHP, DBU, CLAMPS-poly-D-leucine, THF
D: $Na_2CO_3 \cdot 1.5 H_2O_2$, CLAMPS-poly-L-leucine, DME:H_2O (2:1)
E: $Na_2CO_3 \cdot 1.5 H_2O_2$, CLAMPS-poly-D-leucine, DME:H_2O (2:1)
F: UHP, DBU, CLAMPS-poly-L-leucine, i-PrOAc (slow addition of UHP and DBU)
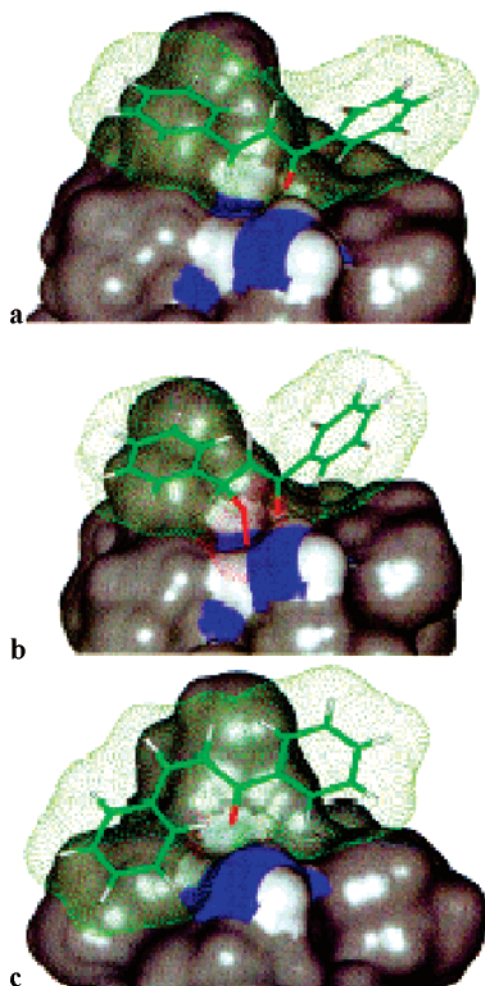
Figure 18. (a) Peptide-bound **37a**. (b) Peroxyenolate resulting from face-selective addition of peroxide. (c) Bound (Z)-**37a**.[111] Reprinted with permission from Berkessel, A.; Gasch, N.; Glaubitz, K.; Koch, C. *Org. Lett.* **2001**, *3*, 3839. Copyright 2001 American Chemical Society.

Scheme 11.
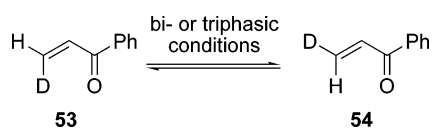
the first three amino acids are not necessary for binding; polyleucine catalysts containing glycine residues at the *N*-terminus [of the structure H₂N(Gly)ₙ(L-Leu)ₘCONH-Tentagel] are effective as long as there are at least four leucine residues incorporated.

Follow-up studies by Berkessel and co-workers[112] addressed the possibility that peptide aggregates may be the catalytically active species. A series of catalysts possessing both L- and D-leucine was synthesized. A linear correlation was found between the percentage of L-leucine and enantioselectivity in the epoxidation of **37a**. The absence of a nonlinear effect suggests that aggregates are *not* catalytically active.

Roberts and co-workers have also performed experiments directed toward delineating the mode of substrate and peroxide binding to the poly-L-leucine catalyst. In kinetic studies of the epoxidation of chalcone (**37a**) using THF-soluble PEG–polyleucine, it was found that the system behaves in an enzyme-like manner.[113,114] That is, saturation
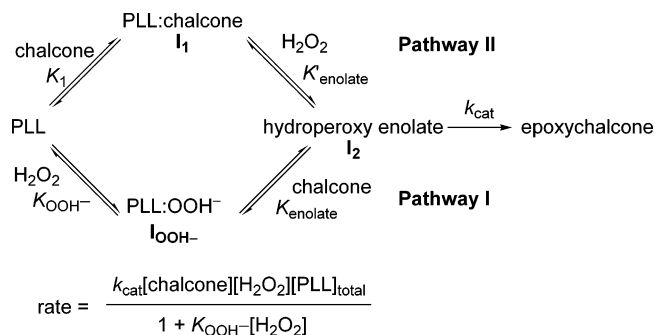
Figure 19. Steady-state random bireactant system and kinetic rate model for poly-L-leucine-catalyzed epoxidation.[113,114,117] Reprinted with permission from Mathem, S. P.; Gunathilagan, S.; Roberts, S. M.; Blackmond, D. G. *Org. Lett.* **2005**, *7*, 4847. Copyright 2005 American Chemical Society.

kinetics were found for both substrate and peroxide. The kinetic profile is consistent with a steady-state random bireactant system[115] in which both substrate and peroxide must bind to catalyst before reaction occurs, with peroxide favored to bind first. A subsequent study has proposed that the first step of the epoxidation process is the reversible addition of peroxide anion, as evidenced by the isomerization of (Z)-3-[²H₁]-phenylprop-2-enone (**53**) to **54** under the reaction conditions (Scheme 11). While isomerization occurs in the absence of catalyst, the rate is accelerated by an order of magnitude in the presence of catalyst.[116a]
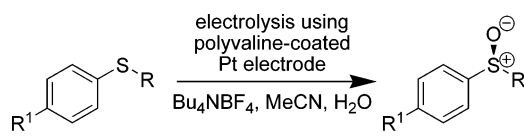
Kelly and Roberts have also developed a model for the mode of asymmetric induction of the Juliá–Colonna epoxidation based on MMX computational studies.[116b] While related to the Berkessel model, there are key differences. Kelly and Roberts propose that poly-L-leucine adopts a helical conformation in which the *N*-terminal amide NH groups are not internally hydrogen-bound. These terminal groups may bind peroxide or water under the reaction conditions. A complex is formed when chalcone (**37a**) displaces the molecules bound at the adjacent *n*-1 and *n*-2 positions, with peroxide still bound at the *n*-3 position. The helical conformation of the complex shields one face of **37a**, allowing face-selective addition of peroxide to occur.

Blackmond and co-workers carried out a detailed kinetic analysis of the Juliá–Colonna epoxidation using calorimetry to monitor the reaction rate.[117] It was found that, after an induction period, the reaction displays a steady-state catalytic cycle (Figure 19). After measuring the reaction rate at many different chalcone concentrations using three chalcone substrates, the data was found to fit a simplified kinetic model in which there is a common binding constant for catalyst binding to hydroperoxide (K_{OOH^-}) and a separate rate constant for each chalcone substrate (k_{cat}). These data suggest that pathway I is operative for the epoxidation while pathway II is negligible.

3.2. Electrochemical Oxidation of Sulfides

A number of oxidation–reduction reactions may be carried out electrochemically, and there has been a great deal of research focused on developing enantioselective versions of such processes. One of the successful strategies is the use of peptide-coated electrodes. Both oxidation and reduction reactions have been accomplished with moderate-to-excellent enantioselectivities using this approach.

Early work on asymmetric electrochemical oxidation by Miller and co-workers showed that graphite electrodes

Table 35. Electrochemical Oxidation of Sulfides[a]

Entry	R	R[1]	Yield (%)	ee (%)
1	Me	H	not reported	2
2	n-Bu	H	not reported	20
3	i-Bu	H	69	44
4	i-Pr	H	56	77
5	c-Hex	H	not reported	54
6	c-Hex	Me	not reported	22
7	t-Bu	H	45	93

[a] For current efficiency, anodic potential and more reaction details, see reference 119.

Scheme 12.
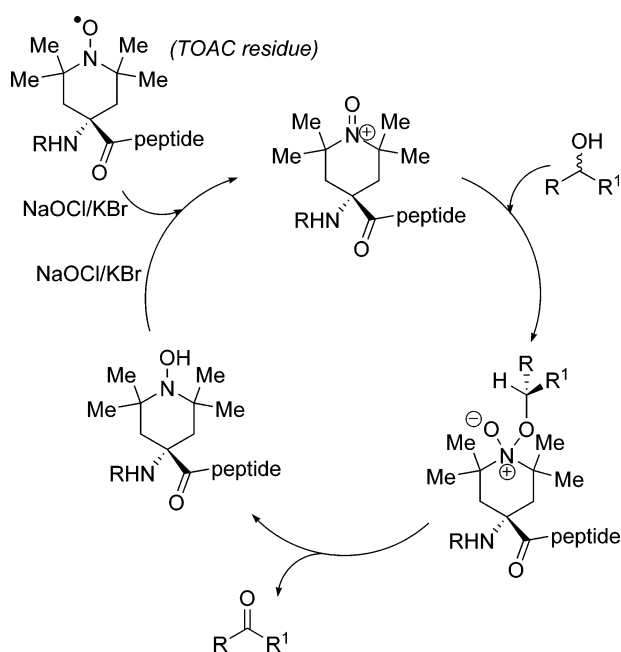
modified with L-phenylalanine methyl ester were capable of inducing enantioselectivity in the oxidation of aryl methyl sulfides to sulfoxides (albeit low, 2.5% ee).[118] Komori and Nonaka further developed this process using poly(amino acid)-coated electrodes.[119,120] It was found that platinum electrodes coated with poly-L-valine provided the best results. The most effective method for poly-L-valine deposition onto the electrode is by first treating the electrode with polypyrrole such that covalent binding occurs, then dip-coating it with a solution of poly(amino acid). Table 35 shows the range of sulfoxides that may be produced nonracemically using this method.

3.3. Oxidation of Secondary Alcohols

In addition to the above-described enantioselective oxidation reactions, peptide catalysts have been employed in asymmetric alcohol oxidation reactions. Specifically, the kinetic resolution of secondary alcohols has been achieved by the use of nitroxyl-containing peptide catalysts. Toniolo and co-workers have demonstrated that a non-natural amino acid, 2,2,6,6-tetramethylpiperidine-1-oxyl-4-amino-4-carboxylic acid (TOAC), can be embedded within a peptide

Scheme 13.
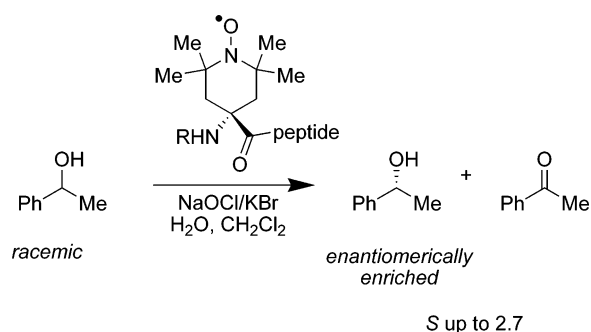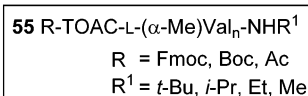
and effectively serve as a redox agent in the presence of alcohols and a NaOCl/KBr solution (Scheme 12).[121]

TOAC was selected as the catalytically active residue not only for its ability to participate in redox reactions but also because of its propensity to induce β-turns due to the C^α-tetrasubstitution pattern. Although TOAC itself is achiral, the strategy creates a chiral environment around this residue through the secondary structure of a peptide. A set of peptide catalysts was designed that possessed TOAC, one-to-several turn-inducing residues (α-methylvaline), and protecting groups for the N- and C-termini (catalysts of type **55** and **56**, Scheme 13). Data from FTIR experiments indicated that these catalysts adopted a β-turn structure, which is corroborated by X-ray diffraction analysis. The catalysts were evaluated for efficacy in the oxidative kinetic resolution of sec-phenylethanol (Scheme 13). It was found that the resolution may be accomplished with S values of up to 2.7. The most selective catalysts possess large lipophilic protective groups at both termini, as well as TOAC at the N terminus. Catalysts that contain valine in place of (C^α-methyl)-valine were found to be inferior, supporting the hypothesis that a β-turn conformation is important for achieving the conformational bias necessary for enantioselectivity.

TOAC-containing peptide catalysts were also evaluated in electrochemical oxidations. Under these conditions, platinum electrodes pass current through a two-phase system of nitroxyl catalyst and alcohol in CH_2Cl_2 (0.017 nitroxyl/alcohol) and buffered aqueous NaBr. The reaction may be monitored over time, and analysis of remaining alcohol shows that the oxidation is modestly enantioselective, with S values up to 1.8. Reduction of the temperature results in a small improvement, with S values up to 3.1 at -10 °C.

4. Enantioselective Reductive Methods

Polypeptides have been used as asymmetric mediators of reduction reactions in the arena of electrochemistry.[122] Several classes of compounds have been enantioselectively reduced including alkenes, carbonyl compounds, oximes, and dihalides.

4.1. Electrochemical Reduction of Alkenes

In 1983, Nonaka and co-workers reported the enantioselective reduction of alkenes conjugated to carbonyls via electrolysis with poly-L-valine-coated graphite electrodes (Scheme 14).[123] The polypeptide may be prepared using the

Scheme 14.

Scheme 15.
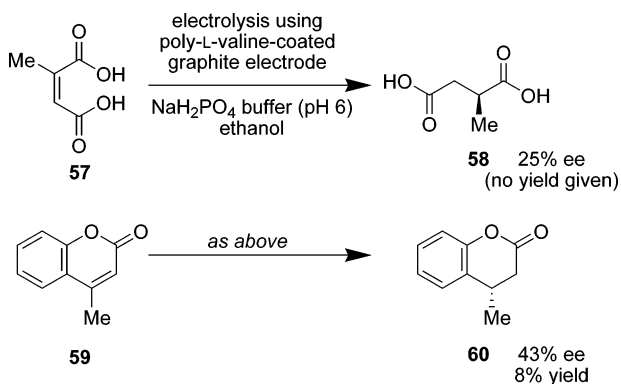
NCA method (described in section 3.1.1) and applied to graphite electrodes using a dip-coating procedure. Electrolysis reactions are best conducted in weakly acidic buffered solutions of substrate in ethanol, while charges of varying amounts and densities were applied with the poly-L-valine-coated graphite electrodes. It was found that citraconic acid (**57**) may be reduced up to 25% ee under these conditions. Increasing the amount of charge and decreasing the reaction time results in a 21% isolated yield of **58** in 21% ee. Under similar conditions, 4-methylcoumarin (**59**) may be enantioselectively reduced to provide **60** in 8% yield, with 43% ee. After one use, the poly-L-valine dip-coated graphite electrodes begin to degrade and exhibit lower enantioselectivity in subsequent runs.[124] To address this durability problem, Nonaka investigated chemically modified electrodes. Graphite plates were treated with 1,3-diaminopropane and then exposed to L-valine NCA. The resulting electrodes were employed in the electrochemical reduction of **37**, and while the enantioselectivity of the process is lower in comparison to the dip-coated electrode runs, the chemically modified electrodes proved to be much more robust. Virtually identical levels of enantioselectivity can be achieved in four consecutive runs.

Follow-up studies were aimed at optimization of the enantioselective electrochemical reduction.[125] Several parameters were examined in the reduction of **57**. First, a series of poly(amino acid)-coated electrodes was prepared and evaluated for asymmetric induction. It was found that among poly-L-valine, poly-D-valine, poly-L-leucine, poly-L-tryptophan, poly-γ-benzyl-L-glutamate, and poly(N-acryloyl-L-valine methyl ester) as coatings for electrodes, poly-L-valine is the best agent for the enantioselective reduction. Interestingly, poly-D-valine-coated electrodes favored the same enantiomer of **58** as poly-L-valine-coated electrodes, although it is lower in enantiomeric excess. This observation is attributed to the chirality of the whole polymer structure, which may not have a simple correlation to the optical rotating power of the monomer units.

In addition to the nature of the polypeptide, the electrode base metal was also examined for effects on enantioselectivity. Graphite was found to be superior to both lead and zinc. Furthermore, an increase in the thickness of the electrode coating did not result in an increase in enantioselectivity.

Temperature was found to have a significant effect on asymmetric induction. While decreasing the temperature from 23 to 0 °C results in a boost in enantioselectivity, further reduction to −20 °C produces a marked decrease in enantioselectivity. Nonaka suggests this may be due to a change in the polypeptide film properties.
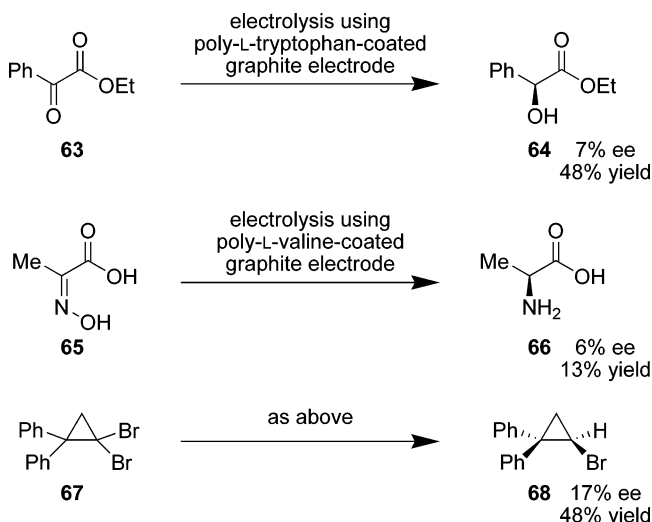
Next, the electrochemical variables were explored. It was found that optimal conditions involve a low cathode potential, a current density of 1.2 A dm^{-2}, and as small amount of charge passed as possible. (More charge, or a longer electrolysis time, results in significantly lower enantioselectivity).

Finally, two other substrates were subjected to the enantioselective electrochemical reduction. Mesaconic acid (**61**), the geometrical isomer of **57**, was reduced under optimal conditions. It was found that **58** is produced with the same absolute configuration but in lower enantiomeric excess than when generated from the reduction of **57**. Under the same conditions, dimethyl citraconate (**62**) was found to undergo essentially nonselective reduction. These results suggest interaction with the chiral electrode coating via hydrogen bonding, and Nonaka proposes that the mode of asymmetric induction involves asymmetric electron transfer rather than enantioselective protonation.
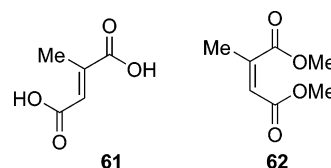
4.2. Electrochemical Reduction of Ketones, Oximes, and Dihalides

In further studies of enantioselective electrochemical reduction processes, Nonaka and co-workers found that prochiral substrates beyond alkenes may be enantioselectively reduced using poly(amino acid)-coated electrodes (Scheme 15).[126] Ethyl phenylglyoxylate (**63**) is reduced to **64** with 7% ee when poly-L-tryptophan is used as the electrode coating (poly-L-valine is much less effective). Interestingly, the reduction of phenylglyoxylic acid is nonselective (<1% ee) under all conditions reported. Pyruvic acid oxime (**65**) was found to undergo reduction using the poly-L-valine-coated electrode, producing alanine (**66**) in 6% ee. Phenylglyoxylic acid oxime is reduced in 2% ee. Finally, exposure of dibromide **67** to the electrolysis conditions produces monobromide **68** in 17% ee.

5. Enantioselective Protonation

In this section, the use of peptide catalysts for enantioselective protonation will be discussed. Two different strategies

Scheme 16.

$$69 + HS\!-\!\!\!\curlyvee\!\!\!Me + \text{chiral amine catalyst} \rightarrow \text{product} \quad (1)$$
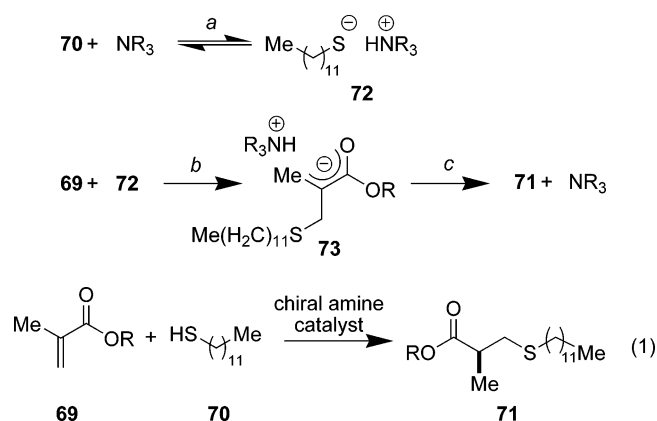
have been employed: enolate generation via conjugate addition to α,β-unsaturated carbonyl compounds followed by enantioselective protonation and direct enantioselective protonation of lithium enolates.

5.1. Protonation of Enolates Generated via Conjugate Addition

One of the earliest examples of peptides as asymmetric catalysts is the enantioselective protonation of enolates derived from a conjugate addition process, developed by Inoue in the 1970s. Preceding work on amine-catalyzed addition of lauryl mercaptan to α,β-unsaturated carbonyl compounds laid the groundwork. In these early studies, it was found that both low molecular weight chiral amines, such as (S)-isobutylethylenimine and corresponding polymeric chiral amines, catalyze the process shown in eq 1 with a modest degree of enantioselectivity.[127] Substrates bearing a β-substituent were examined such as crotonates, maleates, and fumarates. These lead to products with a stereogenic center at the β-carbon atom (at which the addition occurs), but the extent of asymmetric induction is generally more limited than that with methyl acrylates (e.g., **69**).

The proposed mechanism is shown in Scheme 16. In the first step (step a), the amine catalyst deprotonates thiol **70** in a reversible manner to produce ion pair **72**. This ion pair interacts with substrate **69** such that the thiolate undergoes conjugate addition to **69**, producing ammonium enolate **73** (step b). Finally, enantioselective proton transfer generates product **71** and liberates the amine catalyst (step c).

Second-generation studies led to the discovery that poly-(amino acids) catalyze the thiol addition process with a higher degree of enantioselectivity than previously observed (Table 36). The first poly(amino acid) investigated was poly(γ-benzyl-L-glutamate) (**75a**), generated via the corresponding NCA.[128] It was found that an approximate polymer length of 10 provides the highest selectivity in CHCl$_3$ (entries 1, 3, and 5). This degree of polymerization corresponds to a high degree of right-handed α-helicity, indicating that the conformation of the peptide is important for asymmetric induction. To further investigate this hypothesis, poly(β-benzyl-L-aspartate) (**75b**) was prepared, as it is known to adopt a left-handed α-helical conformation that is less stable than **75a**.[129] Interestingly, when compared with runs employing catalyst **75a**, the favored product enantiomer (**74**) does not change when **75b** is used (entries 11, 13, 15, and 17) but **74** is delivered in lower optical yield. These results support the

Table 36. Peptide-Catalyzed Thiol Addition−Enantioselective Protonation

catalysts	
R = (CH$_2$)$_2$CO$_2$Bn	**75a**
R = CH$_2$CO$_2$Bn	**75b**
R = Me	**75c**
L-alanine ethyl ester	**76**
L-alanine propylamide	**77**

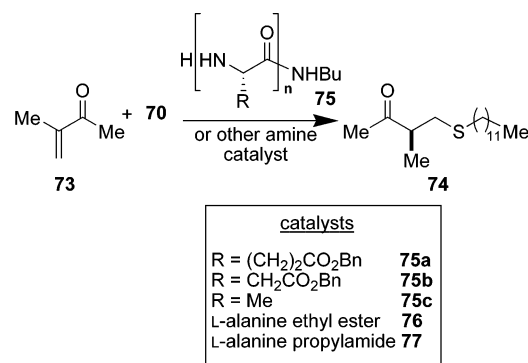| Entry	Catalyst	n	Solvent (v/v)	$[\alpha]_D$ **74**	ee (%)	Ref.
1	**75a**	1	CHCl$_3$	- 0.4	-	127
2	**75a**	1	CHCl$_3$/EtOH (30/2)	- 1.0	-	129
3	**75a**	6	CHCl$_3$	- 0.32	-	127
4	**75a**	6	CHCl$_3$/EtOH (30/2)	- 1.6	-	129
5	**75a**	10	CHCl$_3$	- 2.5	-	127
6	**75a**	10	CHCl$_3$/EtOH (30/2)	- 6.4	37	129, 131
7	**75a**	10	DCE/EtOH (30/1.5)	- 8.2	47	131
8	**75a**	20	DCE/EtOH (30/1.5)	- 7.2	41	131
9	**75a**	25	CHCl$_3$	- 0.68	-	129
10	**75a**	25	CHCl$_3$/EtOH (30/2)	- 4.0	-	129
11	**75b**	1	CHCl$_3$	- 0.3	-	128
12	**75b**	1	CHCl$_3$/EtOH (30/1)	- 0.54	-	129
13	**75b**	5	CHCl$_3$	- 0.05	-	128
14	**75b**	5	CHCl$_3$/EtOH (30/1)	+ 0.12	-	129
15	**75b**	10	CHCl$_3$	- 0.48	-	128
16	**75b**	10	CHCl$_3$/EtOH (30/1)	+ 0.44	-	129
17	**75b**	20	CHCl$_3$	- 0.24	-	128
18	**75b**	20	CHCl$_3$/EtOH (30/1)	+ 0.6	-	129
19	**75c**	3	CHCl$_3$	- 2.0	-	130
20	**75c**	3	CHCl$_3$/EtOH (30/2)	- 2.96	17	130, 131
21	**75c**	5	CHCl$_3$	- 1.28	-	130
22	**75c**	5	CHCl$_3$/EtOH (30/2)	- 2.14	12	130, 131
23	**75c**	10	CHCl$_3$	- 0.84	-	130
24	**75c**	10	CHCl$_3$/EtOH (30/2)	- 1.57	-	130
25	**76**	1	CHCl$_3$	- 0.34	-	130
26	**76**	1	CHCl$_3$/EtOH (30/2)	- 0.64	-	130
27	**77**	1	CHCl$_3$	- 0.65	-	130
28	**77**	1	CHCl$_3$/EtOH (30/2)	- 1.06	6	130, 131

assertion that a stable peptide catalyst conformation is important for asymmetric induction and also suggest that the sense of induction is dictated by the chirality at the N-terminus of catalyst and not the overall handedness of the helix.

Inoue and co-workers also studied the effect of performing the peptide-catalyzed conjugate addition-enantioselective protonation sequence in ethanol.[130,131] As found in earlier studies using nonpeptidic catalysts, with **75a**, **75b**, and poly-(L-alanine) (**75c**), the optical yield increases in the presence of ethanol (i.e., Table 36, compare entries 1−2, 3−4, 5−6, 11−12, 19−20, 21−22, and 23−24), allowing **74** to be isolated in up to 47% ee.[132] In most cases with catalyst **75b**, an inversion in the favored enantiomer occurs in the presence of ethanol (entries 13−14, 15−16, and 17−18). Through IR studies, it was shown that the α-helical tendency of the catalysts did not change to any significant extent in the presence of ethanol. Thus, the increase in enantioselectivity is attributed to a strong association between the catalyst and ethanol, allowing facile proton transfer to the enolate.

It was discovered that product **74** racemizes slowly when exposed to catalyst in CHCl$_3$, but this pathway is mostly

Scheme 17.

Table 37. Dipeptide-Catalyzed Enantioselective Protonation of Enolates

Entry	Substrate	Method	Yield (%)	ee (%)
1	OLi, Me	A / B	71–79 / 65	76–80 / 81
2	OLi, Et	A / B	59 / 61	88 / 13
3	OLi, n-Pr	A	83	24
4	OLi, Me, OMe	A / B	85 / 86	70 / 64
5	OLi, Me, MeO	A / B	91 / 94	45 / 41
6	OLi, Me, O	A / B	nr[b] / 67	15 / 20
7	OLi, Ph	A	65	69

[a] According to Scheme 14; (10 mol %) catalyst **81** used with either method A or B. [b] Not reported.
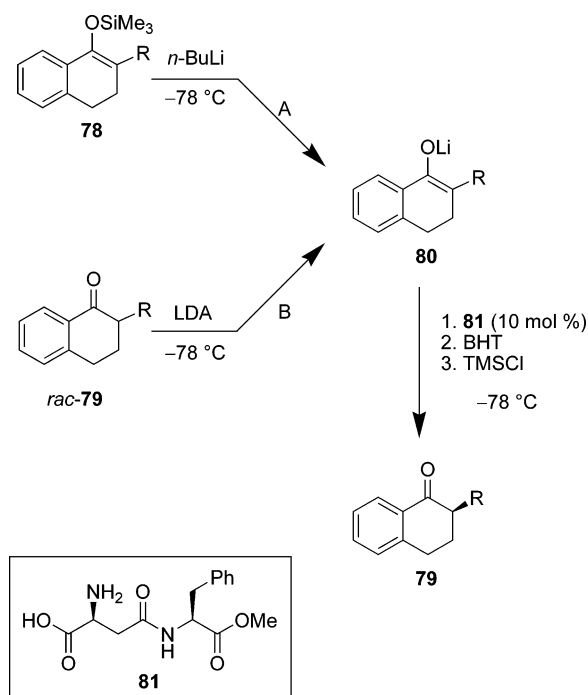
suppressed in the presence of ethanol.[133] The mechanism of racemization is believed to proceed through Schiff base formation between **74** and the free amino group of the catalyst. The suppression is explained by interaction of ethanol with the catalyst amide carbonyl bond,[131] which serves to lower the basicity of the free amino group of the catalyst and slow Schiff base formation.

The importance of secondary structure and catalyst conformation to enantioselectivity is underscored by the inferiority of alanine ethyl ester (**76**) and alanine propylamide (**77**) (Table 36, entries 25–28) compared to peptides **75a** and **75c**.[131] Studies of polymeric peptide catalysts that adopt α-helical and β-sheet structures have led to similar findings: a greater degree of ordered secondary structure tends to give higher enantioselectivity in the conjugate addition–asymmetric protonation sequence.[134] Additionally, peptide catalysts possessing an N-terminal ethylene diamine are less selective, because of the active amino group being farther from the folded portion of the peptide.[135]

5.2. Protonation of Lithium Enolates

Nearly three decades after Inoue's work on peptide-catalyzed enantioselective protonation, Yanagisawa and co-workers[136] reported a complementary strategy for asymmetric peptide-catalyzed protonation of enolates primarily derived from tetralone derivatives. In this strategy, lithium enolates are preformed by treatment of silyl enol ethers (**78**) with n-butyllithium or by direct deprotonation of ketones (**79**) by LDA (Scheme 17, method A or B). Subsequent exposure of the resulting lithium enolate (**80**) to a catalytic amount of a chiral dipeptide proton donor, **81**, and a stoichiometric amount of achiral acid (2,6-di-t-butyl cresol, BHT) results in asymmetric protonation to generate enantiomerically enriched ketone products.

The dipeptide-catalyzed protonation process is enantioselective for a variety of tetralone derivatives (Table 37).[136] Additionally, a simple cyclohexanone-derived enolate also

Scheme 18.

A–H = achiral proton source
*A–H = chiral proton source

undergoes protonation with moderate enantioselectivity (entry 7). For most substrates, the choice of enolate generation method does not significantly change the enantioselectivity (with one exception: entry 2, method A is far superior).

Interestingly, stoichiometric screening of a variety of amino acids, amino acid derivatives, and dipeptides did not provide products with >13% ee; only the catalytic system described above provides good enantioselectivity. The catalytic cycle is believed to proceed as described in Scheme 18.[136] Successful catalytic asymmetric protonation rests upon the relative reactivity of the two possible proton donors. If the achiral acid (BHT) reacts more quickly with the depro-

Scheme 19.

Table 38. Peptide-Catalyzed Enantioselective Conjugate Addition of Azide

Entry	Substrate (R)	Catalyst (°C)	Yield (%)	ee (%)	Ref.
1	**85a** (Me)	**87a** (25)	97	63	137
2		**87b** (25)	90	78	138
3		**87b** (-10)	90	86	138
4	**85b** (Et)	**87a** (25)	91	71	137
5		**87b** (25)	95	77	138
6		**87b** (-10)	83	85	138
7	**85c** (cyclohexyl)	**87a** (25)	79	85	137
8		**87b** (25)	88	89	138
9		**87b** (-10)	65	92	138
10	**85d** (i-Pr)	**87a** (25)	84	82	137
11	**85e**	**87a** (25)	85	71	137
12		**87b** (25)	95	80	138
13		**87b** (-10)	79	87	138
14	**85f**	**87a** (25)	85	45	137
15		**87b** (25)	82	71	138
16		**87b** (-10)	44	78	138
17	**85g** EtO...Me	**87a** (25)	0	--	138

tonated chiral dipeptide proton source than with the lithium enolate, enantioselective catalysis may occur.

6. Enantioselective Conjugate Addition of Azide

Approximately three decades after Inoue's first reports of the poly(amino acid)-catalyzed conjugate addition of thiols/enantioselective protonation protocol, it has been found that peptides are effective catalysts for direct enantioselective conjugate addition reactions. Specifically, Miller and co-workers have reported the enantioselective addition of azide to α,β-unsaturated carbonyl compounds. The products of this method are easily converted to β-amino acids and triazoles with conservation of enantiomeric purity.

In 1999, the discovery of an amine-catalyzed addition of TMSN$_3$ to α,β-unsaturated carbonyl compounds was communicated.[137] As shown in Scheme 19, treatment of enone with an excess of acid and TMSN$_3$ in the presence of a tertiary amine results in smooth azidation. A variety of amine catalysts are effective, including triethylamine, DBU, pyridine, and N-methyimidazole. It was found that resin-bound peptide catalyst **84**, containing a Pmh residue, is a highly competent catalyst for the process, providing azide **83** from enone **82** in 90% yield.

The initial finding that the -Pro-Aib-, β-turn-forming catalyst **84** promotes conjugate azidation led to further studies of chiral peptide catalysts in an attempt to develop an enantioselective version of the process. Screening of β-turn peptides similar to catalyst **84** revealed that, while such catalysts are generally quite effective for conjugate azide addition, they provide racemic products.[138,139] A related class of histidine-containing peptides was studied, those in which the nitrogen distal to the amino acid side chain (the τ nitrogen) is alkylated, as in catalysts **87a** and **87b**. Such peptides turned out to be very promising catalysts, providing products with substantial enantiomeric excesses. The most successful substrates for the azidation a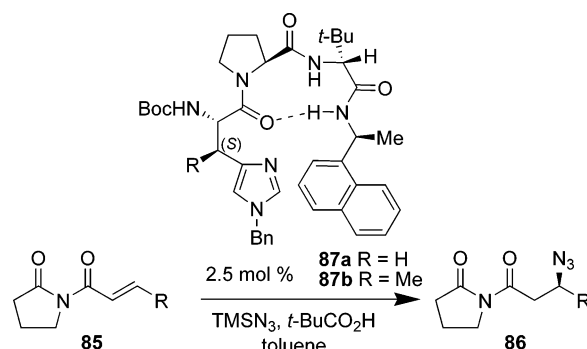re α,β-unsaturated pyrrolidinone-derived imides such as **85**. Peptide **87a** was initially identified as a hit catalyst.[138] As shown in Table 38, azides of structure **86** may be isolated in good yield and in up to 85% ee when the reaction is conducted using **87a** at ambient temperature (entries 1, 4, 7, 10, and 11). Stereochemical and structural changes were made to the β-turn scaffold of **87a** and were found to significantly change and reduce the enantioselectivity of the azidation. Additionally, while simple catalysts possessing only τ-benzyl histidine

promote the reaction, the products are racemic, indicating the important role of the peptidic secondary structure for asymmetric induction.

Further attempts to optimize the enantioselective conjugate azidation procedure focused on dihedral angle restriction within the side chain of the τ-benzyl histidine residue.[139] To accomplish this conformational rigidification, a substituent was introduced at the β-position of the catalytically active histidine residue (as in catalyst **87b**, R = Me). The effects of several substituents were evaluated and, while the enantioselectivity of the azidation was affected differently in each case, methyl-substituted catalyst **87b** consistently provides higher enantioselectivities than those possible with parent catalyst **86a** (see Table 38, substrates **85a**−**85f**). Reduction of the reaction temperature to −10 °C provides optimal results, with azides isolated in up to 92% ee.

Elaboration of the enantiomerically enriched azide products was demonstrated in two ways. First, the azidoimides may undergo reduction, methanolysis, and hydrolysis to the corresponding β-amino acid **88** in good yield over multiple steps (eq 2). Second, the azide products have been shown to participate in both intra- and intermolecular 1,3-dipolar cycloadditions with alkynes (such as **89**, eqs 3 and 4), furnishing triazoles (**90** and **91**) with conservation of enantiomeric excess from the azidation process.

$$(2)$$

86a → **88**
52% Yield
over all steps

$$(3)$$

89 → **90**
86% ee
83% Yield

$$(4)$$

85c → **91**
92% ee
73% Yield
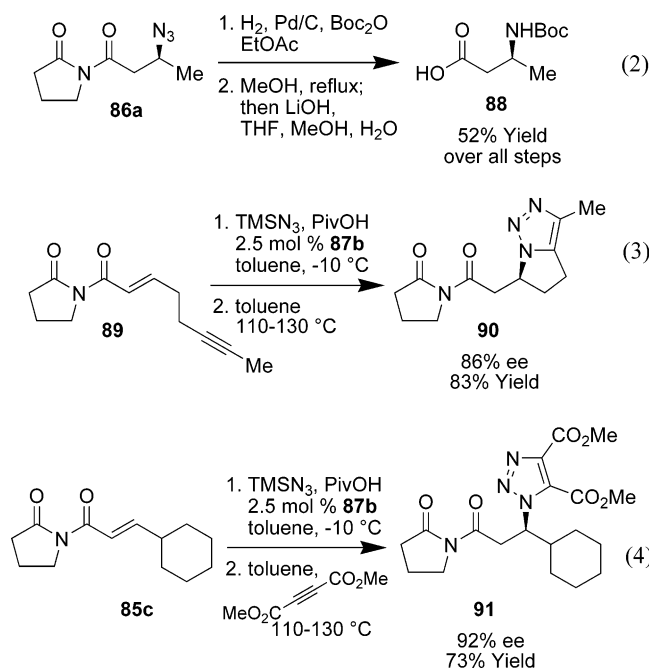
7. Peptide-Catalyzed Hydrolysis of Esters

7.1. Peptide Dimers, Trimers, or Tetramers in Micellar and/or Vesicular Systems

Enzymatic hydrolysis has been well-studied. Secondary structure of enzymes and the interaction between active binding pockets with substrates provide efficient reactivity and selectivity in many cases. Increasing attention has been focused on the development of smaller hydrolysis catalysts that could mimic enzymatic mechanisms to introduce efficiency and selectivity toward a variety of substrates.

Micellar and vesicular catalysis[140] have been studied since the 1970s in order to develop stereoselective hydrolyses of enantiomeric esters and to understand the origin of stereoselectivity in proteolytic enzymes.[141] Normal surfactants[140a] as well as amino acid-functionalized surfactants[140b−e] have been used to induce stereoselectivity in the hydrolysis of

Table 39. Effects of Acyl Chain Length in the Enantioselective Hydrolysis of p-Nitrophenyl N-Acylphenylalanylates (92) by a Dipeptide (93) in a Cationic Chiral Surfactant-(+)-SUR$_{18}$

92 → **93** (+)-SUR$_{18}$
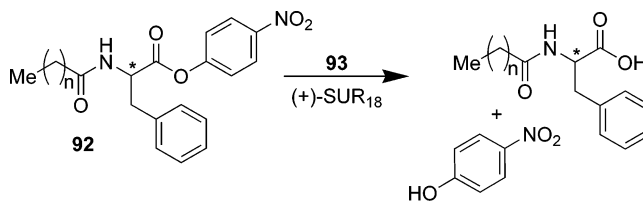
Entry[a]	n	k_{cat}/l mol^{-1} s^{-1}		k_{cat}^{L}/k_{cat}^{D}
		L	D	
1	0	33	34	1.0
2	4	186	71	2.6
3	8	286	52	5.5
4	10	332	58	5.7
5	12	346	61	5.7
6	14	334	61	5.5

[a] Tris buffer (0.08 M) containing 0.08 M KCl at 25 °C (pH 7.61) in 10% (v/v) MeCN-H$_2$O; [**93**] = 9 × 10^{-5} M, [**92**] = 5 × 10^{-5} M, and [(+)-SUR$_{18}$] = 1.8 × 10^{-3} M.

racemic esters of amino acids. Single amino acid derivatives,[140f−p] especially N^α-protected histidine derivatives, have been well-examined in ester hydrolysis with either chiral or achiral surfactants. Significant rate enhancements and reasonable stereoselectivities have been observed.

Later efforts were focused on the catalytic system of dipeptide- or tripeptide-type nucleophiles with surfactants. In 1980, Ohkubo, Ueoka, and co-workers[142] reported the

Substrate: **92**
(n = 0, 8,12)
p-nitrophenyl-N-acylphenylalanylates

Catalyst:
R = OCH$_2$Ph, R' = CH$_2$Ph   Z-L-Phe-L-His-OH
R = OCH$_2$Ph, R' = CH$_2$Ph   Z-D-Phe-L-His-OH
R = OCH$_2$Ph, R' = CH$_2$CHMe$_2$ Z-L-Leu-L-His-OH
R = (Dod)C$_{11}$H$_{23}$, R' = CH$_2$CHMe$_2$ Dod-L-Leu-L-His-OH

R = OCH$_2$Ph   Z-L-His-OH
R = C$_{11}$H$_{23}$ Dod-L-His-OH

Surfactant:

N,N-didodecyl-N,N-dimethylammonium bromide
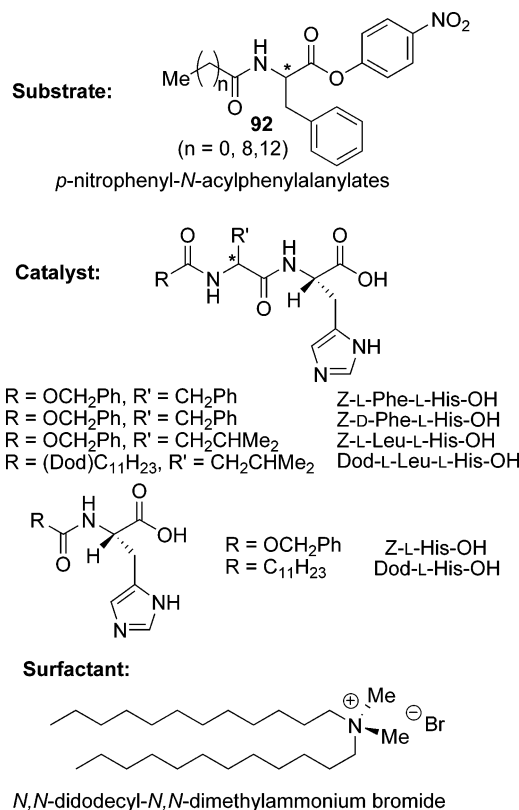
Figure 21. Peptide catalysts for hydrolysis of p-nitrophenyl N-acylphenylalanylates (**92**) in a surfactant.

Substrate: **92**
p-nitrophenyl-N-acylphenylalanylates

Surfactant: (+)-SUR$_{18}$

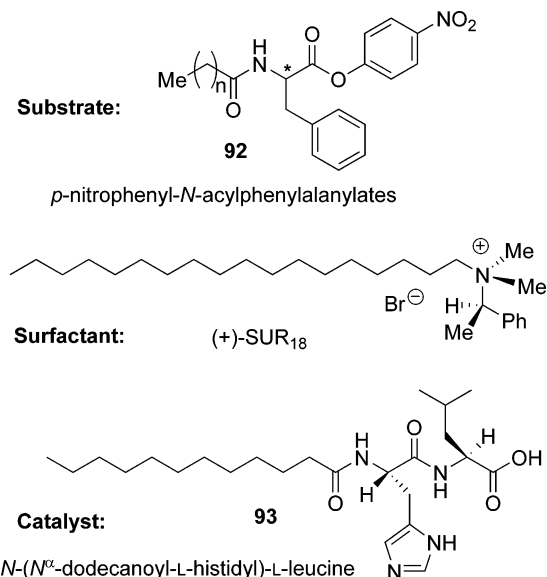**Catalyst:** **93**
N-(N$^\alpha$-dodecanoyl-L-histidyl)-L-leucine

Figure 20. Enantioselective hydrolysis of p-nitrophenyl N-acylphenylalanylates (**92**) by a dipeptide (**93**) in a cationic chiral surfactant ((+)-SUR$_{18}$).

Table 40. Peptide Catalysts for Hydrolysis of *p*-Nitrophenyl *N*-acylphenylalanylates (92) in a Surfactant

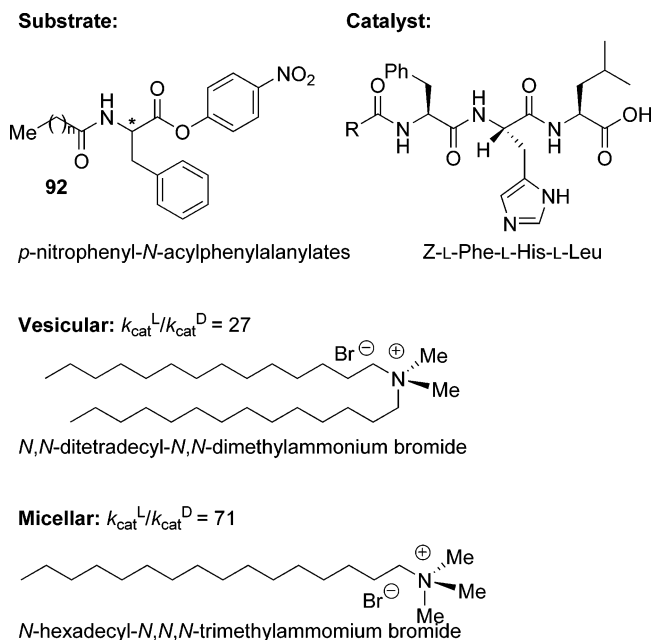| | | | $k_{cat}/1\ mol^{-1}\ s^{-1}$ | | | | | |
| | | | 92; n = 0 | | 92; n = 8 | | 92; n = 12 | |
Entry[a]	Catalyst		25 °C	10 °C	25 °C	10 °C	25 °C	10 °C
1	Z-L-Phe-L-His-OH	L	640	340	4506	2596	2094	978
		D	50	18	152	62	160	42
		L/D	12.8	18.9	**29.6**	**41.9**	13.8	**23.3**
2	Z-D-Phe-L-His-OH	L	88	34	434	286	388	122
		D	72	14	222	94	180	58
		L/D	1.2	2.4	2.0	3.0	2.3	2.1
3	Z-L-Leu-L-His-OH	L	380	154	2282	836	1016	320
		D	38	4	104	10	92	4
		L/D	10.2	**38.0**	**22.5**	**83.6**	11.0	**80.0**
4	Dod-L-Leu-L-His-OH	L	1084	542	4318	2148	1654	764
		D	156	56	654	270	538	190
		L/D	6.9	9.8	6.6	8.0	3.0	4.0
5	Z-L-His-OH	L	20		44		68	
		D	34		62		40	
		L/D	0.6		0.7		1.5	
6	Dod-L-His-OH	L	392	200	1768	1100	1550	598
		D	240	114	380	200	398	144
		L/D	1.6	1.8	4.7	5.5	3.9	4.2

[a] Tris buffer (0.08 M) containing 0.08 M KCl at 10-25 °C (pH 7.68) in 3% (v/v) MeCN-H$_2$O, and the stock solutions were prepared by dissolving the nucleophile and (**92**) in Tris-KCl buffer by sonication at 45 °C for 1 h: [catalyst] = 5 x 10^{-5} M, [surfactant] = 1 x 10^{-3} M, and [substrate (**92**)] = 1 x 10^{-5} M.

enantioselective deacylation of long chain *p*-nitrophenyl *N*-acyl phenylalanylates (**92**) by *N*-(*N$^\alpha$*-dodecanoyl-L-histidyl)-L-leucine (**93**) and a cationic chiral surfactant, (*R*)-(+)-*N*-α-methylbenzyl-*N,N*-dimethyloctadecyl ammonium bromide ((+)-SUR$_{18}$) (Figure 20). Enhanced enantioselectivity (k_{cat}^L/k_{cat}^D = 5.7, *n* = 10, 12; Table 39, entries 4 and 5, respectively) was observed for substrates with relatively longer acyl chains.

In 1982, Ohkubo and co-workers[143] reported a highly stereoselective hydrolysis of amino acid esters in bilayer vesicular systems. Dipeptide-type nucleophiles (Figure 21) were examined for hydrolysis by using an achiral cationic double-chain surfactant, *N,N*-didodecyl-*N,N*-dimethylammonium bromide. Dipeptide Z-L-Leu-L-His-OH was the most general and selective catalyst for enantioselective hydrolysis, providing k_{cat}^L/k_{cat}^D up to 83.6 at 10 °C (Table 40, entry 3).

An enhanced enantioselective hydrolysis with a tripeptide catalyst in a mixed surfactant system was reported by Ueoka and co-workers in 1984.[144] Enantioselective hydrolysis of *p*-nitrophenyl-*N*-dodecanoyl (D,L)-phenylalanylate (**92**, *n* = 10) by tripeptide Z-L-Phe-L-His-L-Leu-OH gave k_{cat}^L/k_{cat}^D = 27 in the vesicular system (*N,N*-ditetradecyl-*N,N*-dimethyl-ammonium bromide) (Figure 22). The selectivity was significantly improved by the addition of micelles (*N*-hexadecyl-*N,N,N*-trimethylammomium bromide) at 25 °C, providing k_{cat}^L/k_{cat}^D = 71.[145a] It has been suggested that the hydrophobic microenvironment of the membrane matrix changed at the optimum temperature for the enhancement of stereoselectivity.[145]

Structural studies have been undertaken in order to elucidate the origin of enantioselectivity. Two active peptide catalysts for hydrolysis, Z-L-Phe-L-His-L-Leu-OH and Z-L-Phe-L-His-OH, share the same specific circular dichroism (CD) patterns in MeOH−H$_2$O (235 nm),[146] suggesting the

Substrate: **Catalyst:**

92

p-nitrophenyl-*N*-acylphenylalanylates   Z-L-Phe-L-His-L-Leu

Vesicular: k_{cat}^L/k_{cat}^D = 27

N,N-ditetradecyl-*N,N*-dimethylammonium bromide

Micellar: k_{cat}^L/k_{cat}^D = 71

N-hexadecyl-*N,N,N*-trimethylammomium bromide

Figure 22. Hydrolysis in a vesicular−micellar system.

rigid conformation of L-Phe-L-His. Peptide Z-L-Phe-L-His-L-Leu-OH shows an α-helix-like CD curve, and its CD spectrum was also compared to that of a known α-helix peptide (mastoparan).[147] It appears that a hydrophobic pocket forms through intramolecular interactions between amino acid residues. The L-enantiomer may be properly oriented for hydrolysis, while the D-enantiomer does not fit as well. Optimizing the composition of coaggregates improved the hydrophobic microenvironment to induce the highest enantioselectivity.
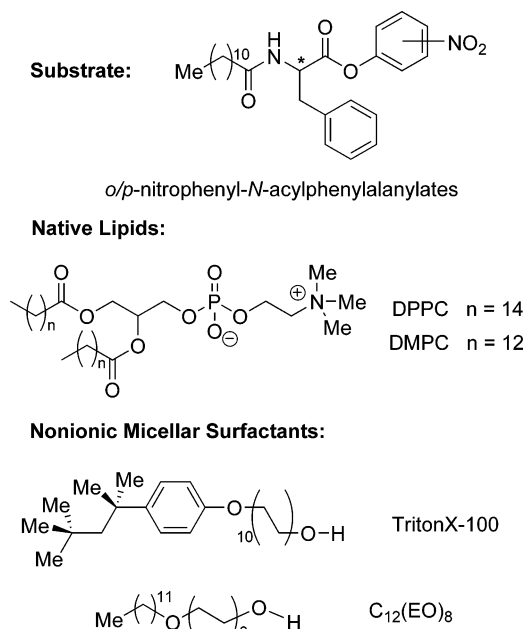
Substrate:

o/p-nitrophenyl-*N*-acylphenylalanylates

Native Lipids:

DPPC n = 14
DMPC n = 12

Nonionic Micellar Surfactants:

TritonX-100

$C_{12}(EO)_8$

Figure 23. Native lipids and nonionic micellar surfactants.

D-ester (Z-L-Leu-L-His-OH)

94

95
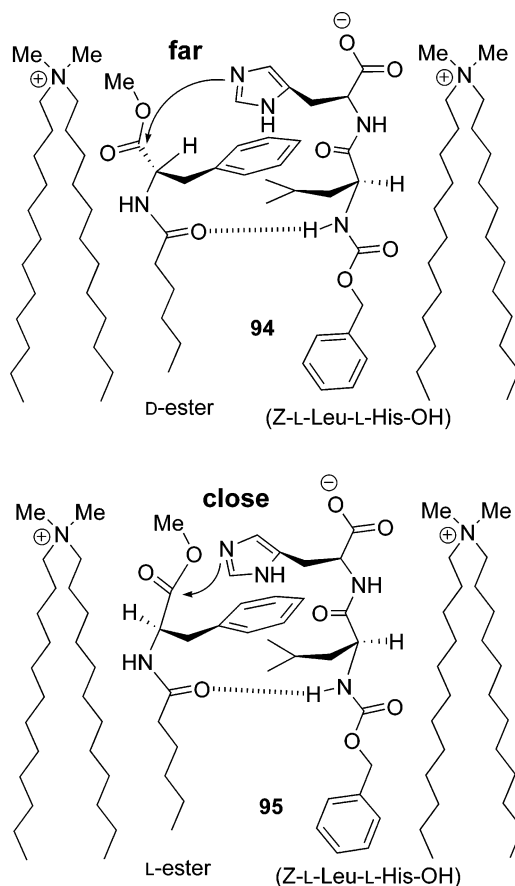
L-ester (Z-L-Leu-L-His-OH)

Figure 24. Interaction between peptide catalyst (*Z*-L-Leu-L-His-OH) and D- or L-methyl *N*-acylphenylalanylate in the double-chain surfactants.

The sequence of the peptide,[148] change in surfactant composition and concentration,[149] isokinetic temperature,[149d,150] experimental temperature,[149d,151] and ionic strength factors[152] have been fully studied in detail by different research groups.

In the additional studies of enantioselective hydrolysis of amino acid esters, Ueoka and co-workers also applied hybrid liposomes composed of native lipid[153] (L-α-dipalmitoylphos-

Scheme 20. Hydrolysis of Peptide Esters with Thio-Functionalized Surfactant
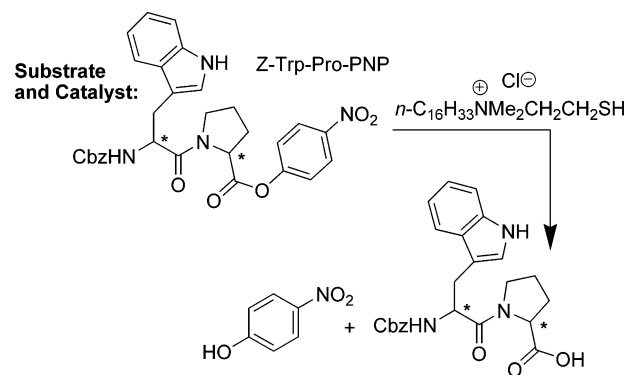
phatidylcholine (DPPC)[153a] or L-α-dimyristoylphosphatidyl-choline (DMPC)[153b]) and nonionic micellar surfactant (TritonX-100[153a] or polyoxyethylene lauryl ether $(C_{12}(EO)_8)$[153b]) (Figure 23).

For the hydrolysis of amino acid esters in a natural lipid coaggregate system, the reaction temperature and the composition of surfactants influence the stereoselectivity by means of changing the hydrophobicity and the fluidity. It is noteworthy that significant enantioselectivity enhancements can be obtained around the phase separation and/or the phase-transition temperature of the surfactants.

In order to investigate the details of membrane-promoted stereoselective esterase-like activity of the peptide catalysts, and also to understand why dipeptide Z-L-Leu-L-His-OH or tripeptide Z-L-Phe-L-His-L-Leu-OH is the most efficient in terms of catalytic and stereoselective activities, Ohkubo and co-workers[154] showed the role of the membrane-assisted hydrophobic interactions between the peptide catalyst and the enantiomeric substrates by ^{1}H NOESY (nuclear Over-hauser enchancement spectroscopy) spectra.[154a,b] NOESY experiments of Z-L-Leu-L-His-OH and *N*-hexanoyl-L/D-Phe methyl esters in the vesicular system (Figure 24) indicated the interactions between the phenyl side chain of the substrate with L-Leu and L-His side chains of catalyst. Although an intermolecular amide hydrogen bond might be present, it was not detected, probably because of H−D exchange in D_2O. Both L- and D-substrates shared identical NOESY spectra,[154b,c] indicating the origin of stereoselectivity is in the catalyst−substrate reaction step instead of the catalyst−substrate binding process.

High stereoselectivity was obtained by intensifying hydrophobic interactions between catalyst and substrates. Membrane played a key role in bringing the catalyst and the substrate together. Good hydrolysis activity and substrate-specificity for the L-ester resulted from the facilitated formation of catalyst−substrate complex and then enantiomer recognition in the reaction step of the complex. The distance between the nucleophilic nitrogen site of the His moiety in peptide Z-L-Leu-L-His-OH and the sp^2 carbon center of the D-esters allowed the D-esters to undergo hydrolysis at a much slower rate than the L-esters (Figure 24; **94**, with D-esters; **95**, with L-esters). A similar interaction mode for the corresponding tripeptide (Z-L-Phe-L-His-L-Leu-OH) has also been proposed.[154c]

In a different approach to the stereoselective hydrolysis of amino acid esters, peptide esters were also examined as the substrates for diastereoselective hydrolysis by the groups of Moss,[140p,155a−f] Ueoka,[155e−j] Ohkubo,[155k] Cho,[155l] and Nolte.[155m] In these cases, the catalyst is also the substrate.

Table 41. Diastereoselectivity for the Hydrolysis of Dipeptide Esters in Buffer Solution

Entry[a]	Substrate/Catalyst Dipeptide esters	k_s (s^{-1}) DL	LL	D.R.	Temp (°C)
1	Z-Phe-Phe-PNP	0.356	0.00351	DL/LL = **101**	32.5
2	Z-Phe-Leu-PNP	0.266	0.00372	DL/LL = **71**	32.5
3	Z-Leu-Phe-PNP	0.0194	0.389	LL/DL = 20	28.5
4	Z-Leu-Leu-PNP	0.164	0.377	LL/DL = 2.3	30.0

[a] pH 9.5, 0.02 M Carbonate buffer (0.05 M KCl), 10% (v/v) CH$_3$CN-H$_2$O, [Sub] = 5 X 10^{-6} M

Thiol-functionalized surfactant (n-C$_{16}$H$_{33}$N$^+$Me$_2$CH$_2$CH$_2$-SHCl$^-$) micelles have been used[155d] to facilitate the hydrolysis of Z-Trp-Pro p-nitrophenyl esters (Scheme 20). Ester cleavage of the L,L-substrate was 5−6 times faster than that of its D,L-diastereomer.

In the hydrolysis of diastereomeric dipeptide p-nitrophenyl esters, Z-D/L-Pro-L-Pro-PNP or Z-D/L-Trp-L-Pro-PNP in micelles,[155f] there is a modest preference for LL-diastereoselectivity for Z-Pro-Pro-PNP dipeptide esters in the intermolecular hydrolysis.

Preferred conformations and energies of the substrate (Z-Pro-Pro-PNP) in the ground state and at the tetrahedral intermediate stage (formed during attack on the ester carbonyl by a nucleophile) were calculated by a combination of molecular mechanics and molecular orbital calculations. The calculated energy difference was consistent with the observed LL-selectivity. The dihedral angle strains (torsions) of the peptide and involved bonds that rehybridized from sp^2 to sp^3 in the transition state contributed to the diastereoselectivity of the hydrolysis process. The strain was greater for the DL substrate, thus reacting more slowly.[155f]

In the case of Z-AA-Pro-PNP (AA = Ala, Phe, Leu, Val, and Trp),[155a−b,f] the hydrolysis was DL-diastereoselective. The reaction proceeded mainly through intramolecular cyclization to the corresponding 2,5-diketopiperazines and through intermolecular attack by hydroxide ion. The Pro-PNP moiety in these substrates played an important role. The intramolecular cyclization was more favorable for the DL-isomer, which afforded a larger k_{DL}/k_{LL}. The nature of nucleophile had a significant effect on the diastereoselectivities. The hydrolysis proceeding through direct attack of hydroxide ion was LL-diastereoselective. For example, the hydrolysis for Z-Trp-Pro-PNP was DL-diastereoselective at pH 8.0 because of the more favorable diketopiperazine cyclization. However, LL-diastereoselectivity, which could be significantly enhanced in functional micellar systems, was obtained at a higher pH (10.0). At this pH, attack by hydroxide ion at the ester carbonyl was dominant.[155f]

Ueoka and co-workers[155g−j] reported highly diastereoselective hydrolytic processes of dipeptide esters in a buffered solution without the use of surfactants. In the hydrolysis of peptide esters, diastereoselectivity could be regulated by controlling temperature, substrate concentration, and pH of the reaction medium.[155i,j] As shown in Table 41, at the optimum temperature (32.5 °C), peptide Z-Phe-Phe-PNP gave $k_{DL}/k_{LL} = 101$ (entry 1) while the peptide Z-Phe-Leu-PNP provided $k_{DL}/k_{LL} = 71$ (entry 2) in a 0.02 M buffered solution at pH 9.5.[155h] The rate of the hydrolysis of Z-D-Phe-Phe-PNP increased with the temperature elevation from 31.5 to 32.5 °C, but this was not the case for the Z-L-Phe-L-Phe-PNP substrate. The temperature effect was the opposite

Scheme 21. Synthesis of Disulfide-Bridged Peptide Dendrimers

	A^3	A^2	A^1
96	Ser	Asp	His
97	Asp	Ser	His
98	Asp	His	Ser
99	Ser	His	Asp
100	His	Asp	Ser
101	His	Ser	Asp

Dendrimers **96-101**

21 dimeric dendrimers
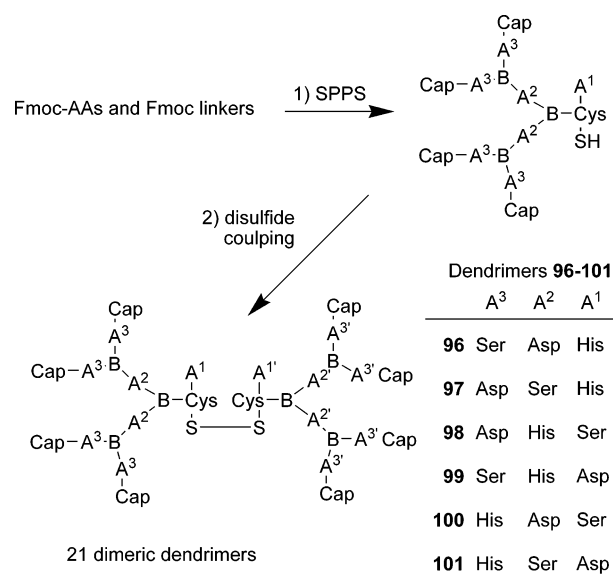
Scheme 22. Peptide Dendrimer-Catalyzed Ester Hydrolysis Reactions

$\lambda_{exc} = 350$ nm
$\lambda_{em} = 505$ nm

102a (R = Me)
102b (R = C$_5$H$_{11}$)
102c (R = CHMe$_2$)

(R)-**102d** R =
(S)-**102d** R =

Branch Unit 103a   **Branch Unit 103b**   **Branch Unit 103c**

Cap=

Branch Unit 103d
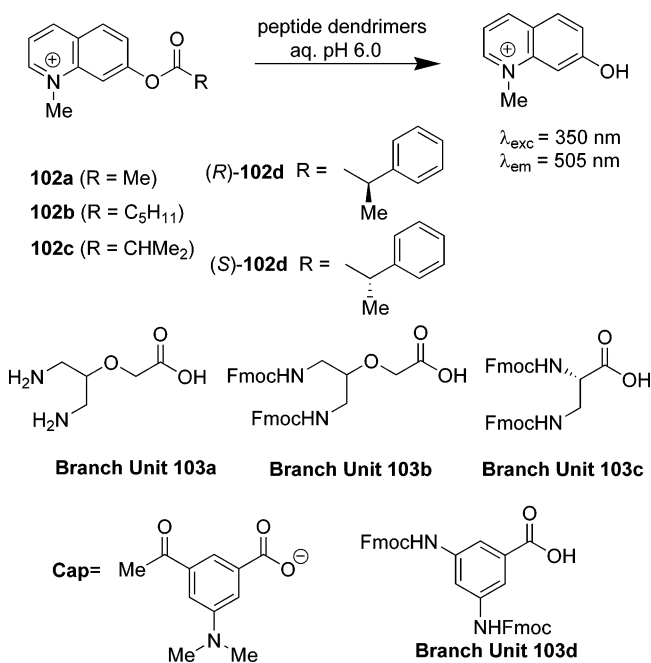
for the Z-Leu-Phe-PNP substrates. Dipeptide esters (Z-Phe-Phe-PNP and Z-Phe-Leu-PNP) having a common Z-Phe unit usually produced larger rate enhancements for the hydrolysis of DL-esters than LL-isomers. On the other hand, hydrolysis of peptide esters with a common Z-Leu unit (Z-Leu-Phe-PNP and Z-Leu-Leu-PNP) favored the LL-diastereomers.

7.2. Peptide Dendrimers and Other Polypeptides

Dendrimers are treelike macromolecules of well-defined size, which emerged as a new class of compounds in the 1970s. Reymond and co-workers[156] applied the dendritic architecture to peptides for artificial enzyme studies.

Dendrimeric peptides (**96−101**) were synthesized with the sequence ((CapCONH-A^3)$_2$(Branch)A^2)$_2$-(Branch)-Cys-A^1-NH$_2$ by alternating amino acids with a branching unit (Scheme 21),[156d] using solid-phase peptide synthesis (SPPS).
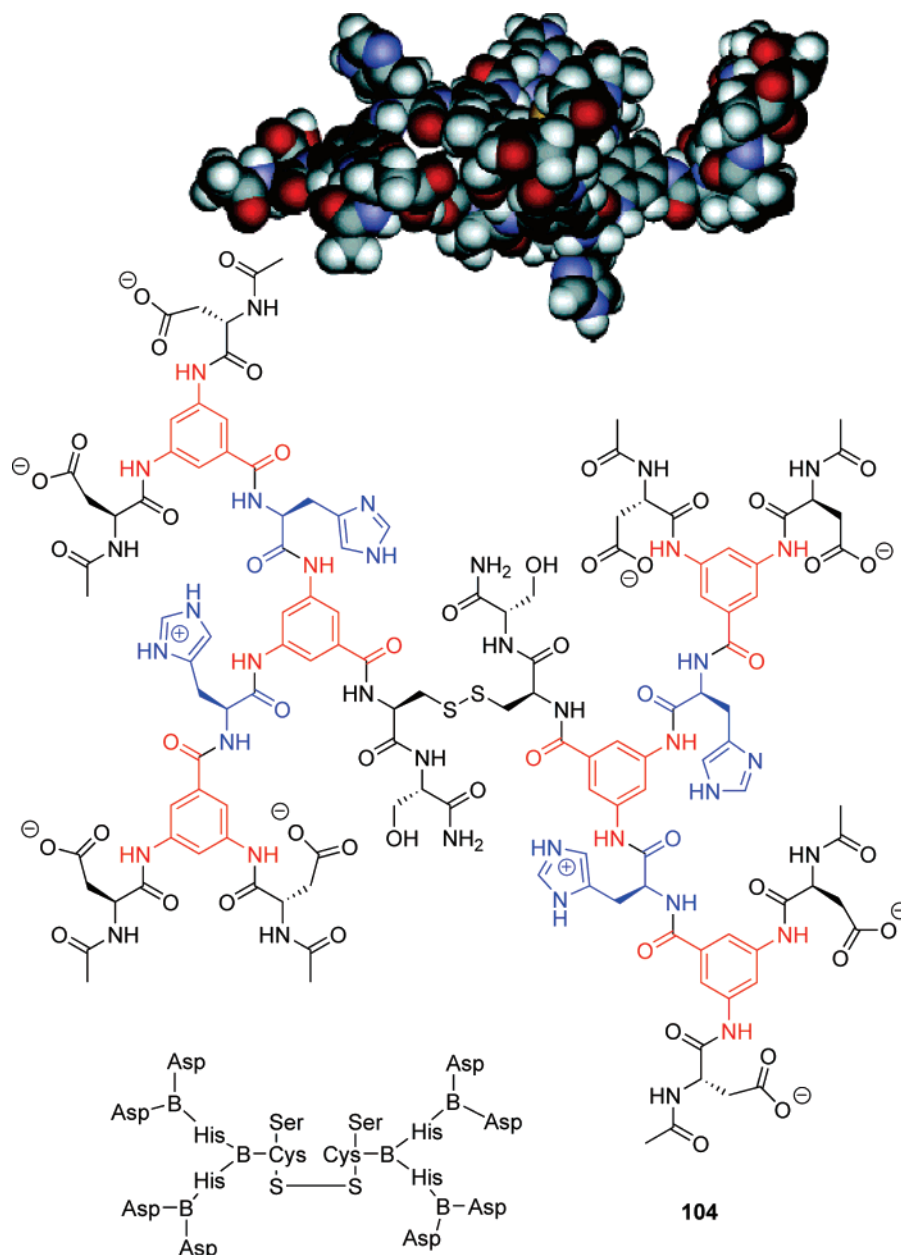
Figure 25. Structural formula and energy-minimized model of dendrimer **104** containing 3,5-diaminobenzoic acid (**103**) as a branching unit.[156d] Reprinted with permission from Darbre, T.; Reymond, J.-L. *Acc. Chem. Res.* **2006**, *39*, 925. Copyright 2006 American Chemical Society.

Monomers were then dimerized by disulfide bond formation through cysteine residues. Peptide dendrimers were obtained with a molecular weight of 3−5 kDa, with three layers of two amino acids close to the core, four in the middle layer, and eight near the surface.
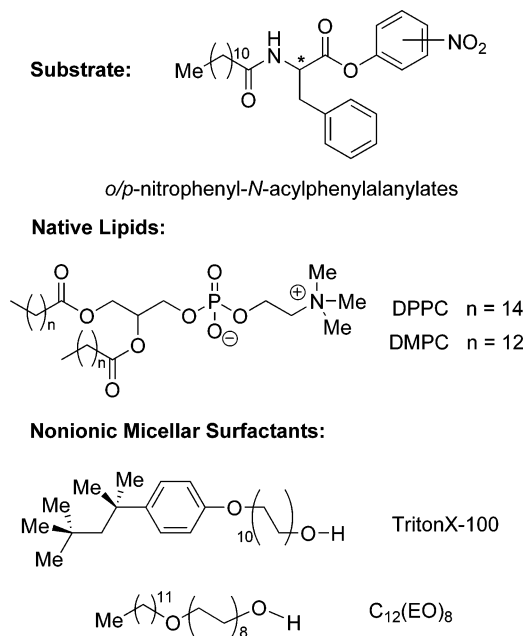
Aspartate (Asp), histidine (His), and serine (Ser), the functional groups present in most esterases[154c] and lipases, were chosen to take positions A[1], A[2], and A[3], respectively. Dendrimer peptides were capped by 3-dimethylaminoisoph-thalamide (Cap, inserted as the mono-*t*-butyl ester), which could introduce additional interaction with substrates (Scheme 22).

The peptide dendrimer library was studied for the hydrolysis of a series of fluorogenic esters (Scheme 22). When symmetrical δ,δ-diamino acid **103a** and symmetrical bis-β-alanine **103b**[156a] or α,β-diaminopropionic acid **103c**[156b] were used as branching units, significant rate acceleration was

obtained. Enantiomeric esters (***R/S***)-**102d** were also accepted as the substrates. However, no significant chiral discrimina-tion by the dendrimers was observed.[156b,d]

3,5-Diaminobenzoic acid **103d** was then examined as a rigid branching unit.[156c] The structure of **103d** would be able to induce favorable hydrophobic or π-stacking interactions with substrates. Dendrimers derived from **103d** were simply acetylated at the *N*-terminus. These dendrimer peptides adopt a more extended and relatively open structure, which allows substrate access to the interior of the catalyst. Dendrimers in this library demonstrated good catalytic activities and selectivities. Strong catalytic activity with substrates **102a**−**102d** were shown by 2 out of 21 dimers, while the other 19 were essentially inactive.

The most active dendrimer (**104**, monomeric dendrimer; Figure 25), containing peripheral aspartate and internal histidine residues, also exhibited significant chiral discrimi-

Scheme 23. Mechanistic Proposal for Dendrimer-Catalyzed Ester Hydrolysis

o/p-nitrophenyl-*N*-acylphenylalanylates

Native Lipids:

DPPC   n = 14

DMPC   n = 12

Nonionic Micellar Surfactants:

TritonX-100

$C_{12}(EO)_8$

nation toward enantiomeric esters 2-phenylpropionate **(S)-102d** and **(R)-102d**, with an enantiomeric ratio $E = 2.8$ [$E = (k_{cat}/K_M((S)\text{-}\mathbf{102d}))/(k_{cat}/K_M((R)\text{-}\mathbf{102}))$] in favor of the (S)-enantiomer (Scheme 22).[156c] It has been suggested that electrostatic interactions between the surface aspartates and the cationic quinolinium group contribute to the selectivity. Significant chiral discrimination in the hydrolysis of chiral substrate **102d** confirmed substrate−catalyst interactions. Dendrimer-catalyzed hydrolysis of hydroxypyrenetrisulfonate esters (−OPTS)[156e−h,j] (Scheme 23) have also been reported.

A structure−activity-relationship (SAR) study of the hydrolysis reaction was carried out by an alanine scan. Exchange of histidine-to-alanine of the active dendrimers resulted in inactive dendrimers. However, corresponding serine-to-alanine replacement had only a small effect on reaction rate, suggesting that histidine catalysis occurred without the direct participation of the serine hydroxyl groups.[156a,d]

It is noteworthy that alanine replacement for only one single histidine resulted in a 75% activity loss. Nondimerized monomers (such as **96−101**, Scheme 21) with only two histidines were inactive for hydrolysis. This evidence indicated a cooperative effect of these residues. On the basis of the results from pH−k_{cat} studies, bifunctional catalysis by two histidine residues was suggested, with one serving as a nucleophile path a, Scheme 23 or a general base path b, Scheme 23 and another protonated histidine stabilizing the oxyanion intermediate.[156d]

These results were similar to those observed by Baltzer and co-workers with a four-helix-bundle histidine-based peptide catalyst,[157] which suggested that histidine catalysis occurred without direct participation of the serine and aspartate residues.

In the de novo catalyst design by Baltzer and co-workers, NMR, as well as CD spectroscopy,[157a] was applied to the structural study of designed polypeptides. Polypeptides (42-AA) folded into a helix-loop−helix motif in solution, which dimerized in an antiparallel mode to form four-helix bundles. Analogues of peptide KO-42 (Figure 26) were prepared by
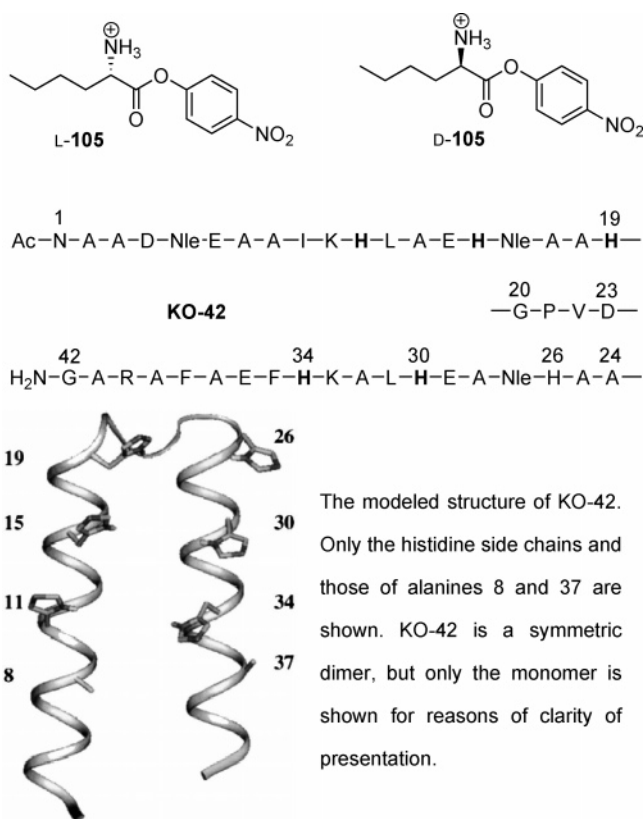

KO-42

The modeled structure of KO-42. Only the histidine side chains and those of alanines 8 and 37 are shown. KO-42 is a symmetric dimer, but only the monomer is shown for reasons of clarity of presentation.

Figure 26. Enantiomeric *p*-nitrophenyl ester substrates and peptide catalyst KO-42.[157m] Reprinted with permission from Baltzer, L.; Broo, K. S.; Nilsson, H.; Nilsson, J. *Bioorg. Med. Chem.* **1999**, *7*, 83. Copyright 1999 Elsevier.

Table 42. Rate Constant Ratios of Peptide-Catalyzed Hydrolysis of L-105 and D-105 at pH 5.1 and 290 K

Entry	Peptide	Residue			$\dfrac{k_2(\text{D-}\mathbf{105})}{k_2(\text{L-}\mathbf{105})}$
		26	30	34	
1	KO-42	H	H	H	1.4
2	MNKK	Q	K	K	2.0
3	MNRR	Q	R	R	1.7
4	MNKR	Q	K	R	1.7
5	MNRK	Q	R	K	2.0

the replacement of histidine residues at the 30 and 34 positions of KO-42 with charged residues such as arginine and lysine (Table 42). These peptides showed great rate enhancements for the hydrolysis of *p*-nitrophenyl esters. In addition, enantioselective differentiation by the polypeptides was observed for the first time. Norleucine substrate D-**105** was hydrolyzed faster than L-**105** with $k_2(\text{D})/k_2(\text{L}) = 2.0$ (Figure 27), when MNKK (Table 42, entry 2) or MNRK (Table 42, entry 5) was used as a catalyst.

^{1}H NMR studies demonstrated the formation of a substrate−peptide complex.[157a,i] The hydrolysis of *p*-nitrophenyl esters with helical peptides was pH-dependent, which suggested that the reaction underwent cooperative nucleophilic and general-acid catalysis by HisH$^+$-His pairs.[157h] In the rate-determining step, the histidine side chain attacks the ester to form an acylamide intermediate, which then reacts with the most potent nucleophile (hydroxide in this case) to form the product in the second step.[157o]

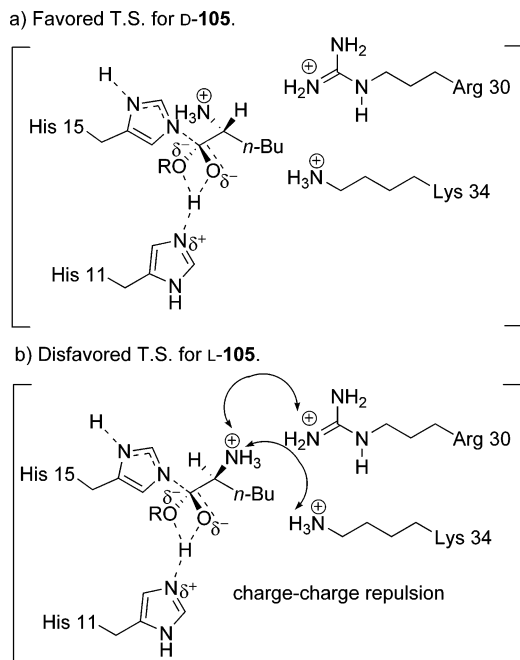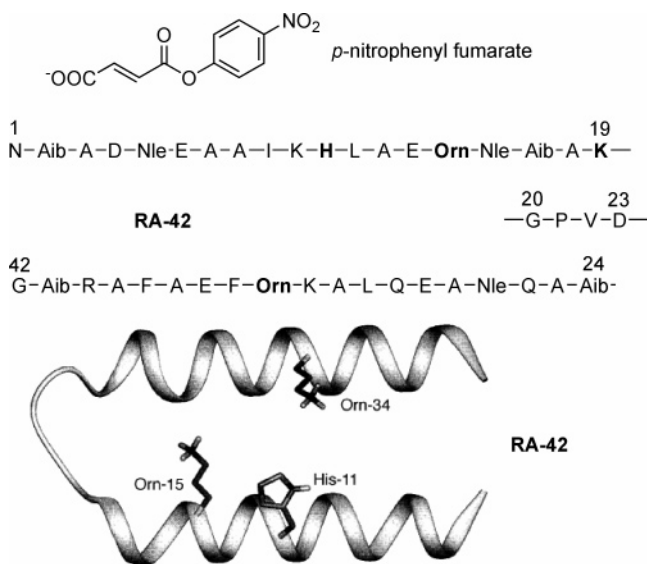The enantioselectivity was proposed to originate from the charge−charge repulsions between positively charged amine

a) Favored T.S. for D-**105**.

b) Disfavored T.S. for L-**105**.

Figure 27. Proposed transition states of MNRK-catalyzed hydrolysis of **105**.

p-nitrophenyl fumarate

RA-42

Figure 28. Ester substrate and peptide catalyst RA-42.[157d] Reprinted with permission from Lundh, A.-C.; Broo, K. S.; Baltzer, L. *J. Chem. Soc., Perkin Trans. 2* **1997**, 209. Copyright 1997 Royal Society of Chemistry.

functionality in the substrate and positively charged amino acid residues in the adjacent helix. The transition state for attack on the L-**105** was destabilized in this way, which made the hydrolysis of L-enantiomer slower than that of the D-enantiomer (Figure 27). Manipulation of the peptide sequence by installing Arg, Lys, and His residues in the proper positions facilitates chiral recognition for enantiomeric ester substrates.

The hydrolysis activity depended on the HisH[+]-His pair at (*i*, *i* + 4) in one helix and the presence of Arg and Lys in the adjacent helix.[157m] It has also been reported that peptides with two His residues (*i* = His, *i* + 3 = His) provide good reactivities. Histidine residues of the active HisH[+]-His pair in this case came from two different helices of the bundle.[157l]

Scheme 24. Mechanism of RA-42 Self-Catalyzed Site-Selective Functionalization
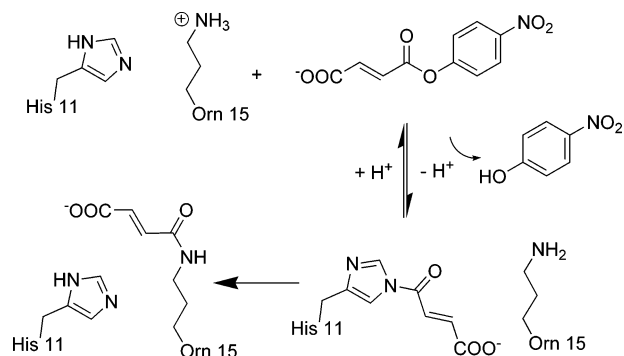

Helical bundle catalysts were also found to undergo site-selective self-functionalization.[157b−f,o] Bundle "RA-42" catalyzed the cleavage of *p*-nitrophenyl fumarate (Figure 28) to form an amide at the side chain of ornithine-15 (Orn-15). His-11, as a nucleophile, attacked the PNP esters to generate an acylamide intermediate in the rate-determining step, releasing *p*-nitrophenol. The acyl group was then transferred to the deprotonated side chain of Orn-15 on RA-42 (Scheme 24).[157c] Three residues, His-11, Orn-15, and Orn-34, are involved in the reaction center. Orn-15 stabilizes the developing oxyanion in the transition state, and Orn-34 interacts with the carboxylate anion of the substrate.[157d] Lysine, ornithine, and 1,3-diaminobutyric acid residues were found to be acylated when they were positioned at *i* − 3 and *i* + 4 relative to *i* = His.[157f]

The helix-loop−helix motif was also used to catalyze the hydrolysis of other challenging substrates, phosphate esters, with metal-ion binding as a key mechanistic affect.[157r] Regarding these phosphate ester substrates, Brack and co-workers found that polypeptides[158] were able to accelerate the corresponding hydrolysis process. In 1980, they studied polypeptides having alternating hydrophilic and hydrophobic residues with both L- and D-residues. Segments containing seven or more residues of the same chirality adopted a β-sheet structure, and the rest of the chain adopted a random coil. Partial hydrolysis of the unordered portion resulted in recovery of L-enriched β-sheet.[159]

Polycationic polypeptides containing basic and hydrophobic amino acids could accelerate the hydrolysis of phos-
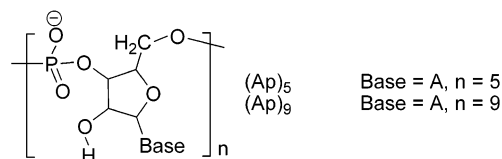
Catalysts:
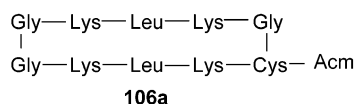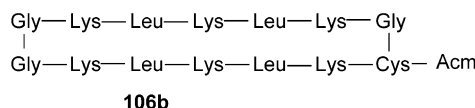
Substrates:

Figure 29. Structure of two cyclic peptides **106a** and **106b** and the hydrolysis substrates.

Table 43. Rate Constants of the Hydrolysis of (Ap)$_9$A by Different Basic Polypeptides Exemplifying the Role of the β-Sheet Conformation[a]

Entry	Polypeptide	k (min^{-1})	Rate Enhancement
1	control	1.1×10^{-6}	
2	poly(Pro-Leu-Lys-Leu-Lys)	1.2×10^{-5}	11
3	poly(D,L-Leu-D,L-Lys)	1.85×10^{-5}	17
4	poly(Ala-Lys)	2.2×10^{-5}	20
5	poly(Leu-Lys)	1.7×10^{-4}	155

[a] Experimental conditions: 37 °C, 7 days in 0.1 M Gly-Gly buffer (pH 7.5), (Ap)$_9$A 4×10^{-4} M in phosphate, peptide 10^{-3} M in basic amino acids.

Table 44. Rate Constants of the Hydrolysis of (Ap)$_9$A by Different Basic Polypeptides Exemplifying the Role of the α-Helix Conformation[a]

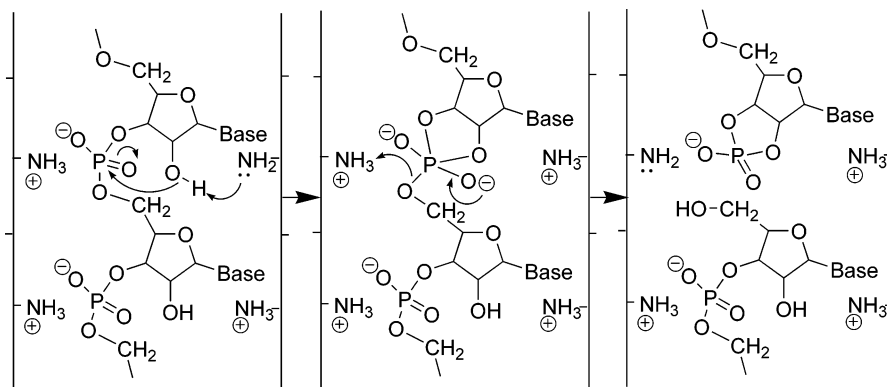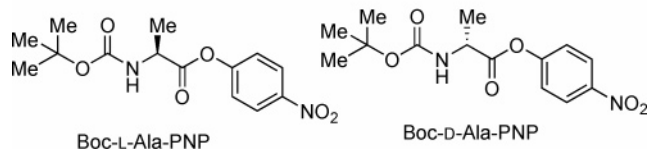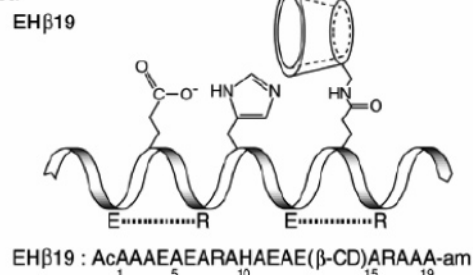| Entry	Polypeptide	k (min^{-1})	Rate Enhancement
1	control	1.1×10^{-6}	
2	poly(Pro-Lys-Lys-Leu)	4.5×10^{-6}	4
3	poly(Leu-Lys-Lys-Leu)	1.1×10^{-4}	100

[a] Experimental conditions: 37 °C, 7 days in 0.1 M Gly-Gly buffer (pH 7.5), (Ap)$_9$A 4×10^{-4} M in phosphate, peptide 10^{-3} M in basic amino acids.

Figure 31. Structure of ester substrates and peptide EHβ19 with three functional groups: carboxylate, imidazole, β-CD; from N- to C-Terminus.[166] Reprinted with permission from Tsutsumi, H.; Hamasaki, K.; Mihara, H.; Ueno, J. *J. Chem. Soc., Perkin Trans. 2* **2000**, 1813. Copyright 2000 Royal Society of Chemistry.

phodiester bonds. The first example employed a β-sheet polypeptide.[160] Both all-D-poly(leucyl-lysyl) and all-L-polymer were active catalysts[161] that adopted a β-sheet conformation when complexed with the substrates. However, the alternating poly(D,L-Leu-D,L-Lys) formed a random coil, showing poor activities. The hydrolytic activity significantly depended on β-sheet proportion, indicating that chemical activity was closely related to the geometry of the chain.

Two cyclopeptides[162] were prepared in order to mimic two adjacent strands of the β-sheet structure of linear (Leu-Lys)$_{25}$. Peptides **106a** and **106b** (Figure 29) were found to adopt β-sheet conformations, supported by IR absorption data.[163] Peptide **106b** showed competitive hydrolytic activities with oligoribonucleotide substrates (Ap)$_5$ and (Ap)$_9$ comparable to polypeptide catalysts.

Brack and co-workers reported that polypeptides needed to present a regular distribution of basic groups in either β-sheet or α-helix[164] to be active. Lys-based polypeptides with β-sheet (Table 43) or α-helix (Table 44) structures were able to enhance the hydrolysis of oligoribonucleotide substrates.[165] A tentative model (Figure 30) was provided for the mechanism of hydrolysis of a polyribonucleotide by poly-(Leu-Lys).

Of particular note is the fact that poly(L-His) did not show significant rate enhancement[165] for a similar hydrolysis, as

histidine is present in many active sites of enzymes.[154c] Authors suggested that conformational factors and the absence of strong basic groups were responsible for the inefficiency of poly(L-His).

In 2000, Ueno and co-workers[166] reported an interesting example of enantioselective hydrolysis by cyclodextrin–peptide hybrids (CD–peptides). These CD–peptides adopt stable α-helix conformations. In these hydrolyses, three functional groups, β-cyclodextrin, imidazole, and carboxylate, are positioned on the same side of the α-helix (Figure 31). The presence of the carboxylate moiety enhanced substrate selectivity for the hydrolysis of esters.

A mechanism was proposed for the hydrolysis catalyzed by peptide EHβ19 (Figure 32). EHβ19 gave a 7-fold higher k_{cat}/K_M value for Boc-D-Ala-PNP than for the L-enantiomer. The substrate selectivity was found to be determined by the order of functional groups, β-CD, imidazole, and carboxylate, from N-terminus or C-terminus.[166]

8. Peptide-Catalyzed Asymmetric Acylation

8.1. Kinetic Resolution of Alcohols

Acylation can be the reverse process of hydrolysis. Nature provides examples of enzymatic acyl transfer with high efficiency and specificity, showing the importance of the
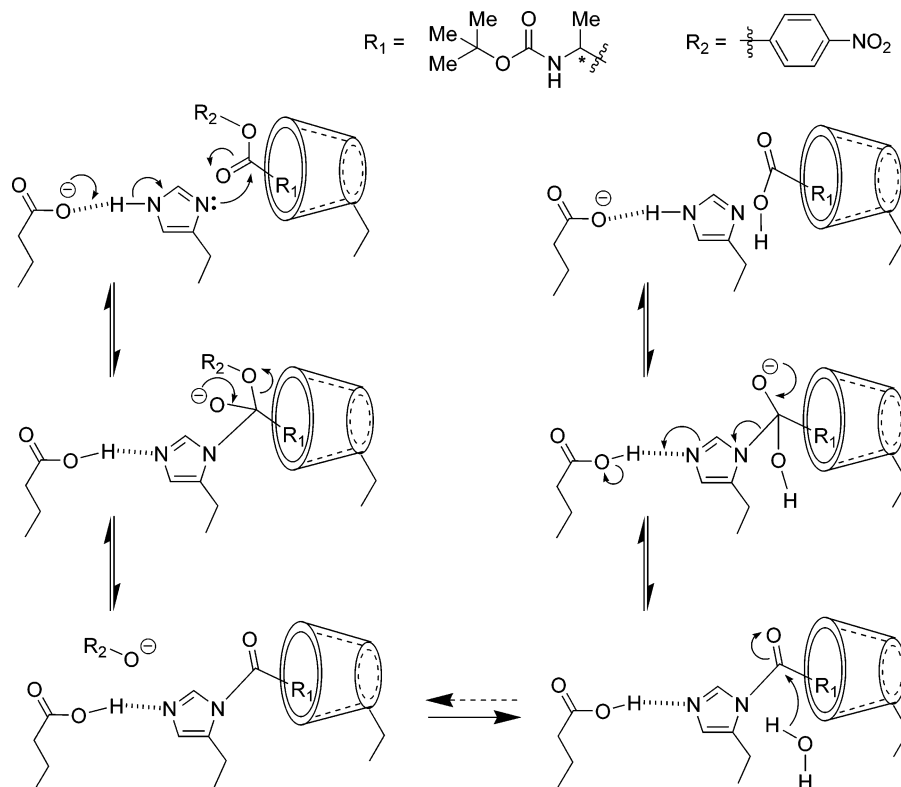

Figure 30. Tentative model for the mechanism of hydrolysis of a polyribonucleotide by poly(Leu-Lys).

Figure 32. Schematic illustration of ester hydrolysis performed by the cooperation of imidazole, carboxylate, and β-CD units.
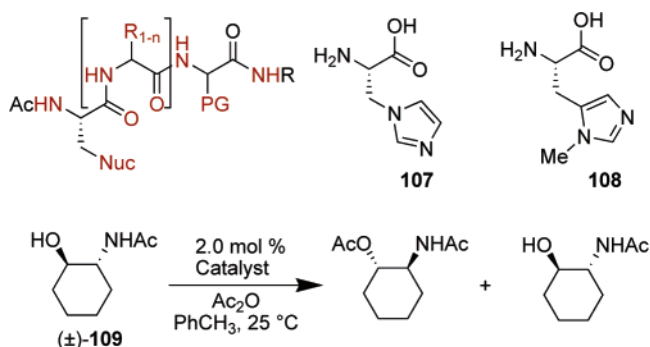

Figure 33. Histidine analogues and designed peptide structure with an embedded nucleophile.

polypeptide structure of catalyst and the multipoint interactions (such as hydrogen bonding, ionic interactions, $\pi-\pi$ stacking, and hydrophobic interactions) between catalyst and substrate. Design and development of small molecules for efficient asymmetric catalytic reactions have always been a challenge. Successful representative catalysts reported to date for asymmetric acylations include phosphine catalysts,[167] chiral pyridine derivatives,[168] other N-heterocycles,[169] and peptide-based catalysts.[53]

Inspired by the enzymatic models, Miller and co-workers applied nucleophilic moiety-embedded peptide structures to the discovery of low molecular-weight enzyme-like catalysts for asymmetric acyl transfer reactions. During the beginning of their study, histidine analogues **107** and **108** (Figure 33) were chosen to serve as nucleophiles in a series of β-turn-type small peptides for the kinetic resolution of *trans*-1,2-acetamidocyclohexanol ($\pm$)-**109**.[170] The amide functionality within substrate **109** was designed to introduce potential hydrogen-bonding interactions with the peptide catalyst.

β-Turn tripeptide **110** afforded $k_{rel} = 17$, favoring the (S,S)-enantiomer of substrate **109** (Figure 34). The control catalyst
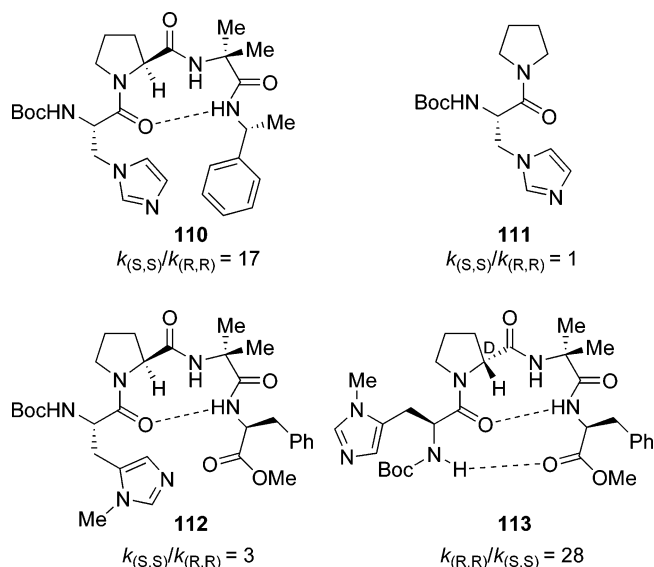

Figure 34. Catalysts for kinetic resolution.

111, with only one stereogenic center, gave no selectivity, because of the lack of secondary structure. Catalysts with different stereochemistry on the proline residue (L- or D-) in the peptide backbone, peptides **112** and **113** exhibited dramatically different conformations and reactivities. Containing a D-proline moiety, catalyst **113** adopted a β-hairpin conformation with two intramolecular hydrogen bonds involved. It afforded a $k_{rel} = 28$, favoring the other enantiomer ((R,R)-enantiomer of **109**). This fact suggests that the rigidity of the β-hairpin structure greatly influenced the enantioselectivity (Figure 34).[171]

This hypothesis was further supported when octapeptide **114** afforded $k_{rel} > 51$, while peptide **115** gave poor selectivity ($k_{rel} = 7$) because of its more flexible structural character. Another analogue of **114**, peptide **117**, provided
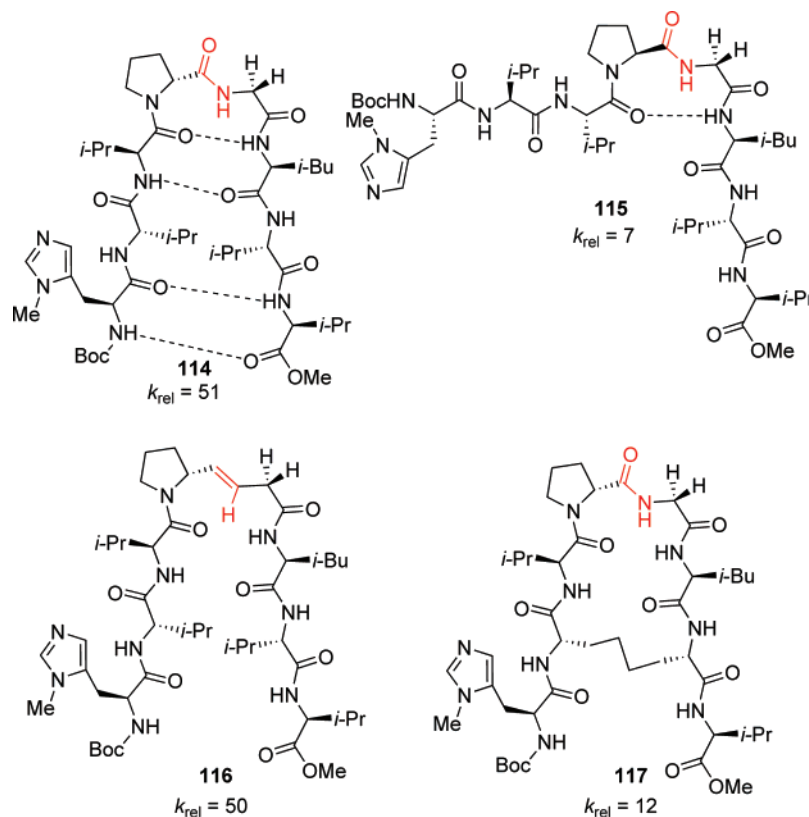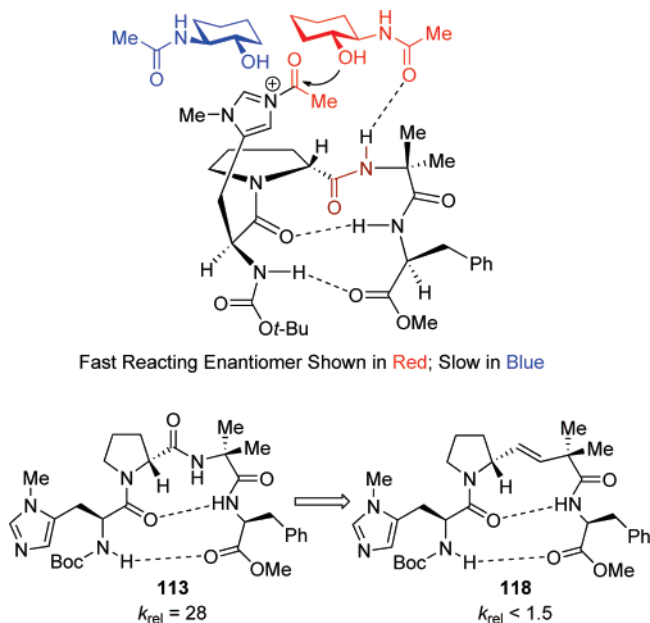
Figure 35. Peptide **114** and its analogues.

Fast Reacting Enantiomer Shown in Red; Slow in Blue

Figure 36. Mechanistic model with peptide **113**.

Figure 37. Interactions between substrate and peptide in order to induce enantioselectivity.

modest selectivity ($k_{rel} = 12$), indicating that some degree of conformational flexibility was required for high enantioselectivity (Figure 35).[172]

Kinetic studies showed that the reactions were first order in alcohol substrate and peptide catalyst. A mechanistic model was proposed to explain the enantioselectivity induced by the secondary structure of peptide catalyst. As shown in Figure 36,[173] one enantiomer (red) is easily acylated by the acylimidazolium moiety because of the favorable hydrogen bonding interactions with the amide N−H of peptide **113**. The experiment with peptide **118**, which lacks the amide functionality, provided almost no selectivity. These results
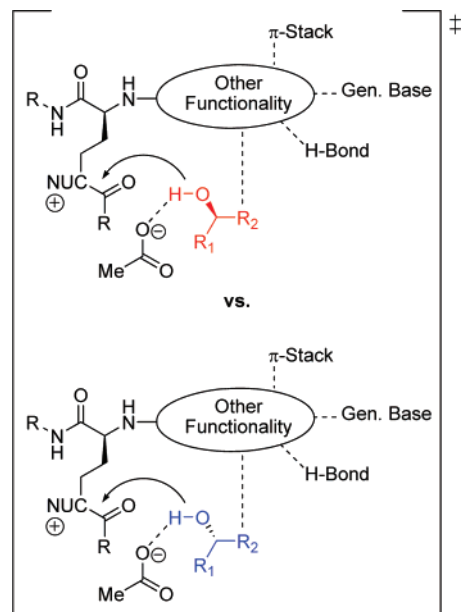
are consistent with the model, confirming that the D-Pro-Aib linkage has a great impact on enantioselectivity. However, octapeptides **114** and **116** both afforded decent selectivities ($k_{rel} > 50$), suggesting that the D-Pro-Gly linkage, which is more remote from the reaction center in this case, contributes only to the structural rigidity.

The efficient peptide catalysts for asymmetric acyl transfer are required to have a proper secondary structure wherein one enantiomer has preferential interactions with other functionalities in the peptide backbone (Figure 37).

Toniolo and co-workers examined Miller and co-workers' catalysts to probe the effects of conformational rigidity on

enantioselectivity with a set of related catalysts.[174] Within this catalyst set, the β-turn-inducing residue Aib was replaced by C^α-tetrasubstituted amino acids, which are also known to induce β-turns (Figure 38). Conformational analysis by ^{1}H NMR spectroscopy and FTIR absorption showed that the more selective catalysts adopt β-hairpin structures while the less selective catalyst **121** does not, corroborating Miller's original assertions regarding the origin of asymmetric induction.

One advantage of peptide-based catalysts is that very large and diverse libraries may be prepared. For example, a diverse peptide library can be easily prepared on solid support with high efficiency. However, evaluation of very large catalyst libraries is not trivial. The exercise requires the development of practical and efficient assays for catalyst screening. Miller and co-workers developed a fluorescent-labeled assay in order to find the most active peptide catalysts; the assay was used as a filter to limit the size and nature of catalyst libraries to be screened for enantioselectivity. Such a filter leads to a focus on those catalysts within a massive library that exhibit high activity, a generally desirable property for a catalyst. Thus, a split-pool peptide library was prepared on solid phase with a proton-activated fluorophore (Figure 39, **122**).[175]

This resin-bound, sensor-functionalized library was applied in the acylation of racemic alcohols with acetic anhydride as the acylating agent. The brightest beads under the fluorescence microscope were indeed found to carry the most active catalysts. In this manner, octapeptide **123** was found to be an efficient and general catalyst for the kinetic resolution of a series of secondary alcohol substrates without the acetamide functionality (eq 5). In addition to high enantioselectivities for a range of secondary alcohols, catalyst **123** afforded $k_{rel} = 4$ for 2-butanol, indicating its promising ability to differentiate between methyl and ethyl groups. Mechanistic studies employing an alanine scan suggest the critical importance of the π-Me-His moiety and the τ-Bn-His moiety.[176] The former may play a nucleophilic role and the latter may act as a general base, although a definitive elucidation of mechanism is ongoing.
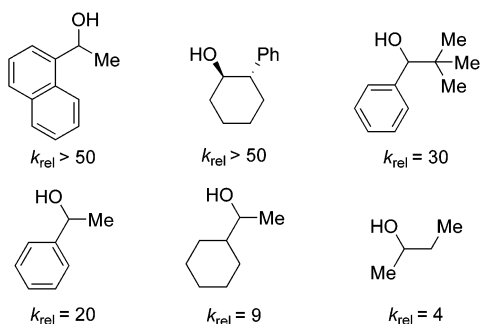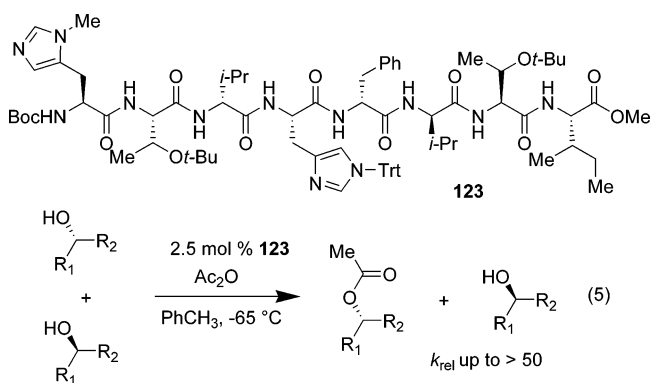
This general type of assay was also applied to the asymmetric acylation of tertiary alcohols (±)-**124** (eq 6),[177a] which are difficult substrates because of their sluggish reactivities. Pentapeptide **125** was able to provide modest enantioselectives ($k_{rel} = 9$ to >50). Interestingly, peptide **126**[177b] with a β-Me-π-Me-His moiety demonstrated improved selectivities for certain substrates. Again, these results elucidated that enantioselectivity could be enhanced by manipulation of the secondary structure of the peptide catalyst. A small change may have a great impact.
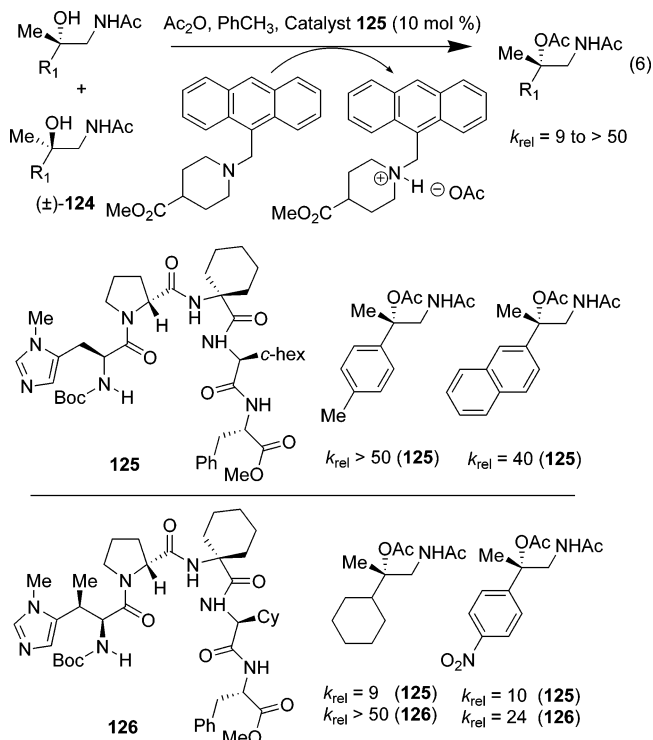
In natural-product chemistry, convenient preparations of enantiomerically pure intermediates are essential for the success of the synthesis. Kinetic resolution by small synthetic catalysts provides a practical tool to obtain optically pure important intermediates. Peptide **127** catalyzed the kinetic resolution of substrate (±)-**128** with $k_{rel} = 27$ to deliver (−)-**128**, which was then carried on to (−)-mitosane, a key intermediate for mitomycin C synthesis (Scheme 25).[178]

8.2. Site-Selective Functionalization

Site-selective functionalization of polyfunctional substrates is also a difficult and potentially useful goal in the synthesis of polyfunctional molecules. In some cases, enzymes demonstrate their high efficiency and selectivity in such processes. However, each known enzymatic model has a very limited substrate scope. The structure of a small peptide catalyst can be easily manipulated, and the efficient synthesis of a small peptide library makes it a potentially practical tool in regioselective functionalization studies.

Griswold and Miller have studied peptide-catalyzed regioselective acylation on monosaccharides.[179] N-Methylimidazole-catalyzed acylation of glucosamine derivative **129** provided two monoacetoxy products and one bis-acetoxy product in a ratio of **130/131/132** = 50:22:28 (Table 45, entry 1). Pentapeptides **133** and **134**, identified from a screen of a
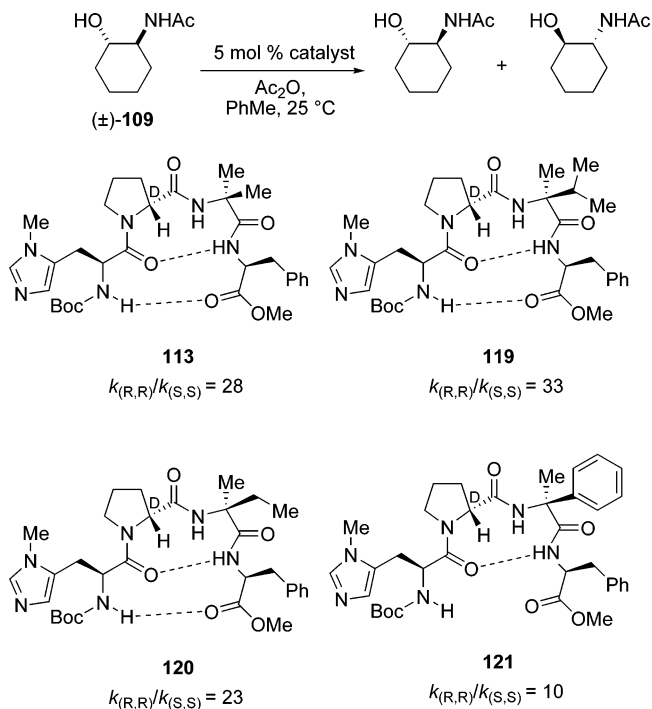
Figure 38. Catalysts with C$^\alpha$-tetrasubstituted amino acid residues replacing Aib.
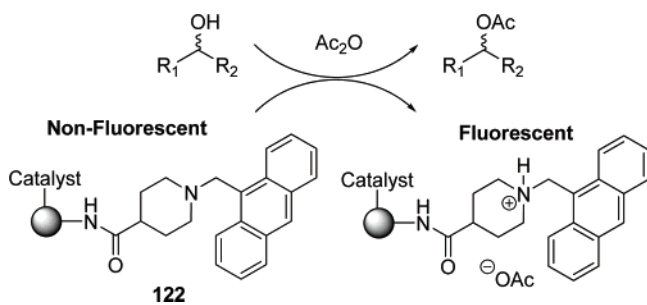

Figure 39. Fluorescent-labeled catalyst on solid support for kinetic resolution.

Scheme 25. Kinetic Resolution in the Synthesis of the Core Structure of Mitomycin C

Table 45. "Hit" Catalysts Compared with *N*-Methylimidazole (NMI)
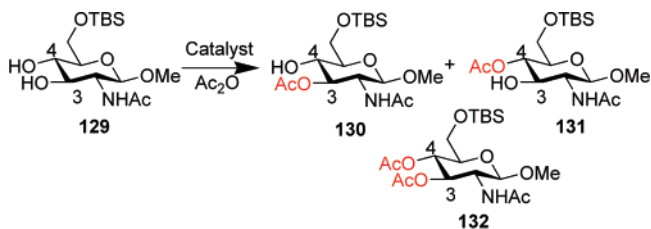
Entry[a]	Catalyst	130	131	132	Total Conversion
1	NMI	50	22	28	86%
2	**133**	97	3	0	88%
3	**134**	53	47	0	80%

[a] 2 mol % catalyst, PhCH$_3$, 25 °C, 15 h.

150-member random peptide library, delivered only monoacetoxy products under the same reaction conditions. In particular, catalyst **133** afforded mainly the 3-acylated monoacetoxy **130** (entry 2).

Glucoside **135** was then chosen as a more challenging substrate for site-selective acylation (Table 46), requiring differentiation of four hydroxyl groups. A 36-member peptide library was screened. The *N*-methylimidazole-catalyzed reaction showed poor selectivity, providing primary acetate **139** as the major product along with two other monoacetoxy compounds products (**137** and **138**), but not monoacetoxy **136**. Peptide **140**, however, exhibited much higher activity and provided monoacetoxy **138** as the major product (entry 2).

Another challenging target for site-selective functionalization explored by the Miller group was the natural product erythromycin A (**141**).[180] Erythromycin A has three secondary alcohol functionalities with different reactivities (2′-OH > 4″-OH > 11-OH). The NMI-catalyzed acylation of **141** with a limited amount of Ac$_2$O (1.0 equiv) delivered mainly C2′-monoacetate **142** (eq 7). With additional Ac$_2$O (2.0

equiv), 4″-OH was acylated to form the diacetate, which could be reverted to C4″-monoacetate **143** upon methanol quench to cleave the 2′-acetate (eq 8). The acylation at C11-OH catalyzed by NMI is quite sluggish. On the basis of the sequential screen of peptide libraries, *β*-turn-type peptide **144** was found to provide a 1:5 ratio for **143**/**145**, favoring the C11-monoacetate **145** (eq 9). Thus, the relative reactivity
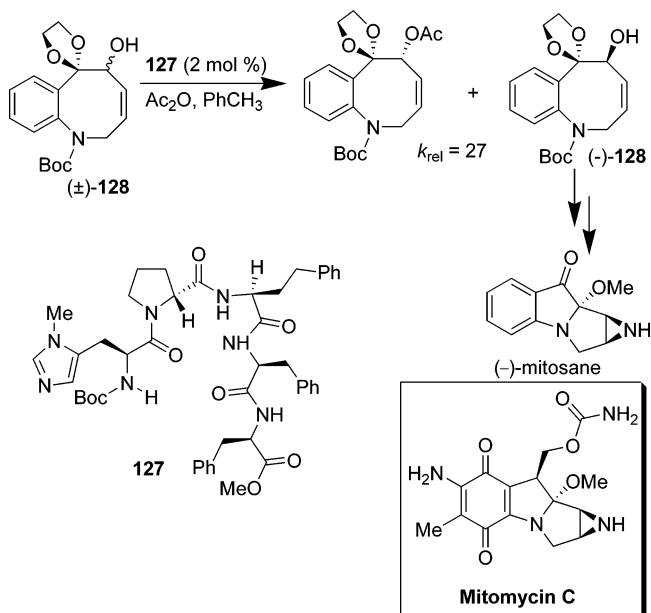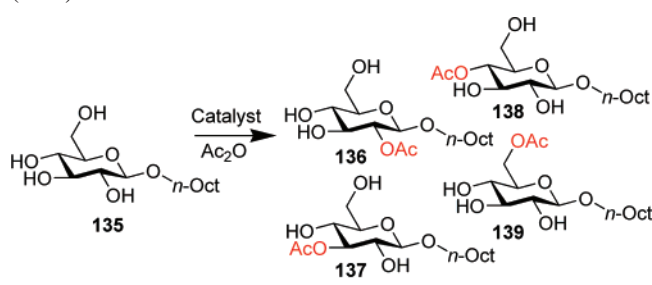
Table 46. "Hit" Catalysts Compared with N-Methylimidazole (NMI)

Entry[a]	Catalyst	136	137	138	139	Total Conversion
1	NMI	0	20	16	64	14%
2	140	9	11	58	22	100%

[a] 2 mol % catalyst, PhCH$_3$/CH$_2$Cl$_2$, 0 °C, 15 h.
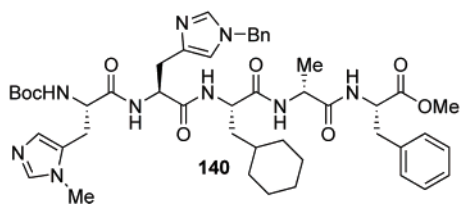
has been reversed by peptide catalyst **144**. In addition, the reactions with peptide **144** proceed much faster than the NMI-catalyzed reactions. The significant reactivity reversal over NMI by peptide **144** was also observed when other anhydride acylating agents were used for the site-selective derivatization of erythromycin A.
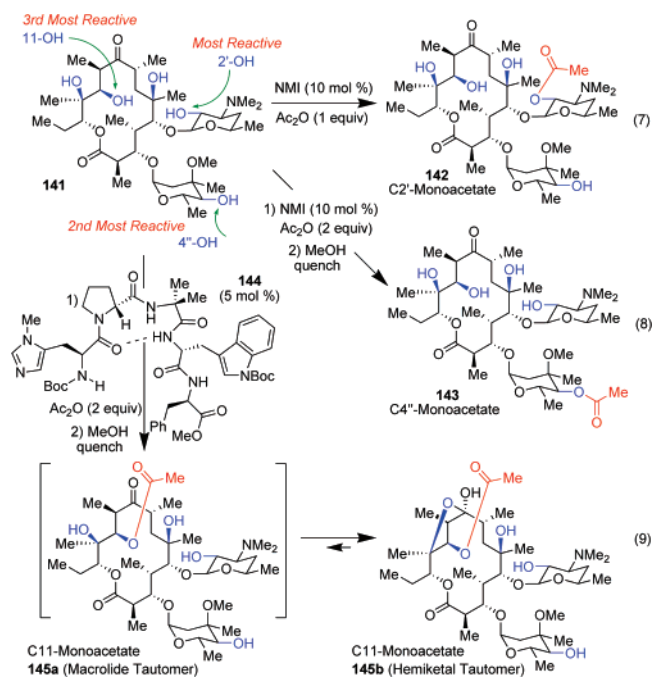
8.3. Desymmetrization of Alcohols by Peptide-Catalyzed Acylation

Peptide-catalyzed acylation has also been applied to the desymmetrization of meso compounds. The more remote the desymmetrization site is from the prochiral center, the more challenging it is to find a low-molecular-weight catalyst to achieve the desymmetrization.

(10)

Initial Library Design
Green - Aromatic
Blue - aliphatic
Red - Aromatic
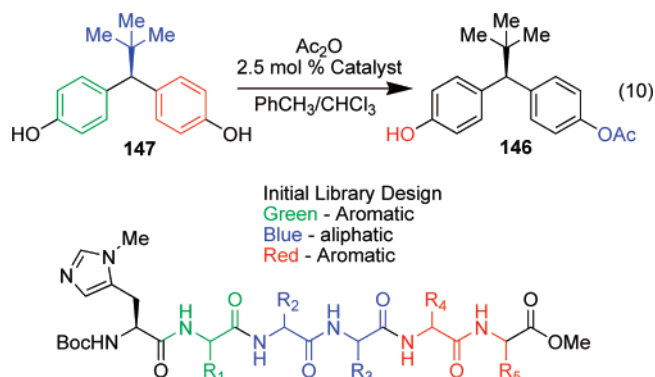

In order to obtain optically pure **146** from meso compound **147**, **147** was initially transformed to bisacetate and subjected to enzymatic hydrolysis. Despite screening over 450 lipases, the enzymatic approach proved unsatisfactory (Scheme 26).[181] Miller, Hansen, and co-workers attempted the desymmetrization of **147** (eq 10) with peptide-based catalysts.[181] After the study of five directed peptide libraries followed by optimization of reaction conditions, a "hit" peptide, catalyst **148**, was found to demonstrate good enantioselectivity. Of particular note was the fact that there was minimal secondary resolution involved when hexapeptide **148** was used as the catalyst (Figure 40).

In order to determine which part of the peptide is critical for the highly enantioselective outcome, truncation experiments of **148** have been performed. Cleavage of 1−2 residues at the C-terminus did not affect the enantioselectivity significantly. Additional optimization of the C-terminus for the truncated tetrapeptide led to catalyst **149**, which afforded (**R**)-**146** with 95% ee and 80% isolated yield (Scheme 27). The extraordinary activity and enantioselectivity observed using tetrapeptide amide **149** and other active peptide catalysts demonstrated the powerful substrate recognition or reaction-site recognition induced by low-molecular-weight catalysts with relatively flexible structures.

Miller and co-workers also studied the desymmetrization of meso substrates with primary alcohol functionalities. Enzymatic desymmetrization of monobenzylated glycerol substrate **150** provided monoacetate **151a** with 96% ee and a ratio of mono/di = 57:43 (eq 11).[182a] The sequential screening of random peptide libraries, followed by the evaluation of a focused library, led to the identification of pentapeptide **152**, which delivered enantiomer **151b** with

Scheme 26. Initial Approach by Using Lipase-Catalyzed Hydrolysis of Bis(acetate)
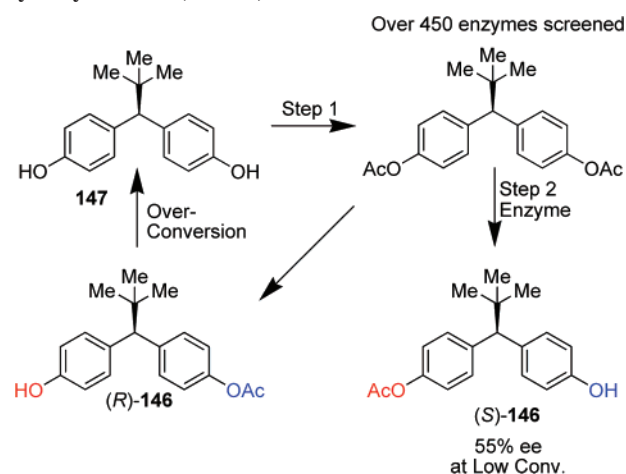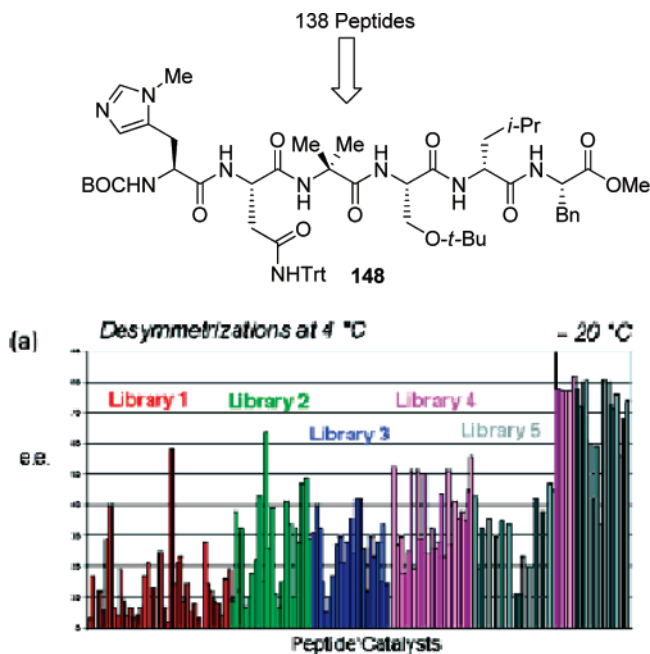
Figure 40. Histogram of complete set of peptide catalysts that were screened and the "Hit" peptide.[181] Reprinted with permission from Lewis, C. A.; Chiu, A.; Kubryk, M.; Balsells, J.; Pollard, D.; Esser, C. K.; Murry, J.; Reamer, R. A.; Hansen, K. B.; Miller, S. J. *J. Am. Chem. Soc.* **2006**, *128*, 16454. Copyright 2006 American Chemical Society.

94% ee and a ratio of mono/di = 39:61 (eq 12).[182b] Once again, a β-turn-type peptide shows the competitive activity as well as selectivity when compared with enzymatic catalysis.
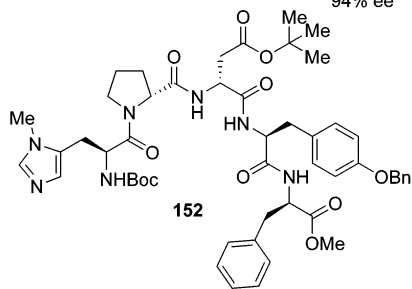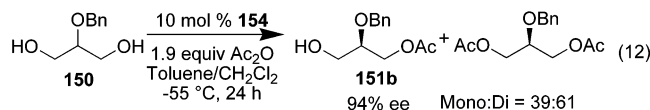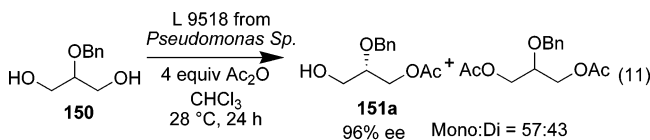
9. Phosphorylation

It is well-known that phosphoryl transfer plays a very important role in many cell signaling pathways. Specifically, there are kinases that use histidine as a nucleophile to attack ATP and become phosphorylated. The phosphate is subsequently transferred to the downstream effector to transmit the signal. Miller and co-workers applied their peptide catalysts with the π-Me-His moiety to the study of asymmetric phosphorylation. Nucleophilic attack on the phosphorylating agent by the peptide catalyst generates a reactive phosphoryl imidazolium species, which then reacts with an

Scheme 27. Peptide-Catalyzed Desymmetrization
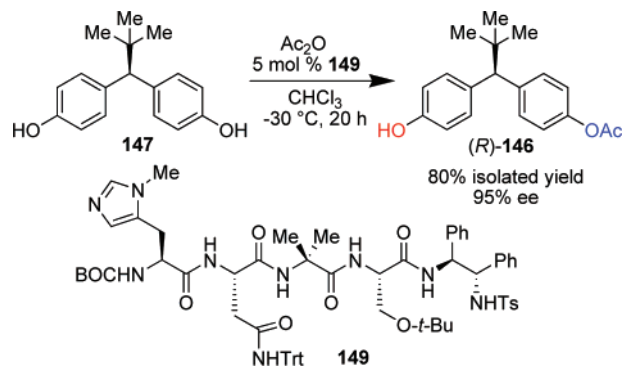
Scheme 28. Catalytic Cycle for Peptide-Catalyzed Asymmetric Phosphorylation
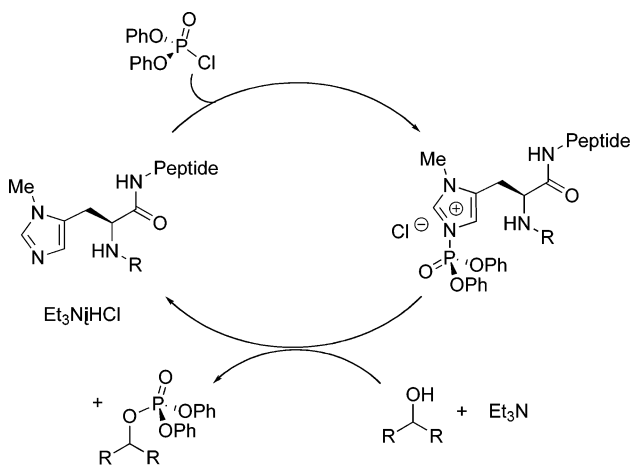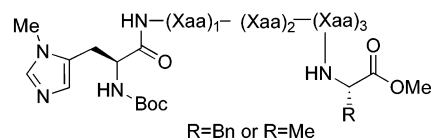
alcohol substrate to form the corresponding phosphorylated product. A sterically hindered base, such as triethylamine, removes the byproduct HCl to complete the catalytic cycle (Scheme 28).[183]

In nature, there is an abundance of phosphorylated inositol natural products. *myo*-Inositol, the important "starting material" for a series of secondary messengers and their precursors, is a difficult substrate for desymmetrization because of its insolubility in most organic solvents. Miller and co-workers selected trisubstituted inositol derivative **155** as the meso substrate for their peptide-catalyzed phosphorylation studies (Scheme 29). On the basis of the sequential screening of random peptide libraries followed by the evaluation of a focused library, two pentapeptides (**156** and **157**) were identified that were able to produce enantiomeric D-*myo*-inositol-1-phosphate and D-*myo*-inositol-3-phosphate derivatives (**158a** and **158b**), respectively, with very high selectivity. In the same catalytic reactions, only trace amounts of the 5-phosphorylated product were observed because of the lower activity of 5-OH. The enantiodivergent syntheses of two small natural products, D−I-1-P and D−I-3-P, were successfully achieved one more step from **158a** and **158b**.[183]

It is noteworthy that these two nonenantiomeric peptides (**156** and **157**) delivered two enantiomeric products with high regio- and enantioselectivity, while they behaved differently

Scheme 29. Peptide-Catalyzed Desymmetrization of a *meso*-Inositol Derivative[183b] (Reprinted with permission from Sculimbrene, B. R.; Morgan, A. J.; Miller, S. J. *J. Am. Chem. Soc.* 2002, *124*, 11653. Copyright 2002 American Chemical Society.
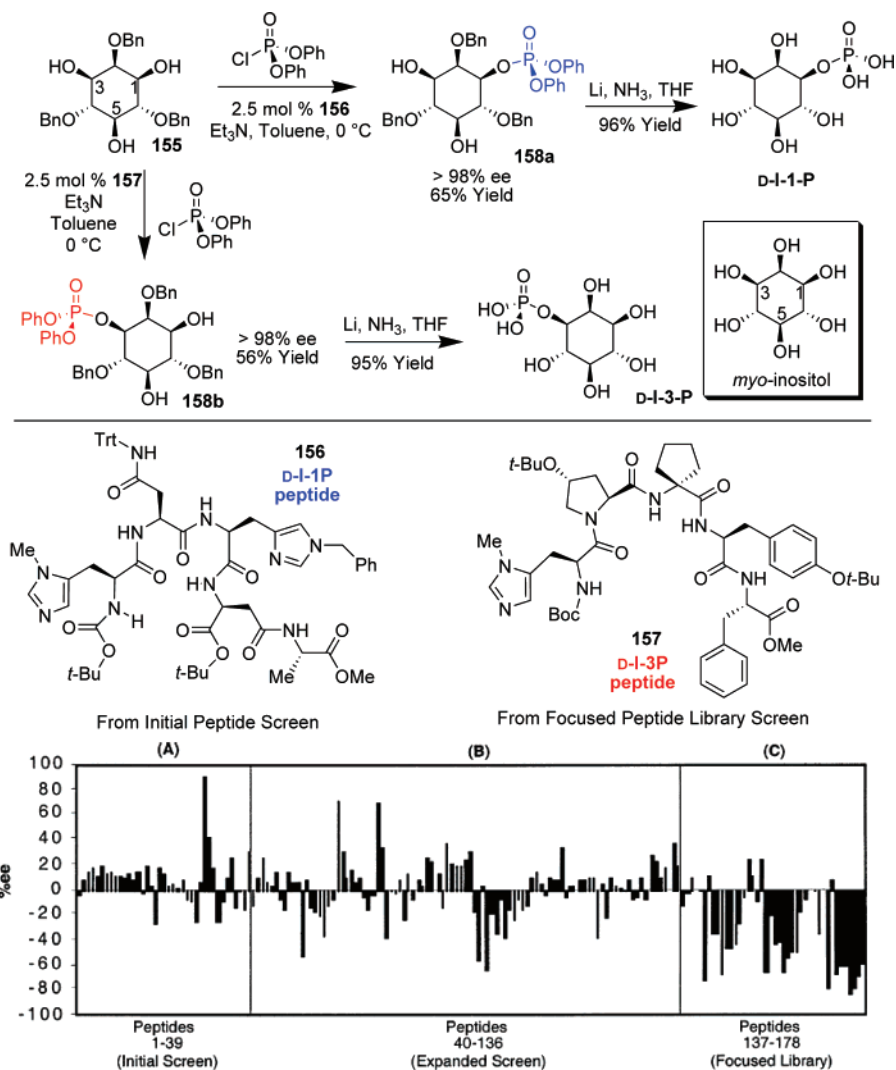
Table 47. Survey of Protecting Groups for Phosphorylation
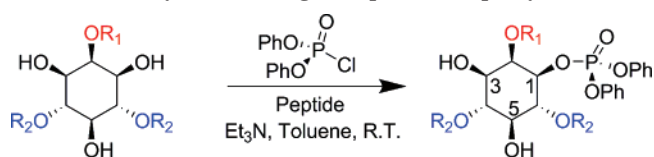
Entry	R₁	R₂	ee (%) 156	ee (%) 157
1	Bn	Bn	98	-98
2	Bn	allyl	94	-97
3	PMB	PMB	98	-98
4	Bn	PMB	97	-98

PMB, *para*-methoxybenzyl

in different solvent systems. Inositol substrates with various protecting groups have been examined for the asymmetric phosphorylation catalyzed by these two peptides.[184] Small modifications on protecting groups do not affect their reactivities. The two peptides behave very similarly for all the cases, providing excellent enantioselectivities (Table 47).

The asymmetric phosphorylation methodology was applied successfully to the syntheses of a series of natural products and their synthetic analogues. For example, four inositol polyphosphates were synthesized by using another *meso*-

inositol substrate **155b** (Figure 41).[184a] In addition, several deoxygenated analogues of inositol phosphate were synthesized for their biological studies.[184b]

Syntheses of phosphatidylinositol (PI) and phosphatidylinositol phosphates (PIPs) usually involve classical resolution as well as complex protecting-group strategies, which result in very long reaction sequences and low overall yields.[185] Peptide-catalyzed asymmetric phosphorylation initiates a new entry for the syntheses of these complex molecules. By using this methodology, Miller and co-workers achieved the syntheses of some representative PI and PIP compounds, in both the synthetic version and natural version with the unsaturated side chains.[186] In addition, convergent syntheses of a series of deoxygenated PI and PIP analogues were also accomplished, in which the Mitsunobu protocol was first applied for the installation of the PI functionality (Figure 42).[187]

10. Sulfinyl Transfer

Chiral sulfur compounds, especially sulfoxides, are efficient chiral auxiliaries for many important asymmetric transformations.[188] Chiral sulfinate esters have served as the primary sources to achieve chiral sulfur compounds. In 2004, Miller, Ellman, and co-workers reported the peptide-based, catalytic enantioselective synthesis of sulfinate esters based

Figure 41. Syntheses of inositol polyphosphates based on peptide-catalyzed asymmetric phosphorylation.

Figure 42. Total syntheses of PI, PIPs, and their deoxygenated analogues through peptide-catalyzed asymmetric phosphorylation.

on the dynamic resolution of racemic *t*-butanesulfinyl chloride (eq 13, **158**).[189]

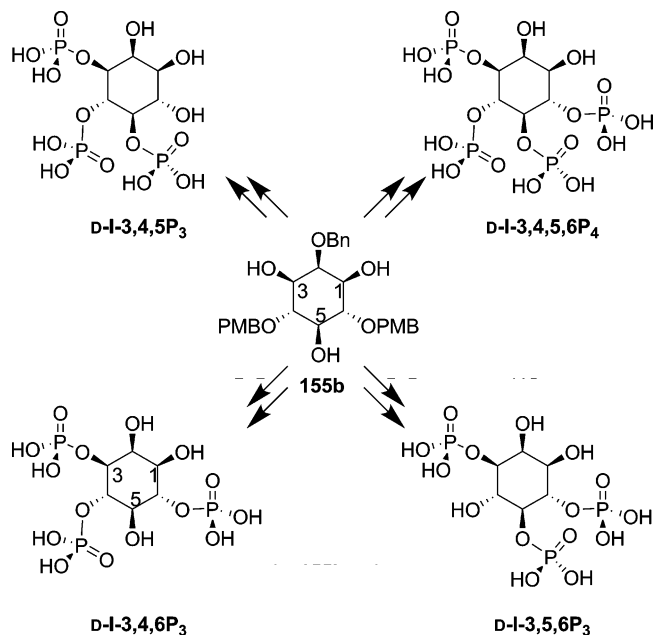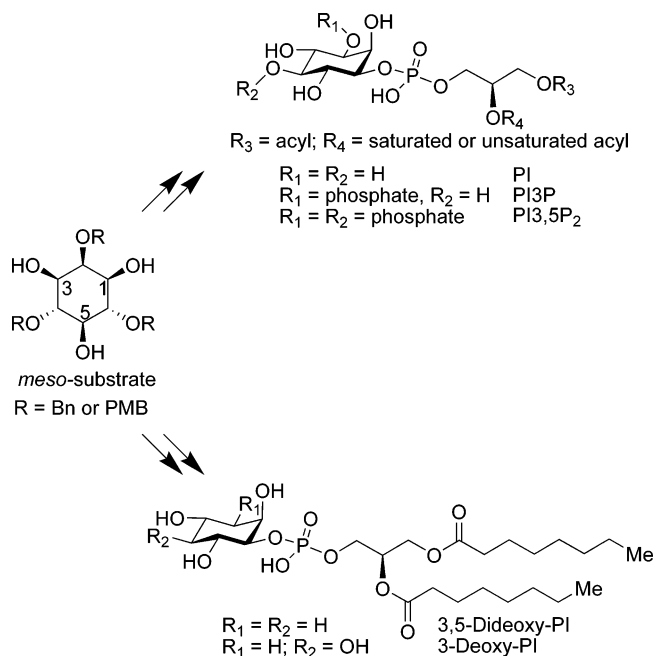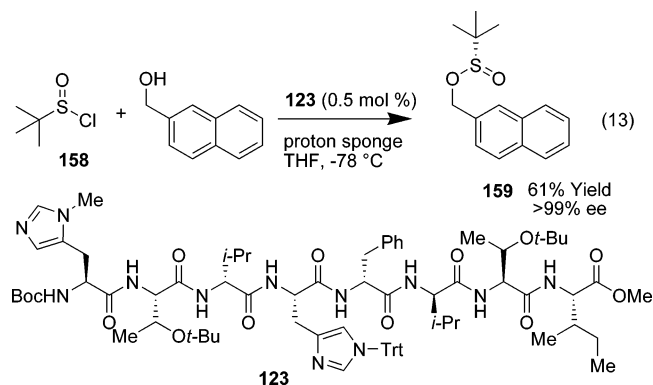Non-nucleophilic bases, such as proton sponge, provided no background reaction at low temperatures. The general peptide catalyst **123**, identified in previous asymmetric acylation studies, was studied in this reaction as well as some chiral DMAP derivatives. Peptide **123** demonstrated dramatically enhanced activity and enantioselectivity over chiral DMAP catalysts. Sulfinate esters were obtained with high enantioselectivities at high conversions, indicating that dynamic resolution occurred through rapid epimerization of the sulfinyl stereocenter. Under the optimized reaction conditions, sulfinate **159**, precursor for a variety of optically pure, chiral sulfur compounds, was obtained with >99% ee and 61% yield after recrystallization. An alanine scan of peptide **123** elucidated again the critical role of π-Me-His moiety in the peptide backbone for the asymmetric sulfinyl transfer reactions. It is noted that this process is also effectively carried out in a dynamic kinetic resolution mode employing cinchona alkaloid-based catalysts.[190]

11. Conclusions

The use of peptide-based catalysts has now exploded into both a thriving area of fundamental research and also a viable arena for the development of practical processes. From early beginnings that included inspiration from biological systems, to the present when biological concepts are routinely applied in the development of these catalysts, there is now a venerable history in this not-so-young field that also serves an exciting prologue for continuous new developments well into the future.

12. Acknowledgments

13. References

(1) Strecker, A. *Liebigs Ann. Chem.* **1850**, *75*, 27.
(2) Enders, D.; Shilvock, J. P. *Chem. Soc. Rev.* **2000**, *29*, 359.
(3) Oku, J.; Inoue, S. *Makromol. Chem.* **1979**, *180*, 1089.
(4) Becker, W.; Freund, H.; Pfeil, E. *Angew. Chem., Int. Ed. Engl.* **1965**, *4*, 1079.
(5) Bredig, G.; Fiske, P. S. *Biochem. Z* **1912**, *46*, 7.
(6) Oku, J.; Inoue, S. *J. Chem. Soc., Chem. Commun.* **1981**, 229.
(7) Oku, J.; Ito, N.; Inoue, S. *Makromol. Chem.* **1982**, *183*, 579.
(8) Asada, S.; Kobayashi, Y.; Inoue, S. *Makromol. Chem.* **1985**, *186*, 1755.
(9) Kobayashi, Y.; Asada, S.; Watanabe, I.; Hayashi, H.; Motoo, Y.; Inoue, S. *Bull. Chem. Soc. Jpn.* **1986**, *59*, 893.
(10) Tanaka, K.; Mori, A.; Inoue, S. *J. Org. Chem.* **1990**, *55*, 181.
(11) Shvo, Y.; Gal, M.; Becker, Y.; Elgavi, A. *Tetrahedron: Asymmetry* **1996**, *7*, 911.
(12) Danda, H. *Synlett* **1991**, 263.
(13) Hogg, D. J. P.; North, M.; Stokoe, R. B.; Teasdale, W. G. *Tetrahedron: Asymmetry* **1993**, *4*, 1553.
(14) Kim, H. J.; Jackson, W. R. *Tetrahedron: Asymmetry* **1992**, *3*, 1421.
(15) (a) Callant, D.; Coussens, B.; Maten, T. V. D.; de Vries, J. G.; de Vries, N. K. *Tetrahedron: Asymmetry* **1992**, *3*, 401. (b) Hulst, R.; Broxterman, Q. B.; Kamphuis, J.; Formaggio, F.; Crisma, M.; Toniolo, C.; Kellogg, R. M. *Tetrahedron: Asymmetry* **1997**, *8*, 1987.
(16) Apperley, D.; North, M.; Stokoe, R. B. *Tetrahedron: Asymmetry* **1995**, *6*, 1869.
(17) (a) Williams, R. M. *Synthesis of Optically Active α-Amino Acids*; Pergamon Press: Oxford, U.K., 1989; Chapter 5, p 208. (b) Duthaler, R. O. *Tetrahedron* **1994**, *50*, 1539.

(18) (a) Groger, H. *Chem. Rev.* **2003**, *103*, 2795. (b) Spino, C. *Angew. Chem., Int. Ed.* **2004**, *43*, 1764.

(19) Su, J. T.; Vachal, P.; Jacobsen, E. N. *Adv. Synth. Catal.* **2001**, *343*, 197−200 and references therein.

(20) Iyer, M. S.; Gigstad, K. M.; Namdev, N. D.; Lipton, M. *J. Am. Chem. Soc.* **1996**, *118*, 4910.

(21) Becker, C.; Hoben, C.; Schollmeyer, D.; Scherr, G.; Kunz, H. *Eur. J. Org. Chem.* **2005**, 1497.

(22) Machajewski, T. D.; Wong, C. H. *Angew. Chem., Int. Ed.* **2000**, *39*, 1352.

(23) For recent reviews of proline catalyzed reactions, see: (a) List, B. *Tetrahedron* **2002**, *58*, 5573. (b) List, B. *Synlett* **2001**, 1675.

(24) List, B.; Lerner, R. A.; Barbas, C. F., III *J. Am. Chem. Soc.* **2000**, *122*, 2395.

(25) Kofoed, J.; Nielsen, J.; Reymond, J.-L. *Bioorg. Med. Chem. Lett.* **2003**, *13*, 2445.

(26) Martin, H. J.; List, B. *Synlett* **2003**, 1901.

(27) Tang, Z.; Yang, Z.-H.; Cun, L.-F.; Gong, L.-Z.; Mi, A.-Q.; Jiang, Y.-Z. *Org. Lett.* **2004**, *6*, 2285.

(28) Notz, W.; List, B. *J. Am. Chem. Soc.* **2000**, *122*, 7386.

(29) Shi, L.-X.; Sun, Q.; Ge, Z.-M.; Zhu, Y.-Q.; Cheng, T.-M.; Li, R.-T. *Synlett* **2004**, 2215.

(30) For examples of micelles accelerating aldol reactions, see: (a) Dickerson, T. J.; Janda, K. D. *J. Am. Chem. Soc.* **2002**, *124*, 3220. (b) Peng, Y. Y.; Ding, Q. P.; Li, Z. C.; Wang, P. G.; Cheng, J. P. *Tetrahedron Lett.* **2003**, *44*, 3871.

(31) Akagawa, K.; Sakamoto, S.; Kudo, K. *Tetrahedron Lett.* **2005**, *46*, 8185.

(32) Tang, Z.; Jiang, F.; Yu, L. T.; Cui, X.; Gong, L. Z.; Mi, A. Q.; Jiang, Y. Z.; Wu, Y. D. *J. Am. Chem. Soc.* **2003**, *125*, 5262.

(33) Andreae, M. R. M.; Davis, A. P. *Tetrahedron: Asymmetry* **2005**, *16*, 2487.

(34) Krattiger, P.; McCarthy, C.; Pfaltz, A.; Wennemers, H. *Angew. Chem., Int. Ed.* **2003**, *42*, 1722.

(35) Krattiger, P.; Kovásy, R.; Revell, J. D.; Ivan, S.; Wennemers, H. *Org. Lett.* **2005**, *7*, 1101.

(36) Krattiger, P.; Kovásy, R.; Revell, J. D.; Wennemers, H. *QSAR Comb. Sci.* **2005**, *24*, 1158.

(37) Revell, J. D.; Gantenbein, D.; Krattiger, P.; Wennemers, H. *Biopolymers (Pept. Sci.)* **2006**, *84*, 105.

(38) Kofoed, J.; Darbre, T.; Reymond, J.-L. *Org. Biomol. Chem.* **2006**, *4*, 3268.

(39) Luppi, G.; Cozzi, P. J.; Monari, M.; Kaptein, B.; Broxterman, Q. B.; Tomasini, C. *J. Org. Chem.* **2005**, *70*, 7418.

(40) Tsogoeva, S. B.; Wei, S. *Tetrahedron: Asymmetry* **2005**, *16*, 1947.

(41) Zou, W.; Ibrahem, I.; Dziedzic, P.; Sudén, H.; Córdova, A. *Chem. Commun.* **2005**, 4946.

(42) Dziedzic, P.; Zou, W.; Háfren, J.; Córdova, A. *Org. Biomol. Chem.* **2006**, *4*, 38.

(43) Pizzarello, S.; Weber, A. L. *Science* **2004**, *303*, 1151.

(44) Weber, A. L.; Pizzarello, S. *Proc. Natl. Acad. Sci. U.S.A.* **2006**, *103*, 12713.

(45) Córdova, A.; Zou, W.; Dziedzic, P.; Ibrahem, I.; Reyes, E.; Xu, Y. *Chem.—Eur. J.* **2006**, *12*, 5383.

(46) Córdova, A.; Ibrahem, I.; Casas, J.; Sundén, H.; Engqvist, M.; Reyes, E. *Chem.—Eur. J.* **2005**, *11*, 4772.

(47) (a) Notz, W.; Tanaka, F.; Barbas, C. F., III, *Acc. Chem. Res.* **2004**, *37*, 580. (b) Berner, O. M.; Tedeschi, L.; Enders, D. *Eur. J. Org. Chem.* **2002**, 1877. (c) Gil, M. V.; Roman, E.; Serrano, J. A. *Trends Org. Chem.* **2001**, *9*, 17.

(48) Xu, Y.; Zou, W.; Sundén, H.; Ibrahem, I.; Córdova, A. *Adv. Synth. Catal.* **2006**, *348*, 418.

(49) Tsogoeva, S. B.; Jagtap, S. B. *Synlett* **2004**, 2624.

(50) Tsogoeva, S. B.; Jagtap, S. B.; Ardemasova, Z. A. *Tetrahedron: Asymmetry* **2006**, *17*, 989.

(51) Tsogoeva, S. B.; Jagtap, S. B.; Ardemasova, Z. A.; Kalikhevich, V. *Eur. J. Org. Chem.* **2004**, 4014.

(52) Hanessian, S.; Pham, V. *Org. Lett.* **2000**, *2*, 2975.

(53) Miller, S. J. *Acc. Chem. Res.* **2004**, *37*, 601.

(54) Linton, B. R.; Reutershan, M. H.; Aderman, C. M.; Richardson, K. A.; Brownell, K. R.; Ashley, C. W.; Evans, C. A.; Miller, S. J. *Tetrahedron Lett.* **2007**, *48*, 1993.

(55) Morita, K.; Suzuki, Z.; Hirose, H. *Bull. Chem. Soc. Jpn.* **1968**, *41*, 2815.

(56) Baylis, A. B.; Hillman, M. E. D. German Patent 2155113, 1972; *Chem. Abstr.* **1972**, *77*, 34174q.

(57) Hoffman, H. M. R.; Rabe, J. *Angew. Chem., Int. Ed.* **1983**, *22*, 795.

(58) Price, K. E.; Broadwater, S. J.; Walker, B. J.; McQuade, D. T. *J. Org. Chem.* **2005**, *70*, 3980.

(59) Copeland, G. T.; Miller, S. J. *J. Am. Chem. Soc.* **2001**, *123*, 6496.

(60) (a) Sculimbrene, B. R.; Miller, S. J. *J. Am. Chem. Soc.* **2001**, *123*, 10125. (b) Sculimbrene, B. R.; Morgan, A. J.; Miller, S. J. *J. Am.*

Chem. Soc. **2002**, *124*, 11653. (c) Sculimbrene, B. R.; Morgan, A. J.; Miller, S. J. *Chem. Commun.* **2003**, 1781.

(61) Evans, J. W.; Fierman, M. B.; Miller, S. J.; Ellman, J. A. *J. Am. Chem. Soc.* **2004**, *126*, 8134.

(62) Guerin, D. J.; Miller, S. J. *J. Am. Chem. Soc.* **2002**, *124*, 2134.

(63) Shi, M.; Jiang, J.-K. *Tetrahedron: Asymmetry* **2002**, *13*, 1941.

(64) Iwabuchi, Y.; Nakatani, M.; Yokoyama, N.; Hatakeyama, S. *J. Am. Chem. Soc.* **1999**, *121*, 10219.

(65) Imbriglio, J. E.; Vasbinder, M. M.; Miller, S. J. *Org. Lett.* **2003**, *5*, 3741.

(66) Vasbinder, M. M.; Imbriglio, J. E.; Miller, S. J. *Tetrahedron* **2006**, *62*, 11450.

(67) Seebach, D. *Angew. Chem., Int. Ed.* **1979**, *18*, 239.

(68) Breslow, R. *J. Am. Chem. Soc.* **1958**, *80*, 3719.

(69) Seebach, D.; Corey, E. J. *J. Org. Chem.* **1975**, *40*, 231.

(70) Mennen, S. M.; Blank, J. T.; Tran-Dubé, M. B.; Imbriglio, J. E.; Miller, S. J. *Chem. Commun.* **2005**, 195.

(71) Murry, J. A.; Frantz, D. E.; Soheili, A.; Tillyer, R.; Grabowski, E. J. J.; Reider, P. J. *J. Am. Chem. Soc.* **2001**, *123*, 9696.

(72) Mennen, S. M.; Gipson, J. D.; Kim, Y. R.; Miller, S. J. *J. Am. Chem. Soc.* **2005**, *127*, 1654.

(73) Juliá, S.; Masana, J.; Vega, J. C. *Angew. Chem., Int. Ed. Engl.* **1980**, *19*, 929.

(74) Juliá, S.; Guixer, J.; Masana, J.; Rocas, J.; Colonna, S.; Annūziata, R.; Molinari, H. *J. Chem. Soc., Perkin Trans. 1* **1982**, 1317.

(75) Colonna, S.; Molinari, H.; Banfi, S.; Juliá, S.; Masana, J.; Alvarez, A. *Tetrahedron* **1983**, *39*, 1635.

(76) Banfi, S.; Colonna, S.; Molinari, H.; Juliá, S.; Guixer, J. *Tetrahedron* **1984**, *40*, 5207.

(77) The Julia−Colonna epoxidation has been featured in several previous reviews: (a) Kelly, D. R.; Roberts, S. M. *Biopolymers (Pept. Sci.)* **2006**, *84*, 74. (b) Jarvo, E. R.; Miller, S. J. *Tetrahedron* **2002**, *58*, 2481. (c) Porter, M. J.; Skidmore, J. *Chem. Commun.* **2000**, 1215. (d) Porter, M. J.; Roberts, S. M.; Skidmore, J. *Bioorg. Med. Chem.* **1999**, *7*, 2145. (e) Pu, L. *Tetrahedron: Asymmetry* **1998**, *9*, 1457. (f) Ebrahim, S.; Wills, M. *Tetrahedron: Asymmetry* **1997**, *8*, 3163.

(78) Itsuno, S.; Sakakura, M.; Ito, K. *J. Org. Chem.* **1990**, *55*, 6047.

(79) Flisak, J. R.; Gombatz, K. J.; Holmes, M. M.; Jarmas, A. A.; Lantos, I.; Mendelson, W. L.; Novack, V. J.; Remich, J. J.; Snyder, L. *J. Org. Chem.* **1993**, *58*, 6247.

(80) Lasterra-Sánchez, M. E.; Felfer, U.; Mayon, P.; Roberts, S. M.; Thornton, S. R.; Todd, C. J. *J. Chem. Soc., Perkin Trans. 1* **1996**, 343.

(81) Savizky, R. M.; Suzuki, N.; Bové, J. L. *Tetrahedron: Asymmetry* **1998**, *9*, 3967.

(82) Allen, J. V.; Drauz, K-H.; Flood, R. W.; Roberts, S. M.; Skidmore, J. *Tetrahedron Lett.* **1999**, *40*, 5417.

(83) (a) Bezuidenhoudt, B. C. B.; Swanepoel, A.; Augustyn, J. A. N.; Ferreira, D. *Tetrahedron Lett.* **1987**, *28*, 4857. (b) Augustyn, J. A. N.; Bezuidenhoudt, B. C. B.; Ferreira, D. *Tetrahedron* **1990**, *46*, 2651. (c) Augustyn, J. A. N.; Bezuidenhoudt, B. C. B.; Swanepoel, A.; Ferreira, D. *Tetrahedron* **1990**, *46*, 4429.

(84) van Rensburg, H.; van Heerden, P. S.; Bezuidenhoudt, B. C. B.; Ferreira, D. *Chem. Commun.* **1996**, 2747.

(85) Lasterra-Sánchez, M. E.; Roberts, S. M. *J. Chem. Soc., Perkin Trans. 1* **1995**, 1467.

(86) Kroutil, W.; Lasterra-Sánchez, M. E.; Maddrell, S. J.; Mayon, P.; Morgan, P.; Roberts, S. M.; Thornton, S. R.; Todd, C. J.; Tüter, M. *J. Chem. Soc., Perkin Trans. 1* **1996**, 2837.

(87) Kroutil, W.; Mayon, P.; Lasterra-Sánchez, M. E.; Maddrell, S. J.; Roberts, S. M.; Thornton, S. R.; Todd, C. J.; Tüter, M. *Chem. Commun.* **1996**, 845.

(88) Falck, J. R.; Bhatt, R. K.; Reddy, K. M.; Ye, J. *Synlett* **1997**, 481.

(89) Geller, T.; Gerlach, A.; Krüger, C. M.; Militzer, H.-C. *Tetrahedron Lett.* **2004**, *45*, 5065.

(90) Geller, T.; Krüger, C. M.; Militzer, H.-C. *Tetrahedron Lett.* **2004**, *45*, 5069.

(91) Lopez-Pedrosa, J.-M.; Pitts, M. R.; Roberts, S. M.; Saminathan, S.; Whitall, J. *Tetrahedron Lett.* **2004**, *45*, 5073.

(92) A similar compilation appears in references 77a and 77d.

(93) Bentley, P. A.; Bergeron, S.; Cappi, M. W.; Hibbs, D. E.; Hursthouse, M. B.; Nugent, T. C.; Pulido, R.; Roberts, S. M.; Wu, L. E. *Chem. Commun.* **1997**, 739.

(94) Cooper, M. S.; Heaney, H.; Newbold, A. J.; Sanderson, W. R. *Synlett* **1990**, 533.

(95) Allen, J. V.; Cappi, M. W.; Kary, P. D.; Roberts, S. M.; Williamson, N. M.; Wu, L. E. *J. Chem. Soc., Perkin Trans. 1* **1997**, 3297.

(96) Adger, B. M.; Barkley, J. V.; Bergeron, S.; Cappi, M. W.; Flowerdew, B. E.; Jackson, M. P.; McCague, R.; Nugent, T. C.; Roberts, S. M. *J. Chem. Soc., Perkin Trans. 1* **1997**, 3501.

(97) Chen, W.; Egar, A. L.; Hursthouse, M. B.; Malik, K. M. A.; Mathews, J. E.; Roberts, S. M. *Tetrahedron Lett.* **1998**, *39*, 8495.

(98) Allen, J. V.; Bergeron, S.; Griffiths, M. J.; Mukherjee, S.; Roberts, S. M.; Williamson, N. M.; Wu, L. E. *J. Chem. Soc., Perkin Trans. 1* **1998**, 3171.

(99) Ray, P. C.; Roberts, S. M. *Tetrahedron Lett.* **1999**, *40*, 1779.

(100) Bentley, P. A.; Bickley, J. F.; Roberts, S. M.; Steiner, A. *Tetrahedron Lett.* **2001**, *42*, 3741.

(101) Cappi, M. W.; Chen, W.-P.; Flood, R. W.; Liao, Y.-W.; Roberts, S. M.; Skidmore, J.; Smith, J. A.; Williamson, N. M. *Chem. Commun.* **1998**, 1159.

(102) (a) Geller, T.; Roberts, S. M. *J. Chem. Soc., Perkin Trans. 1* **1999**, 1397. (b) Carde, L.; Davies, H.; Geller, T. P.; Roberts, S. M. *Tetrahedron Lett.* **1999**, *40*, 5421. (c) Baars, S.; Drauz, K.-H.; Krimmer, H.-P.; Roberts, S. M.; Sander, J.; Skidmore, J.; Zanardi, G. *Org. Process Res. Dev.* **2003**, *7*, 509.

(103) Yi, H.; Zou, G.; Li, Q.; Chen, Q.; Tang, J.; He, M. *Tetrahedron Lett.* **2005**, *46*, 5665.

(104) Bentley, P. A.; Cappi, M. W.; Flood, R. W.; Roberts, S. M.; Smith, J. A. *Tetrahedron Lett.* **1998**, *39*, 9297.

(105) Flood, R. W.; Geller, T. P.; Petty, S. A.; Roberts, S. M.; Skidmore, J.; Volk, M. *Org. Lett.* **2001**, *3*, 683.

(106) Tsogoeva, S. B.; Wöltinger, J.; Jost, C.; Reichert, D.; Kühnle, A.; Krimmer, H.-P.; Drauz, K. *Synlett* **2002**, 707.

(107) Bentley, P. A.; Kroutil, W.; Littlechild, J. A.; Roberts, S. M. *Chirality* **1997**, *9*, 198.

(108) Bentley, P. A.; Flood, R. W.; Roberts, S. M.; Skidmore, J.; Smith, C. B.; Smith, J. A. *Chem. Commun.* **2001**, 1616.

(109) Kelly, D. R.; Bui, T. T.; Caroff, E.; Drake, A. F.; Roberts, S. M. *Tetrahedron Lett.* **2004**, *45*, 3885.

(110) Takagi, R.; Shiraki, A.; Manabe, T.; Kojima, S.; Ohkata, K. *Chem. Lett.* **2000**, 366.

(111) Berkessel, A.; Gasch, N.; Glaubitz, K.; Koch, C. *Org. Lett.* **2001**, *3*, 3839.

(112) Berkessel, A.; Koch, B.; Toniolo, C.; Rainaldi, M.; Broxterman, Q. B.; Kaptein, B. *Biopolymers* (*Pept. Sci.*) **2006**, *84*, 90.

(113) Carrea, G.; Colonna, S.; Meek, A. D.; Ottolina, G.; Roberts, S. M. *Chem. Commun.* **2004**, 1412.

(114) Carrea, G.; Colonna, S.; Meek, A. D.; Ottolina, G.; Roberts, S. M. *Tetrahedron: Asymmetry* **2004**, *15*, 2945.

(115) Ferdinand, W. *Biochem. J.* **1966**, *98*, 278.

(116) (a) Kelly, D. R.; Caroff, E.; Flood, R. W.; Heal, W.; Roberts, S. M. *Chem. Commun.* **2004**, 2016. (b) Kelly, D. R.; Roberts, S. M. *Chem. Commun.* **2004**, 2018.

(117) Mathem, S. P.; Gunathilagan, S.; Roberts, S. M.; Blackmond, D. G. *Org. Lett.* **2005**, *7*, 4847.

(118) Firth, B. E.; Miller, L. L.; Mitani, M.; Rogers, T.; Lennox, J.; Murray, R. W. *J. Am. Chem. Soc.* **1976**, *98*, 8272.

(119) Komori, T.; Nonaka, T. *J. Am. Chem. Soc.* **1983**, *105*, 5690.

(120) Komori, T.; Nonaka, T. *J. Am. Chem. Soc.* **1984**, *106*, 2656.

(121) Formaggio, F.; Bonchio, M.; Crisma, M.; Peggion, C.; Mezzato, S.; Polese, A.; Barazza, A.; Antonello, S.; Maran, F.; Broxterman, Q. B.; Kaptein, B.; Kamphuis, J.; Vitale, R. M.; Saviano, M.; Benedetti, E.; Toniolo, C. *Chem.—Eur. J.* **2002**, *8*, 84.

(122) Early work on enantioselective electrochemical reduction using (amino acid)-coated electrodes was carried out by Miller. See: Watkins, B. F.; Behling, J. R.; Kariv, E.; Miller, L. L. *J. Am. Chem. Soc.* **1975**, *97*, 3549.

(123) Abe, S.; Nonaka, T.; Fuchigami, T. *J. Am. Chem. Soc.* **1983**, *105*, 3630.

(124) Abe, S.; Nonaka, T. *Chem. Lett.* **1983**, 1541.

(125) Nonaka, T.; Abe, S.; Fuchigami, T. *Bull. Chem. Soc. Jpn.* **1983**, *56*, 2778.

(126) Abe, S.; Fuchigami, T.; Nonaka, T. *Chem. Lett.* **1983**, 1033.

(127) (a) Inoue, S.; Ohashi, S.; Tabata, A.; Tsuruta, T. *Makromol. Chem.* **1968**, *112*, 66. (b) Ohashi, S.; Inoue, S. *Makromol. Chem.* **1971**, *150*, 105. (c) Ohashi, S.; Inoue, S. *Makromol. Chem.* **1972**, *160*, 69. (d) Inoue, S.; Ohashi, S.; Unno, Y. *Polymer J.* **1972**, *3*, 611.

(128) Fukushima, H.; Ohashi, S.; Inoue, S. *Makromol. Chem.* **1975**, *176*, 2751.

(129) Fukushima, H.; Inoue, S. *Makromol. Chem.* **1975**, *176*, 3609.

(130) Fukushima, H.; Inoue, S. *Makromol. Chem.* **1976**, *177*, 2617.

(131) Ueyanagi, K.; Inoue, S. *Makromol. Chem.* **1976**, *177*, 2807.

(132) Enantiomeric excess of product **74** was determined with chiral shift reagents: Ueyanagi, K.; Inoue, S. *Makromol. Chem.* **1977**, *178*, 235.

(133) Ueyanagi, K.; Inoue, S. *Makromol. Chem.* **1977**, *178*, 375.

(134) Ueyanagi, K.; Inoue, S. *Makromol. Chem.* **1978**, *179*, 887.

(135) Inoue, S.; Kawano, Y. *Makromol. Chem.* **1979**, *180*, 1405.

(136) Mitsuhashi, K.; Ito, R.; Arai, T.; Yanagisawa, A. *Org. Lett.* **2006**, *8*, 1721.

(137) Guerin, D. J.; Horstmann, T. E.; Miller, S. J. *Org. Lett.* **1999**, *1*, 1107.

(138) Horstmann, T. E.; Guerin, D. J.; Miller, S. J. *Angew. Chem., Int. Ed.* **2000**, *39*, 3635.

(139) See ref 62.

(140) (a) Moss, R. A.; Sunshine, W. L. *J. Org. Chem.* **1974**, *39*, 1083. For the use of amino acid-functionalized surfactants, see: (b) Brown, J. M.; Bunton, C. A. *J. Chem. Soc., Chem. Commun.* **1974**, 969. (c) Moss, R. A.; Lukas, T. J.; Nahas, R. C. *Tetrahedron Lett.* **1977**, *44*, 3851. (d) Moss, R. A.; Nahas, R. C.; Lukas, T. J. *Tetrahedron Lett.* **1978**, *6*, 507. (e) Murakami, Y.; Nakano, A.; Yoshimatsu, A.; Fukuya, K. *J. Am. Chem. Soc.* **1981**, *103*, 728. For the use of *N*-protected amino acid derivatives and surfactants, see: (f) Inoue, T.; Nomura, K.; Kimizuka, H. *Bull. Chem. Soc. Jpn.* **1976**, *49*, 719. (g) Ihara, Y. *J. Chem. Soc., Chem. Commun.* **1978**, 984. (h) Yamada, K.; Shosenji, H.; Ihara, H.; Otsubo, Y. *Tetrahedron Lett.* **1979**, *27*, 2529. (i) Yamada, K.; Shosenji, H.; Ihara, H. *Chem. Lett.* **1979**, 491. (j) Ihara, Y. *J. Chem. Soc., Perkin Trans. 2* **1980**, 1483. (k) Ueoka, R.; Matsuura, H.; Nakahata, S.; Ohkubo, K. *Bull. Chem. Soc. Jpn.* **1980**, *53*, 347. (l) Ueoka, R.; Matsumoto, Y.; Ninomiya, Y.; Nakagawa, Y.; Inoue, K.; Ohkubo, K. *Chem. Lett.* **1981**, 785. (m) Ohkubo, K.; Sugahara, K.; Ohta, H.; Tokuda, K.; Ueoka, R. *Bull. Chem. Soc. Jpn.* **1981**, *54*, 576. (n) Ueoka, R.; Murakami, Y. *J. Chem. Soc., Perkin Trans. 2* **1983**, 219. (o) Ihara, Y.; Hosako, R. *J. Chem. Soc., Perkin Trans. 2* **1983**, 5. (p) Moss, R. A.; Lee, Y.-S.; Lukas, T. J. *J. Am. Chem. Soc.* **1979**, *101*, 2499.

(141) Ingles, D. W.; Knowles, J. R. *Biochem. J.* **1968**, *208*, 561.

(142) Okubo, K.; Sugahara, K.; Yoshinaga, K.; Ueoka, R. *J. Chem. Soc., Chem. Commun.* **1980**, *13*, 637.

(143) Ohkubo, K.; Matsumoto, N.; Ohta, H. *J. Chem. Soc., Chem. Commun.* **1982**, *13*, 738.

(144) Ueoka, R.; Matsumoto, Y.; Ihara, Y. *Chem. Lett.* **1984**, *10*, 1807.

(145) (a) Ueoka, R.; Matsumoto, Y.; Moss, R. A.; Swarup, S.; Sugii, A.; Harada, K.; Kikuchi, J.; Murakami, Y. *J. Am. Chem. Soc.* **1988**, *110*, 1588. (b) Ueoka, R.; Matsumoto, Y.; Cho, M.; Ikeda, T.; Kawata, T.; Kato, Y. *Kagaku Kogaku Ronbunshu* **1989**, *15*, 540. (c) Tanoue, O.; Baba, M.; Tokunaga, Y.; Goto, K.; Matsumoto, Y.; Ueoka, R. *Tetrahedron Lett.* **1999**, *40*, 2129.

(146) Ueoka, R.; Matsumoto, Y.; Nagamine, K.; Yashi, H.; Harada, K.; Sugii, A. *Chem. Pharm. Bull.* **1987**, *35*, 3070.

(147) Ueoka, R.; Matsumoto, Y.; Harada, K.; Sugi, A. *Yuki Gosei Kagaku Kyokaishi* **1989**, *47*, 53.

(148) (a) Ueoka, R.; Matsumoto, Y.; Takemiya, N.; Ihara, Y. *Chem. Pharm. Bull.* **1989**, *37*, 2263. (b) Ishida, H.; Donowaki, K.; Suga, M.; Shimose, K.; Ohkubo, K. *Tetrahedron Lett.* **1995**, *36*, 8987. (c) Ohkubo, K.; Urabe, K.; Yamamoto, J.; Sagawa, T.; Usui, S. *J. Chem. Soc., Perkin Trans. 1* **1995**, *23*, 2957.

(149) (a) Ueoka, R.; Moss, R. A.; Swarup, S.; Matsumoto, Y.; Strauss, G.; Murakami, Y. *J. Am. Chem. Soc.* **1985**, *107*, 2185. (b) Ueoka, R.; Matsumoto, Y.; Yoshino, T.; Watanabe, N.; Omura, K.; Murakami, Y. *Chem. Lett.* **1986**, *10*, 1743. (c) Ueoka, R.; Yoshino, T.; Matsumoto, Y. *Nippon Kagaku Kaishi* **1987**, *3*, 378. (d) Ohkubo, K.; Miyake, S. *J. Chem. Soc., Perkin Trans. 2* **1987**, *8*, 995. (e) Ueoka, R.; Dozono, H.; Matsumoto, Y.; Cho, M.; Kitahara, K.; Kato, Y. *Chem. Pharm. Bull.* **1990**, *38*, 219.

(150) (a) Ueoka, R.; Matsumoto, Y.; Kikuno, T.; Okada, K. *J. Mol. Catal.* **1983**, *18*, 267. (b) Ueoka, R.; Matsumoto, Y.; Nagamatsu, T.; Hirohata, S. *Tetrahedron Lett.* **1984**, *25*, 1363. (c) Ueoka, R.; Matsumoto, Y. *J. Org. Chem.* **1984**, *49*, 3774. (d) Ueoka, R.; Matsumoto, Y. *J. Org. Chem.* **1990**, *55*, 5797.

(151) (a) Matsumoto, Y.; Ueoka, R. *Bull. Chem. Soc. Jpn.* **1983**, *56*, 3370. (b) Ueoka, R.; Matsumoto, Y.; Nagamatsu, T.; Hirohata, S. *Chem. Lett.* **1984**, 583.

(152) (a) Ohkubo, K.; Kawata, M.; Orito, T.; Ishida, H. *J. Chem. Soc., Perkin Trans. 1* **1989**, 666. (b) Ueoka, R.; Cho, M.; Matsumoto, Y.; Goto, K.; Kato, Y.; Harada, K.; Sugii, A. *Tetrahedron Lett.* **1990**, *31*, 5335.

(153) (a) Goto, K.; Matsumoto, Y.; Ueoka, R. *J. Org. Chem.* **1995**, *60*, 3342. (b) Tanoue, O.; Ichihara, H.; Goto, K.; Matsumoto, Y.; Ueoka, R. *Chem. Pharm. Bull.* **2003**, *51*, 224.

(154) (a) Ohkubo, K.; Urabe, K.; Yamamoto, J.; Ishida, H.; Ushi, S.; Sagawa, T. *J. Chem. Soc., Chem. Commun.* **1995**, *22*, 2301. (b) Ohkubo, K. *Macromol. Rapid Commun.* **1996**, *17*, 109. (c) For a review, see: Sagawa, T.; Urabe, K.; Ihara, H.; Ohkubo, K. *Recent Res. Dev. Pure Appl. Chem.* **2000**, *4*, 1.

(155) (a) Moss, R. A.; Lee, Y.-S.; Alwis, K. W. *J. Am. Chem. Soc.* **1980**, *102*, 6648. (b) Moss, R. A.; Lee, Y.-S. *Tetrahedron Lett.* **1981**, *22*, 2353. (c) Moss, R. A.; Taguchi, T.; Bizzigotti, G. O. *Tetrahedron Lett.* **1982**, *23*, 1985. (d) Moss, R. A.; Chiang, Y.-C. P.; Hui, Y. *J. Am. Chem. Soc.* **1984**, *106*, 7506. (e) Ueoka, R.; Matsumoto, Y.; Yoshino, T.; Hirose, T.; Moss, R. A.; Kim, K. Y.; Swarup, S. *Tetrahedron Lett.* **1986**, *27*, 1183. (f) Moss, R. A.; Hendrickson, T. F.; Ueoka, R.; Kim, K. Y.; Weiner, P. K. *J. Am. Chem. Soc.* **1987**, *109*, 4363. (g) Matsumoto, Y.; Matsumoto, Y.; Inoue, J.; Ueoka, R. *Chem. Lett.* **1993**, *8*, 1303. (h) Ueoka, R.; Matsumoto, Y.; Ito, T.; Matsumoto, Y.; Kato, Y. *Chem. Pharm. Bull.* **1994**, *42*, 173. (i) Ueoka, R.; Matsumoto, Y.; Goto, K.; Ito, T.; Mori, S.; Matsumoto, Y.; Sakoguchi, A.; Ihara, Y.; Hirata, F. *Tetrahedron Lett.* **1996**, *37*,

3461. (j) Ueoka, R.; Goto, K.; Tanoue, O.; Miki, A.; Yoshimitsu, S.; Imamura, C.; Ihara, Y.; Murakami, Y. *Chem. Lett.* **1999**, 73. (k) Ohkubo, K.; Matsumoto, N.; Nagasaki, M.; Yamaki, K.; Ogata, H. *Bull. Chem. Soc. Jpn.* **1984**, *57*, 214. (l) Cho, I.; Kim, G.-C. *J. Org. Chem.* **1988**, *53*, 5189. (m) Cleij, M. C.; Drenth, W.; Nolte, R. J. M. *J. Org. Chem.* **1991**, *56*, 3883.

(156) (a) Esposito, A.; Delort, E.; Lagnoux, D.; Djojo, F.; Reymond, J.-L. *Angew. Chem., Int. Ed.* **2003**, *42*, 1381. (b) Lagnoux, D.; Delort, E.; Douat-Casassus, C.; Esposito, A.; Reymond, J.-L. *Chem.—Eur. J.* **2004**, *10*, 1215. (c) Douat-Casassus, C.; Darbre, T.; Reymond, J.-L. *J. Am. Chem. Soc.* **2004**, *126*, 7817. (d) Darbre, T.; Reymond, J.-L. *Acc. Chem. Res.* **2006**, *39*, 925. (e) Clouet, A.; Darbre, T.; Reymond, J.-L. *Adv. Synth. Catal.* **2004**, *346*, 1195. (f) Clouet, A.; Darbre, T.; Reymond, J.-L. *Biopolymers (Pept. Sci.)* **2006**, *84*, 114. (g) Delort, E.; Darbre, T.; Reymond, J.-L. *J. Am. Chem. Soc.* **2004**, *126*, 15642. (h) Clouet, A.; Darbre, T.; Reymond, J.-L. *Angew. Chem., Int. Ed.* **2004**, *43*, 4612. (i) Kofoed, J.; Reymond, J.-L. *Curr. Opin. Chem. Biol.* **2005**, *9*, 656. (j) Delort, E.; Nguyen-Trung, N.-Q.; Darbre, T.; Reymond, J.-L. *J. Org. Chem.* **2006**, *71*, 4468.

(157) (a) Olofsson, S.; Johansson, G.; Baltzer, L. *J. Chem. Soc., Perkin Trans. 2* **1995**, 2047. (b) Baltzer, L.; Lundh, A.-C.; Broo, K.; Olofsson, S.; Ahlberg, P. *J. Chem. Soc., Perkin Trans. 2* **1996**, 1671. (c) Broo, K. S.; Brive, L.; Lundh, A.-C.; Ahlberg, P.; Baltzer, L. *J. Am. Chem. Soc.* **1996**, *118*, 8172. (d) Lundh, A.-C.; Broo, K. S.; Baltzer, L. *J. Chem. Soc., Perkin Trans. 2* **1997**, 209. (e) Kjellstrand, M.; Broo, K.; Andersson, L.; Farre, C.; Nilsson, A.; Baltzer, L. *J. Chem. Soc., Perkin Trans. 2* **1997**, 2745. (f) Broo, K. S.; Allert, M.; Andersson, L.; Erlandsson, P.; Stenhagen, G.; Wigstrom, J.; Ahlberg, P.; Baltzer, L. *J. Chem. Soc., Perkin Trans. 2* **1997**, 397. (g) Broo, S. K.; Brive, L.; Ahlberg, P.; Baltzer, L. *J. Am. Chem. Soc.* **1997**, *119*, 11362. (h) Broo, K. S.; Nilsson, H.; Nilsson, J.; Flodberg, A.; Baltzer, L. *J. Am. Chem. Soc.* **1998**, *120*, 4063. (i) Broo, K. S.; Nilsson, H.; Nilsson, J.; Baltzer, L. *J. Am. Chem. Soc.* **1998**, *120*, 10287. (j) Baltzer, L. *Biopolymers* **1998**, *47*, 31. (k) Baltzer, L. *Curr. Opin. Struct. Biol.* **1998**, *8*, 466. (l) Nilsson, J.; Broo, K. S.; Sott, R. S.; Baltzer, L. *Can. J. Chem.* **1999**, *77*, 990. (m) Baltzer, L.; Broo, K. S.; Nilsson, H.; Nilsson, J. *Bioorg. Med. Chem.* **1999**, *7*, 83. (n) Nilsson, J.; Broo, K. S.; Sott, R. S.; Baltzer, L. *Can. J. Chem.* **1999**, *77*, 990. (o) Baltzer, L. *Topics Curr. Chem.* **1999**, *202*, 39. (p) Nilsson, J.; Baltzer, L. *Chem.—Eur. J.* **2000**, *6*, 2214. (q) Willian, N. H.; Wyman, P. *Chem. Commun.* **2001**, 1268. (r) Rossi, P.; Tecilla, P.; Baltzer, L.; Scrimin, P. *Chem.—Eur. J.* **2004**, *10*, 4163.

(158) (a) Guilly, L. L.; Brack, A.; Spach, G. *Makromol. Chem.* **1978**, *179*, 2829. (b) Brack, A. *Pure Appl. Chem.* **1993**, *65*, 1143.

(159) Brack, A.; Spach, G. *J. Mol. Evol.* **1980**, *15*, 231.

(160) Barbier, B.; Brack, A. *J. Am. Chem. Soc.* **1988**, *110*, 6880.

(161) Brack, A.; Barbier, B. *Origins Life Evol. Biosphere* **1990**, *20*, 139.

(162) Malon, P.; Bonmatin, J.-M.; Brack, A. *Tetrahedron Lett.* **1991**, *32*, 5337.

(163) Brack, A.; Spach, G. *J. Am. Chem. Soc.* **1981**, *103*, 6319.

(164) Perello, M.; Barbier, B.; Brack, A. *Int. J. Pept. Protein Res.* **1991**, *38*, 154.

(165) Barbier, B.; Brack, A. *J. Am. Chem. Soc.* **1992**, *114*, 3511.

(166) Tsutsumi, H.; Hamasaki, K.; Mihara, H.; Ueno, A. *J. Chem. Soc., Perkin Trans. 2* **2000**, 1813.

(167) (a) Vedejs, E.; Daugulis, O.; Harper, L. A.; MacKay, J. A.; Powell, D. R. *J. Org. Chem.* **2003**, *68*, 5020. (b) Vedejs, E.; Daugulis, O.; Tuttle, N. *J. Org. Chem.* **2004**, *69*, 1389.

(168) Fu, G. C. *Acc. Chem. Res.* **2004**, *37*, 542.

(169) (a) Birman, V. B.; Jiang, H. *Org. Lett.* **2005**, *7*, 3445−3447. (b) Birman, V. B.; Uffman, E. W.; Jiang, H.; Li, X.; Kilbane, C. J. *J. Am. Chem. Soc.* **2004**, *126*, 12226−12227.

(170) Miller, S. J.; Copeland, G. T.; Papaioannou, N.; Horstmann, T. E.; Ruel, E. M. *J. Am. Chem. Soc.* **1998**, *120*, 1629.

(171) Copeland, G. T.; Jarvo, E. R.; Miller, S. J. *J. Org. Chem.* **1998**, *63*, 6784.

(172) Jarvo, E. R.; Copeland, G. T.; Papaioannou, N.; Bonitatebus, P.; Miller, S. J. *J. Am. Chem. Soc.* **1999**, *121*, 11638.

(173) Vasbinder, M. M.; Jarvo, E. R.; Miller, S. J. *Angew. Chem., Int. Ed.* **2001**, *40*, 2824.

(174) (a) Formaggio, F.; Barazza, A.; Bertocco, A.; Toniolo, C.; Broxterman, Q. B.; Kaptein, B.; Brasola, E.; Pengo, P.; Pasquato, L.; Scrimin, P. *J. Org. Chem.* **2004**, *69*, 3849. (b) Licini, G.; Bonchio, M.; Broxterman, Q. B.; Kaptein, B.; Moretto, A.; Toniolo, C.; Scrimin, P. *Biopolymers (Pept. Sci.)* **2006**, *84*, 97.

(175) (a) See ref 59. (b) Evans, C. A.; Miller, S. J. *Curr. Opin. Chem. Biol.* **2002**, *6*, 333.

(176) Fierman, M. B.; O'Leary, D. J.; Steinmetz, W. E.; Miller, S. J. *J. Am. Chem. Soc.* **2004**, *126*, 6967.

(177) (a) Jarvo, E. R.; Evans, C. A.; Copeland, G. T.; Miller, S. J. *J. Org. Chem.* **2001**, *66*, 5522. (b) Angione, M. C.; Miller, S. J. *Tetrahedron* **2006**, *62*, 5254.

(178) (a) Papaioannou, N.; Blank, J. T.; Miller, S. J. *J. Org. Chem.* **2003**, *68*, 2728. (b) Papaioannou, N.; Evans, C. A.; Miller, S. J. *Org. Lett.* **2001**, *3*, 2879.

(179) Griswold, K. S.; Miller, S. J. *Tetrahedron*, **2003**, *59*, 8869.

(180) Lewis, C. A.; Miller, S. J. *Angew. Chem., Int. Ed.* **2006**, *45*, 5616.

(181) Lewis, C. A.; Chiu, A.; Kubryk, M.; Balsells, J.; Pollard, D.; Esser, C. K.; Murry, J.; Reamer, R. A.; Hansen, K. B.; Miller, S. J. *J. Am. Chem. Soc.* **2006**, *128*, 16454.

(182) (a) Wong, C. H.; Wang, Y. F. *J. Org. Chem.* **1988**, *53*, 3127. (b) Lewis, C. A.; Sculimbrene, B. R.; Xu, Y.; Miller, S. J. *Org. Lett.* **2005**, *7*, 3021.

(183) See ref 60.

(184) (a) Morgan, A. J.; Komiya, S.; Xu, Y.; Miller, S. J. *J. Org. Chem.* **2006**, *71*, 6923. (b) Morgan, A. J.; Wang, Y. K.; Roberts, M. F.; Miller, S. J. *J. Am. Chem. Soc.* **2004**, *126*, 15370.

(185) (a) Bruzik, K. S.; Kubiak, R. J. *Tetrahedron Lett.* **1995**, *36*, 2415. (b) Gilbert, I. H.; Holmes, A. B.; Pestchanker, M. J.; Young, R. C. *Carbohydr. Res.* **1992**, *234*, 117. (c) Painter, G. F.; Grove, S. J. A.; Gilbert, I. H.; Holmes, A. B.; Raithby, P. R.; Hill, M. L.; Hawkins, P. T.; Stephens, L. R. *J. Chem. Soc., Perkin Trans. 1* **1999**, 923. (d) Falck, J. R.; Krishna, U. M.; Katipally, K. R.; Capdevilla, J. H.; Ulug, E. T. *Tetrahedron Lett.* **2000**, *41*, 4271. (e) Falck, J. R.; Krishna, U. M.; Capdevila, J. H. *Bioorg. Med. Chem. Lett.* **2000**, *10*, 1711. (f) Wang, D. S.; Chen, C. S. *J. Org. Chem.* **1996**, *61*, 5905. (g) Chen, J.; Feng, L.; Prestwich, G. D. *J. Org. Chem.* **1998**, *63*, 6511.

(186) Sculimbrene, B. R.; Xu, Y.; Miller, S. J. *J. Am. Chem. Soc.* **2004**, *126*, 13182.

(187) Xu, Y.; Sculimbrene, B. R.; Miller, S. J. *J. Org. Chem.* **2006**, *71*, 4919.

(188) Fernandez, I.; Khiar, N. *Chem. Rev.* **2003**, *103*, 3651.

(189) See ref 61.

(190) Peltier, H. M.; Evans, J. A.; Ellman, J. A. *Org. Lett.* **2005**, *7*, 1733.